

Colors of 2625 Quasars at $0 < z < 5$ Measured in the Sloan Digital Sky Survey Photometric System¹

Gordon T. Richards^{2,3}, Xiaohui Fan^{4,5}, Donald P. Schneider², Daniel E. Vanden Berk⁶, Michael A. Strauss⁴, Donald G. York^{3,7}, John E. Anderson, Jr.⁶, Scott F. Anderson⁸, James Annis⁶, Neta A. Bahcall⁴, Mariangela Bernardi³, John W. Briggs³, J. Brinkmann⁹, Robert Brunner¹⁰, Scott Burles^{3,6}, Larry Carey⁸, Francisco J. Castander^{3,11}, A. J. Connolly¹², J. H. Crocker¹³, István Csabai^{13,14}, Mamoru Doi¹⁵, Douglas Finkbeiner¹⁶, Scott D. Friedman¹³, Joshua A. Frieman^{3,6}, Masataka Fukugita¹⁷, James E. Gunn⁴, Robert B. Hindsley¹⁸, Željko Ivezić⁴, Stephen Kent^{3,6}, G. R. Knapp⁴, D.Q. Lamb³, R. French Leger⁸, Daniel C. Long⁹, Jon Loveday¹⁹, Robert H. Lupton⁴, Timothy A. McKay²⁰, Avery Meiksin²¹, Aronne Merrelli^{10,22}, Jeffrey A. Munn²³, Heidi Jo Newberg²⁴, Matt Newcomb²², R. C. Nichol²², Russell Owen⁸, Jeffrey R. Pier²³, Adrian Pope^{13,22}, Michael W. Richmond²⁵, Constance M. Rockosi³, David J. Schlegel⁴, Walter A. Siegmund⁸, Stephen Smee^{13,26}, Yehuda Snir²², Chris Stoughton⁶, Christopher Stubbs⁸, Mark SubbaRao³, Alexander S. Szalay¹³, Gyula P. Szokoly²⁷, Christy Tremonti¹³, Alan Uomoto¹³, Patrick Waddell⁸, Brian Yanny⁶, Wei Zheng¹³

ABSTRACT

We present an empirical investigation of the colors of quasars in the Sloan Digital Sky Survey (SDSS) photometric system. The sample studied includes 2625 quasars with SDSS photometry: 1759 quasars found during SDSS spectroscopic commissioning

²Department of Astronomy and Astrophysics, The Pennsylvania State University, University Park, PA 16802

³The University of Chicago, Department of Astronomy and Astrophysics, 5640 S. Ellis Ave., Chicago, IL 60637

⁴Princeton University Observatory, Princeton, NJ 08544

⁵Institute for Advanced Study, Olden Lane, Princeton, NJ 08540

⁶Fermi National Accelerator Laboratory, P.O. Box 500, Batavia, IL 60510

⁷The University of Chicago, Enrico Fermi Institute, 5640 S. Ellis Ave., Chicago, IL 60637

⁸University of Washington, Department of Astronomy, Box 351580, Seattle, WA 98195

⁹Apache Point Observatory, P.O. Box 59, Sunspot, NM 88349-0059

¹⁰Department of Astronomy, California Institute of Technology, Pasadena, CA 91125

¹¹Observatoire Midi Pyrenees, 14 ave Edouard Belin, Toulouse, F-31400, France

¹²Department of Physics and Astronomy, University of Pittsburgh, Pittsburgh, PA 15260

¹³Department of Physics and Astronomy, The Johns Hopkins University, 3701 San Martin Drive, Baltimore, MD 21218

¹⁴Department of Physics of Complex Systems, Eötvös University, Pázmány Péter sétány 1

¹⁵Department of Astronomy and Research Center for the Early Universe, School of Science, University of Tokyo, Hongo, Bunkyo, Tokyo, 113-0033, Japan

¹⁶University of California at Berkeley, Departments of Physics and Astronomy, 601 Campbell Hall, Berkeley, CA 94720

¹⁷University of Tokyo, Institute for Cosmic Ray Reserach, Kashiwa, 2778582, Japan

¹⁸Remote Sensing Division, Code 7215, Naval Research Laboratory, 4555 Overlook Ave. SW, Washington, DC 20375

¹⁹Astronomy Centre, University of Sussex, Falmer, Brighton BN1 9QJ, United Kingdom

²⁰University of Michigan, Department of Physics, 500 East University, Ann Arbor, MI 48109

²¹Royal Observatory, Edinburgh, EH9 3HJ, United Kingdom

²²Dept. of Physics, Carnegie Mellon University, 5000 Forbes Ave., Pittsburgh, PA-15232

²³U.S. Naval Observatory, Flagstaff Station, P.O. Box 1149, Flagstaff, AZ 86002-1149

²⁴Physics Department, Rensselaer Polytechnic Institute, SC1C25, Troy, NY 12180

²⁵Physics Department, Rochester Institute of Technology, 85 Lomb Memorial Drive, Rochester, NY 14623-5603

²⁶Department of Astronomy, University of Maryland, College Park, MD 20742-2421

²⁷Astrophysikalisches Institut Potsdam, An der Sternwarte 16, D-14482 Potsdam, Germany

and SDSS followup observations on other telescopes, 50 matches to FIRST quasars, 573 matches to quasars from the NASA Extragalactic Database, and 243 quasars from two or more of these sources. The quasars are distributed in a 2.5 degree wide stripe centered on the Celestial Equator covering ~ 529 square degrees. Positions (accurate to $0.2''$) and SDSS magnitudes are given for the 898 quasars known prior to SDSS spectroscopic commissioning. New SDSS quasars, which range in brightness from $i^* = 15.39$ to the photometric magnitude limit of the survey, represent an increase of over 200% in the number of known quasars in this area of the sky.

The ensemble average of the observed colors of quasars in the SDSS passbands are well represented by a power-law continuum with $\alpha_\nu = -0.5$ ($f_\nu \propto \nu^\alpha$) and are close to those predicted by previous simulations. However, the contributions of the “small blue (or 3000 Å) bump” and other strong emission lines have a significant effect upon the colors. The color-redshift relation exhibits considerable structure, which may be of use in determining photometric redshifts for quasars from their colors alone. The range of colors at a given redshift can generally be accounted for by a range in the optical spectral index with a distribution $\alpha_\nu = -0.5 \pm 0.65$ (95% confidence), but there is a red tail in the distribution. This tail may be a sign of internal reddening, especially since fainter objects at a given redshift tend to exhibit redder colors than the average. Finally, we show that there is a continuum of properties between quasars and Seyfert galaxies and we test the validity of the traditional dividing line ($M_B = -23$) between the two classes of AGN.

Subject headings: quasars: general — surveys — catalogs

1. Introduction

Quasar identification in multicolor surveys relies on the fact that the spectral energy distributions of stars and quasars produce different colors in broad-band photometric systems. At low redshift ($z \leq 2.2$), the lack of a Balmer jump in quasars separates them from hot stars; at higher redshifts the presence of the strong Lyman- α emission line and absorption by the Lyman- α forest cause the broad-band colors of quasars to become increasingly redder with redshift (Sandage 1965; Green et al. 1986; Warren et al. 1991a; Fan 1999). Historically, large area surveys have been based

¹Based on observations obtained with the Sloan Digital Sky Survey; with the Apache Point Observatory 3.5-meter telescope, which is owned and operated by the Astrophysics Research Consortium; with the Hobby-Eberly Telescope, which is a joint project of the University of Texas at Austin, the Pennsylvania State University, Stanford University, Ludwig-Maximilians-Universität München, and Georg-August-Universität Göttingen; with the 2.1-meter telescope at Kitt Peak National Observatory; and at the W. M. Keck Observatory, which is operated as a scientific partnership among the California Institute of Technology, the University of California, and NASA, and was made possible by the generous financial support of the W. M. Keck Foundation.

on photographic plates; the limited photometric accuracy of this technique (~ 0.1 mag) has been one of the primary limitations of the effectiveness of their quasar selection.

The Sloan Digital Sky Survey (SDSS; York et al. 2000) will survey approximately one quarter of the Celestial Sphere in five broad bands spanning the optical region of the spectrum. The expected photometric errors in each filter are less than 5% for objects brighter than 19th magnitude; this should allow identification of approximately 100,000 quasars. In this paper we study the photometric properties in the SDSS system of over 2600 quasars in a stripe 2.5° wide centered on the Celestial Equator; the total area covered is ~ 529 square degrees. Over 1700 of these objects were discovered in the past year and are examined here for the first time.

This paper acts as an empirical companion to Fan (1999), which presented theoretical and simulated colors of quasars and other point sources in the SDSS system. Although the SDSS photometric system is still uncertain at the few percent level, the photometry is better than has ever been accomplished previously for a large area sample of quasars. With the SDSS photometry, we can detect features in the color-redshift distribution that are smaller than the typical error in the colors of quasars from photographic surveys. Using this information, we examine a number of long-standing issues in quasar science.

Section 2 of the paper describes the observations and in Section 3 we describe the catalogs that were used to construct the database for this study. In Section 4 we examine the observed colors of quasars and compare them to the values expected from simulations of their spectral energy distributions, and in Section 5 we discuss how these results will impact a number of issues, including quasar target selection in the SDSS. Finally, Section 6 presents our conclusions.

2. SDSS Imaging

The Sloan Digital Sky Survey (York et al. 2000) will provide accurate photometry and spectroscopy for over 10,000 square degrees of sky. The optical magnitudes of detected objects are measured nearly simultaneously through five broad-band filters (u' , g' , r' , i' , and z' ; Fukugita et al. 1996) with nominal effective wavelengths of 3540 Å, 4760 Å, 6280 Å, 7690 Å and 9250 Å, complete to limiting point source magnitudes of 22.3, 22.6, 22.7, 22.4 and 20.5, respectively (signal-to-noise ratio 5:1). Because the definition of the photometric system is not yet finalized, measured magnitudes are quoted using asterisks (u^* , g^* , r^* , i^* , and z^*) to represent preliminary photometry; the filters themselves are referred to as u' , g' , r' , i' , and z' . SDSS magnitudes are based on the AB magnitude system (Oke & Gunn 1983), and are given as asinh magnitudes (Lupton et al. 1999), which have nice properties at low flux limits. For objects fainter than the 5σ flux limit given above, the asinh magnitude will deviate from normal magnitudes. The analysis in this paper should not be affected by these differences; however, some of the high-redshift quasars have u' and g' magnitudes fainter than these limits.

The survey is being done with a dedicated 2.5m telescope (Siegmund et al. 2001). The telescope

has a wide, well-corrected field and is equipped with a large mosaic CCD camera (Gunn et al. 1998) and a pair of fiber-fed spectrographs (Uomoto et al. 2001a). The camera utilizes thirty 2048×2048 CCDs which take the data in drift-scanning (time-delay-and-integrate, or TDI) mode with a total integration time of 54.1 seconds per filter. The imaging data are obtained using the data acquisition system (Petravick et al. 1994; Annis et al. 2001) at the Apache Point Observatory (APO) and are automatically processed through a set of software pipelines (Kent et al. 2001). The photometric pipeline (Lupton et al. 2001) reduces the imaging data, measuring positions, magnitudes, and shape parameters for all detected objects. The photometric pipeline uses information from the astrometric pipeline (Pier et al. 2001) and the photometric calibration telescope (PT; Smith et al. 2001; Uomoto et al. 2001b; Tucker et al. 2001). After final photometric calibration of the data, the outputs, together with all the observing and processing information, are loaded into the operational database (Yanny et al. 2001). The final parameters are stored in an object-oriented searchable database (SX; Szalay et al. 2001). For an explanation of SDSS technical terms used in the text, please refer to York et al. (2000).

Preliminary analysis shows that there are differences between the real SDSS transmission curves and those shown by Fukugita et al. (1996); see Fan et al. (2001), Appendix A, for a discussion. These differences are believed to be due to the fact that the filters are in vacuo and are not exposed to the air. For a quasar with a typical power-law spectrum of $f_\nu \propto \nu^{-0.5}$ we find that the effective wavelengths of the actual 2.5m filters are 3651, 4679, 6175, 7494, and 8873 Å instead of 3544, 4770, 6231, 7625 and 9135 Å, respectively for u' , g' , r' , i' , and z' . (Since the spectral energy distribution of a quasar is different from the standard stars used to define the SDSS photometric system, the latter effective wavelengths of the passbands are different from those quoted earlier.) These offsets are quite large, but they produce only small effects on the measured colors of the objects discussed herein (~ 0.005 mag). The most current transmission curves are used in all of the analysis throughout the paper. More details on the transmission curves of the 2.5m camera will be shown in a future paper (Doi et al. 2001).

Data from the imaging camera on the 2.5-m are calibrated against patches of the sky observed by the PT. The PT also observes standard stars in order to determine nightly extinction coefficients. While the quality of the current SDSS photometric data is more than adequate for our purposes, the final calibration of the SDSS system is not yet in place, due in part to the SDSS transmission curve uncertainties discussed above. However, the quality of the data in hand suggests that any changes to the quasar color-color and color-redshifts relations will be relatively minor, and should not have a significant impact on the results presented herein.

The SDSS data analyzed herein include the photometric catalog from the four best equatorial scans that were taken between 1998 September 19 and 1999 March 22, which include data “runs” 94, 125, 752 and 756, as described in Table 1. These runs were observed and processed as part of the commissioning phase of the SDSS; they were acquired with the telescope parked on the meridian while pointed at the Celestial Equator. The density of previously known quasars is highest on the Celestial Equator, making these data particularly appropriate for this study. Runs 94 and

125 are from the south Galactic cap, whereas runs 752 and 756 are from the north Galactic cap. A fraction of the data from these runs have been re-reduced. The mean difference between the old magnitudes and the new magnitudes is (0.043, 0.008, 0.007, 0.006, 0.006) in $(u^*, g^*, r^*, i^*, z^*)$ coordinates. Since these differences are negligible, we will use the “old” magnitudes throughout for the sake of consistency.

3. Quasar Catalog

In order to study the colors of quasars in the SDSS photometric system, we first generated a (full sky) master catalog of all known quasars including the newly discovered quasars from the SDSS. We then matched the equatorial SDSS photometric catalog to the equatorial regions of the master catalog. The master quasar catalog used in this study includes quasars from four distinct sources. These four subcatalogs of quasars were combined to form a larger combined catalog. The subcatalogs are described in the following sections.

3.1. NED

One third of the quasars studied herein are previously known quasars that have been cataloged by the NASA Extragalactic Database (NED)²⁸. Our NED subcatalog includes all of the 12,987 objects that NED classified as quasars with known redshifts as of 2000 June 22. Many of these objects will also appear in the other subcatalogs discussed later.

The NED catalog is a compilation of results from the literature. Any bias in the original selection of these objects will also be manifest in this sample. One of the most important selection effects is the definition of what constitutes a quasar. Typically, quasars are defined to be active galactic nuclei (AGN) brighter than $M_B = -23$ ($H_0 = 50 \text{ km s}^{-1} \text{ Mpc}^{-1}$, $q_0 = 0.5$); however, Seyfert galaxies, the fainter cousins of quasars, are often included in compilations of quasars. Such objects from NED are included in our combined catalog for sake of completeness even though their colors may be contaminated by their host galaxy. See § 5.5 for more on this subject.

The primary input to the NED quasar catalog is the catalog produced by Hewitt & Burbidge (1989, hereafter HB89), which includes over 3500 quasars. As with the NED catalog, HB89 is itself a compilation from the literature. The largest uniform sample of quasars (~ 1000) in NED comes from the Large Bright Quasar Survey (LBQS; Hewett et al. 1995). Since LBQS quasars were selected from objective prism plates, the LBQS catalog may include quasars with stronger than average emission lines. Other optical quasar surveys that contribute significantly to the catalog of known quasars include the AAT Survey (Boyle et al. 1990), the CFHT Survey (Crampton et al.

²⁸The NASA/IPAC Extragalactic Database (NED) is operated by the Jet Propulsion Laboratory, California Institute of Technology, under contract with the National Aeronautics and Space Administration.

1988), the Second Byurakan Survey (SBS; Stepanian et al. 1993), and the Palomar Grism Surveys (Schneider et al. 1994, 1999). Not all of these surveys are color-selected surveys; each has its own selection effects. The AAT survey was an ultra-violet excess (UVX) survey and is biased towards $z < 2.2$. The CFHT survey used a blue “grens” to do slitless spectroscopy and was sensitive to $z < 3.3$. The SBS survey was an objective prism survey, whereas the Palomar Grism Surveys used a grism for candidate selection and slit spectroscopy for followup observations. Many of the radio-detected quasars in NED come from Véron-Cetty & Véron (1996), which, like HB89, is a compilation based on a variety of sources. The brightest of these objects are 3C sources (Spinrad et al. 1985), which are brighter than 9 Jy at 178 MHz.

3.2. FIRST

We have attempted to recover, in the SDSS data, quasars detected by the VLA FIRST Survey (Becker et al. 1995), in particular those discovered by the FIRST Bright Quasar Survey (FBQS; Gregg et al. 1996; White et al. 2000; Becker et al. 2001) and the FIRST Faint Quasar Survey (FFQS; Becker et al. 1998). Many of the FBQS quasars also appear in the NED catalog; however, the FBQS is an ongoing survey, so we have included these FIRST quasars explicitly. Although the SDSS will be selecting FIRST sources as quasar candidates, it is valuable to include in our sample those FIRST objects that have already been confirmed as quasars. As with the radio-selected quasars from NED, FIRST quasars are valuable because they have different selection biases than optically-selected quasars. In particular, they can be used to determine the fraction of quasars embedded in the stellar locus and to analyze the effects of reddening and extinction upon quasar target selection.

3.3. SDSS Spectroscopic Commissioning

The largest part of the sample comes from spectroscopic confirmation of quasar candidates from SDSS spectroscopic commissioning (Uomoto et al. 2001a). The SDSS uses two double fiber-fed spectrographs; each has separate red and blue cameras, with a dichroic splitting the light at $\sim 6000 \text{ \AA}$. The fibers are hand-plugged into an aluminum plate (640 fibers per plate); the correspondence between hole number and fiber number is determined by an automated plate mapper. The entire fiber, plate and slit assembly is modular and is removed and replaced for each spectroscopic exposure.

The fibers subtend $3''$ at the focal plane. The resulting spectra cover the range from 3800 \AA to 9200 \AA with a resolution of roughly 1800, over 4096 pixels. Typical exposure times are 45 minutes to an hour, broken into single exposures of 15 minutes each. Reduction on the mountain confirms that the signal-to-noise ratio of the faintest objects meets survey specifications. The wavelength calibration is appreciably better than the specifications of 0.1 \AA . The flux calibration is currently

only approximate, and is carried out with observations of F subdwarfs. The spectrographs are very high throughput, approaching 30% in the red; the resulting spectra have quite high signal-to-noise ratio, of order 4 per pixel for objects as faint as $r' = 20$.

Quasar candidates for spectroscopy were selected by a preliminary version of the SDSS Quasar Target Selection Algorithm (Newberg et al. 2001; Richards et al. 2001), which is primarily a color-selection algorithm. The primary selection criterion is that objects be outliers from the stellar locus, which means that quasars with unusual colors will be targeted. Since one of the goals of the commissioning phase of this project is to define this algorithm, the quasars selected with the current algorithm cannot be considered representative of the final SDSS quasar sample, or in any way to constitute a complete sample. In particular, these are color selected objects selected with color cuts that are not yet final (moreover the color cuts have changed with time), and the quasars do not cover a uniform area on the sky. Nevertheless, they are extremely useful for increasing our knowledge of the colors of quasars.

Quasar candidates were observed with the SDSS fiber spectrographs and the data were reduced with the spectroscopic pipeline (Frieman et al. 2001). Each of the quasar identifications and redshifts were determined by visual inspection by one of us (DEVB), since the automated reduction pipelines are not yet complete. The redshifts and photometry of these 1677 objects are not included in Table 2, but will appear in 2001 as part of a public SDSS data release. A sample of 10 SDSS quasar spectra with $0 < z < 5$ are presented in Figure 1, in order to give the reader an idea of the quality of the spectra.

3.4. SDSS Followup

The remainder of the sample includes 112 quasars discovered during the course of SDSS followup observations using the ARC 3.5m telescope at Apache Point Observatory, the Hobby-Eberly Telescope at McDonald Observatory, and the W. M. Keck Observatory. These observations are part of a number of followup projects that are underway, mostly in search of high- z quasars. Quasar candidates are selected by color and confirmed spectroscopically on these other telescopes in order to confirm objects that the SDSS spectrographs might not observe (e.g., due to faintness, fiber spacing constraints, etc.) or that the SDSS has simply not taken a spectrum of yet. Those SDSS followup objects used in this study have been published by Fan et al. (1999), Fan et al. (2000), Schneider et al. (2000), Zheng et al. (2000), Fan et al. (2001), and Schneider et al. (2001). The redshift and color distribution of this sample of quasars is summarized in the last of these references.

Nearly all of the $z \geq 3.6$ quasars in our sample are from these SDSS followup observations (which cover a larger area of sky than the SDSS spectroscopic commissioning plates). The selection of these quasars introduces a significant feature in the redshift distribution of our sample: certain regions ($3 < z < 3.6$) of color space are apparently underrepresented because of the way that high-redshift follow-up targets were selected. The selection criteria for the $z \geq 3.6$ quasars are presented

by Fan et al. (2001) and references therein.

3.5. Combined Catalog

The combination of these subcatalogs results in a total of 16,446 quasars covering the entire sky, a fraction of which are in the region covered by the SDSS commissioning data from the Celestial Equator. The distribution of quasars is as follows: 12,987 are from the NASA Extragalactic Database (NED), 941 are FIRST quasars, and 2518 were discovered or recovered as part of the SDSS. The quasars found using SDSS data are from both the spectroscopic commissioning data (2406 quasars) and from SDSS followup observations using other telescopes (112 quasars).

In order to create a combined catalog that includes each quasar only once, the NED, FIRST and SDSS subcatalogs were compared to each other. Quasars in more than one catalog whose positions agreed to $5''$ or better, whose redshifts agreed to $\Delta z = 0.1$ or better, and whose differential magnitude differed by less than 3.5 mag were considered to be matches. In all, 508 quasars were found in more than one catalog of quasars, resulting in a total of 15,938 unique quasars in the full-sky catalog.

3.6. SDSS Matches to the Combined Catalog

In four SDSS Equatorial scans studied, 2625 previously known or recently discovered quasars from the combined full-sky catalog of 15,938 quasars are found in the SDSS database. Quasars from the combined catalog were considered to be matches to the SDSS database if the positions of the quasars and the SDSS objects agreed to better than $3''$ and the agreement between the cataloged magnitudes and the SDSS magnitudes were reasonable (root-mean-square of the difference between the predicted and observed g' and r' magnitudes less than 2 magnitudes, where the predicted SDSS magnitudes have been computed by transforming the published magnitude to the SDSS system assuming a spectral index of $\alpha_\nu = -0.5$). The SDSS astrometry is good to $0.2''$ or better per coordinate. See Finlator et al. (2000), Figure 2, for a comparison of the SDSS astrometry that demonstrates this level of accuracy. An additional 235 known quasars had potential matches, but the positions disagreed by more than $3''$. Many of these matches with large positional discrepancies may be correct, but in order to avoid contamination of the empirical colors studies herein, we do not include these in our analysis.

Of these 2625 quasars, 801 are from NED (573 unique), 92 are from FIRST (50 unique), and 1983 quasars are from SDSS data (1759 unique). A total of 243 quasars were found in more than one of the above catalogs. There are more NED quasars in the area covered by these four runs; however, only these 801 had NED coordinates and photometry accurate enough to ensure that the matches to SDSS objects are correct. A more detailed (and labor intensive!) analysis would allow for the matching of additional known quasars and for the correction of their published coordinates.

A histogram of the redshift distribution of all 2625 quasars is given in Figure 2. There is a noticeable lack of quasars between $z = 2.5$ and $z = 3.6$, since the density of quasars at $z \geq 2.5$ is declining and the followup observations specifically target quasars at $z \geq 3.6$. The new SDSS quasars represent over a factor of two increase in the density of known quasars on the Celestial Equator.

The difference between the input magnitude (typically, but not always B_J) and the measured g^* magnitude for the NED and FIRST sources are plotted as a function of g^* in Figure 3. This plot enables us to check the accuracy of the cataloged magnitudes and to look for variability (e.g., Francis 1996). Photometry and astrometry for all previously published quasars (including SDSS quasars discovered during followup observations) is presented in Table 2. Data on the 1677 new SDSS quasars will be published separately as part of an official SDSS data release. Data on the 50 FIRST equatorial quasars was kindly provided in advance of publication by R. Becker and will be presented by Becker et al. (2001). The columns in Table 2 are as follows: (1) is the name of the quasar. (2) is the redshift. The right ascension and declination as measured by the SDSS are given as J2000 coordinates in (3) and (4). The difference between the SDSS position and the cataloged position is given in (5) in units of arcseconds. (6) through (10) give the measured magnitudes and errors in the five SDSS passbands. Errors are photometric errors only and do not include systematic errors, which are on the order of 0.03 mag. Reddening corrections have not been applied, but the reddening vector in $E(g^* - r^*)$ (as determined from Schlegel et al. 1998) is given in (11). The last column indicates the source catalog of each object. A “1” indicates that the object is in the NED catalog. SDSS quasars discovered during followup observations are represented by a “2”. Objects found in more than one catalog are so indicated.

Three quasars were both NED and SDSS sources, and had large discrepancies in their redshifts as reported by NED. The following quasars from NED have incorrect redshifts: UM 203, UM 183, and UM 427. Their correct redshifts as derived from SDSS spectroscopic commissioning data are 1.47, 1.14, and 1.69, respectively. We further note that PC 0036+0032 ($z = 4.51$) is not included because it is improperly classified by NED as a galaxy. Since not all previously known quasars in this area of the sky have new SDSS spectra, it is likely that there are other known quasars in this region with incorrect redshifts, or that are misclassified.

4. Quasar Colors

We present SDSS quasar color-color diagrams in Figure 4, where we plot $(u^* - g^*, g^* - r^*)$, $(g^* - r^*, r^* - i^*)$, and $(r^* - i^*, i^* - z^*)$, respectively. The black points and black countours are 10,000 stellar sources brighter than $i^* = 19$ taken from the run 745 data [Galactic $(l, b) = (248^\circ, 48^\circ)$ to $(18^\circ, 27^\circ)$], which covers approximately the same region of space as run 756. The color points are the quasars, color-coded according to their redshifts: blue points are low-redshift quasars and red points are high-redshift quasars. Only quasars whose errors are small (≤ 0.2 magnitudes each of the three relevant bands) are plotted. The solid black line is the median color-color track of the entire sample. The average Galactic reddening and an extra-Galactic (internal) reddening vector (defined in § 5.1)

are also plotted in the bottom right-hand corner of each panel in Figure 4. In each case, the uppermost vector is the average Galactic reddening vector. Throughout the paper all figures and tables (except Table 2) use magnitudes and colors that have been dereddened using the reddening maps of Schlegel et al. (1998).

The broad-band SDSS colors of quasars as a function of redshift are presented in tabular form in Table 3 and in graphical form in Figure 5. Only quasars whose errors are less than 0.1 mag (10σ detections) in each of the magnitudes that contribute to a given color are included. In each redshift bin, we measure the median colors of the quasars, as well as the limits within which 95% of the quasars lie, which we hereafter refer to as “confidence limits”. Table 3 gives the median and 95% confidence limits of the dereddened colors of quasars in the redshift bins given, plus the number of quasars per bin. In Figure 5, the black dots are point sources as seen by SDSS, whereas magenta dots are extended sources (i.e., the profile is not suitably described by a point-spread function, as determined by the SDSS photometric pipeline) with $z \leq 0.6$. The solid light blue line is the median color-redshift vector for these quasars in redshift bins of size $\Delta z = 0.05$ from $z = 0.05$ to $z = 2.1$, as reported in Table 3. Starting with $z = 2.2$ the bin size is $\Delta z = 0.2$; the $z = 2.2$ bin partially overlaps the $z = 2.1$ bin. The median color-redshift relation in Figure 5 is smoothed by 50% of the bin size for plotting purposes. We use the median to describe the color-redshift vector rather than a mean, since the median is less sensitive to outliers. The dashed red line is similar to the median color-redshift track from Fan (1999); see § 4.4 for further discussion. Two vectors are plotted as solid lines in the lower right-hand corner of each panel. The one on the left shows the magnitude of typical Galactic reddening, whereas the one on the right is representative of the change in color due to extra-Galactic reddening. These are the same vectors as in Figure 4. We discuss reddening in further detail in § 5.1.

The high quality of the data is quite apparent in Figure 4 and can be compared to similar graphs using photometry from photographic plates (e.g., Warren et al. 1991b; Irwin et al. 1991). The tightness of the stellar locus is a result of the high-quality CCD photometry. Clearly, more accurate photometric data allow quasars to be found more easily. A lack of color-degeneracy in the quasar colors as a function of redshift is apparent in the color-color (Figure 4) and the color-redshift diagrams (Figure 5). Quasars with similar redshifts tend to have the same colors, whereas quasars with different redshifts occupy different places in color space. The fact that there is so much structure in the color-redshift relation and that the scatter in the colors at a given redshift is reasonably small may allow for the determination of photometric redshifts for quasars (Richards et al. 2000). Photometric redshifts are now common practice for galaxies (e.g., Budavári et al. 2000), and have recently become possible for quasars (Wolf et al. 2000).

4.1. Theoretical Colors

We begin our analysis with a discussion of the expected colors of quasars in the SDSS photometric system. For a general introduction on the subject see Fan & Chen (1994) and Warren et al.

(1994), or Fan (1999) for a discussion specific to the SDSS. To first order, the spectra of quasars can be characterized as a power-law. A power-law spectrum has the convenient property that it has the same color at any redshift. The color of an object with flux density $f(\nu)$ is given by:

$$m_1 - m_2 = -2.5 \left(\log \frac{\int f(\nu) S_1(\nu) d \log \nu}{\int S_1(\nu) d \log \nu} - \log \frac{\int f(\nu) S_2(\nu) d \log \nu}{\int S_2(\nu) d \log \nu} \right), \quad (1)$$

where $S_1(\nu)$ and $S_2(\nu)$ are the throughput of the system in each bandpass (for a photon counting system). For the SDSS photometric system, there is no additive constant since the SDSS magnitudes are on the *AB* system (Oke & Gunn 1983; Fukugita et al. 1996). This lack of an additive constant is in contrast with the *UBVRI* system, which is Vega based; the computation of colors in the *UBVRI* system requires a correction for the fact that the spectrum of Vega is not perfectly flat in f_ν . For a flat-spectrum source ($\alpha_\nu = 0$), the colors in an *AB* system are always 0. Table 4 gives the expected SDSS colors for a range of spectral indices. The spectral indices are given in both frequency and wavelength units, where α_λ and α_ν are defined such that $\alpha_\lambda = -(2 + \alpha_\nu)$, $f_\nu \propto \nu^{\alpha_\nu}$ and $f_\lambda \propto \lambda^{\alpha_\lambda}$. Expected colors for other spectral indices can be interpolated or extrapolated from those given in Table 4.

From Figure 5 it is clear that the colors of quasars are not strictly power-laws; however, the average colors are consistent with the input power-law distribution of Fan (1999), $\alpha_\nu = -0.5 \pm 0.3$. Whereas the power-law index of the quasar spectrum sets the average colors of a quasar, the colors will deviate from this value as a result of emission and absorption features (e.g. the Lyman- α forest). To identify the nature of these discrepancies, we turn to an analysis of the expected colors of quasars using a composite SDSS quasar spectrum convolved with the SDSS transmission curves.

4.2. Composite Spectrum Colors

A composite quasar spectrum has been constructed from the early SDSS spectroscopic commissioning spectra (Vanden Berk et al. 2000; Vanden Berk et al. 2001). The composite spectrum extends from 1050 Å to 7000 Å, in the rest frame. We have convolved this spectrum with the most recent SDSS transmission curves (Fan et al. 2001, Appendix A). The resulting color-redshift tracks for the composite spectrum are presented in Figure 6.

In Figure 6 the solid blue line is the color-redshift track of the composite spectrum. For comparison, we also re-plot the empirical median color-redshift tracks from Figure 5 (solid black line) and the expected colors from a power-law spectrum of the form $f_\nu \propto \nu^{-0.5}$ (dashed black line; see Table 4). The remaining lines in Figure 6 show what happens when a given emission feature is cut out of the composite spectrum and is replaced with a power-law, i.e. each emission line is removed from the composite spectrum, then the flux values in the wavelength range removed are replaced by a power-law spectrum of the form $f_\nu \propto \nu^{-0.3}$ normalized at 1450 Å, which is a good fit to the composite spectrum (Vanden Berk et al. 2000; Vanden Berk et al. 2001). A small additive constant was also required to make the spliced region fit into the spectrum cleanly. Since

the strength of the Lyman- α forest is a function of redshift and because the composite does not cover the entire optical spectrum for $0 < z < 5$, the ends of the composite spectrum are padded with the average value between 1050 and 1150 Å at the blue end, and 7000 and 8000 Å at the red end. As a result, the absolute colors may not be accurate in the blue colors at high redshift and in the red colors at low redshift. Figure 6 displays what happens when Lyman- α , C IV, Mg II, H β , H α , or the small blue (λ 3000) bump (SBB) are removed. In § 4.4, we will demonstrate the effect that a strong emission line has on the colors of an otherwise power-law spectrum. A knowledge of this effect is helpful to understanding the results in the next section.

4.3. Empirical Colors

The color-redshift relations of quasars in the SDSS bandpasses exhibit considerable structure. We attempt to describe the causes of the features in the color-redshift diagrams. Features in the color-redshift relations are identified by comparing the results from the composite spectrum above (Figure 6) to the measured colors of quasars (Figure 5). All colors used for this analysis are dereddened colors. The emission lines that significantly affect the broad-band colors include Lyman- α , C IV, Mg II, H α , H β , and the λ 3000 bump. The λ 3000 bump consists of Balmer continuum emission and Fe II emission features (Grandi 1982; Peterson 1997). The feature starts at approximately 2300 Å and extends to approximately 3800 Å. The Mg II emission line is nearly centered between these ranges, and contributes significantly to color changes as a function of redshift since it sits on top of the λ 3000 bump.

We identify each of the significant features in the color-redshift curves. Many of the features in the color-redshift relation are caused by more than one feature in the quasar spectrum interacting with the transmission curves. A more detailed understanding of the causes of deviations from power-law colors can be obtained by comparing Figure 6 to Figure 5. Understanding the causes of the color-redshift features is interesting in and of itself, but also is helpful for determining sample completeness for objects with particularly weak or strong emission features.

4.3.1. u' - g'

$z \sim 0.1$ to 0.4 — The colors in this region of redshift have a considerable range; the range is much larger than for the redder SDSS colors. A comparison of the composite spectrum colors to the composite spectrum colors without the λ 3000 bump reveals that some of this range could be due to objects having a wide range of λ 3000 bump strengths, but see § 5.1 for another explanation.

$z \sim 0.3$ — The λ 3000 bump and Mg II are in u' , and cause the color to be blue.

$z \sim 0.6$ — The λ 3000 bump and Mg II are in g' , making the color red.

$z \sim 1.3$ — C IV is in u' and shifts the color to the blue.

$z \sim 1.6$ — Lyman- α is entering u' , while C IV is leaving u' and entering g' .

$z \sim 1.9$ — Lyman- α is in u' , but the effect is tempered by the presence of C IV in g' . The strength of Lyman- α dominates nevertheless, causing a blue dip.

$z \sim 2.3$ to 2.4 — A small plateau-like feature is caused as C IV leaves g' shortly after Lyman- α enters g' .

$z > 2.6$ — The u' - g' color rises rapidly as the Lyman- α forest and Lyman-limit systems cause there to be little or no flux in the u' band.

4.3.2. g' - r'

$z \sim 0.2$ to 0.3 — The presence of H β in r' keeps the average color relatively red.

$z \sim 0.5$ — The $\lambda 3000$ bump is mostly in g' , causing the color to be blue. As with the $z < 0.4$ region in u' - g' , there is evidence for a population of redder objects.

$z \sim 1.2$ — The combination of Mg II and the $\lambda 3000$ bump in r' cause a reddening near this redshift.

$z \sim 1.75$ — The $\lambda 3000$ bump and C IV offset each other as the latter enters g' and the former leaves r' .

$z \sim 2.1$ — The presence of C IV in g' keeps the color bluer than a power-law.

$z \sim 2.5$ to 3.5 — The C IV line pushes the color to the red, whereas Lyman- α pushes the color to the blue. As the redshift increases more and more of the Lyman- α forest enters g' and the color reddens.

$z > 4.0$ — The g' - r' color rises rapidly as the Lyman- α forest and Lyman-limit systems cause there to be little or no flux in the g' band.

4.3.3. r' - i'

$z \sim 0.1$ to 0.2 — H α is in i' and makes the color redder than the average power-law value.

$z \sim 0.3$ — The presence of H β in r' drives the color blueward, which is enhanced when H α leaves r' .

$z \sim 0.5$ — The color moves back to the red while H β is in i' .

$z \sim 0.9$ — The $\lambda 3000$ bump fills the r' filter making the color bluer.

$z \sim 1.2$ — A small kink in the median colors is noticeable here as the $\lambda 3000$ bump and Mg II trade off in influence in the r' filter.

$z \sim 1.4$ to 1.5 — The color makes a sharp transition from blue to red as Mg II leaves r' and enters i' .

$z \sim 1.65$ — A small kink in the median colors is noticeable here as the $\lambda 3000$ bump and Mg II trade off in influence in the i' filter.

$z \sim 1.8$ — A small hump is caused as both Mg II and the $\lambda 3000$ bump push the color redward.

$z \sim 2.0$ to 2.5 — The color is driven back to the blue as the $\lambda 3000$ bump leaves i' .

$z \sim 2.6$ to 3.4 — C IV keeps the color blue, when it would otherwise have reddened.

$z \sim 3.4$ to 4.4 — Lyman- α and C IV offset each other during the period when the former is in r' and the latter is in i' .

$z > 4.5$ — The $r'-i'$ color rises rapidly as the Lyman- α forest and Lyman-limit systems cause there to be little or no flux in the r' band.

4.3.4. $i'-z'$

$z \sim 0.2$ — H α is in i' and keeps the color blue.

$z \sim 0.3$ to 0.4 — H α has moved into z' , causing an abrupt reddening.

$z \sim 0.6$ — H β is in i' , whereas H α is leaving z' , resulting in a blue color.

$z \sim 0.8$ — H β has moved into z' and causes the color to become redder.

$z \sim 1.2$ — The $\lambda 3000$ bump in i' drives the color blueward.

$z \sim 1.9$ to 2.1 — Mg II moves from i' to z' , causing an abrupt reddening.

$z \sim 2.1$ to 2.5 — As with the $z \sim 1.7$ feature in $r'-i'$, a small red hump is formed as both Mg II and the $\lambda 3000$ bump push the color to the red.

$z \sim 3.4$ to 4.2 — C IV keeps the color bluer than the average power-law color.

$z \sim 4.4$ to 5.0 — Lyman- α and C IV offset each other as C IV pushes the color redward at the same time that Lyman- α pushes the color blueward.

4.4. Comparison of Expected and Measured Colors

To characterize the differences between the expected colors of a power-law and the empirical colors of quasars, it is instructive to know what effect the profile of a strong emission line has on the colors of quasars as the line is redshifted through each of the filters. Figure 7 shows what happens when a top hat emission line with an observed equivalent width of 200 \AA that is 20 \AA wide

is redshifted through each of the filters. The emission line starts centered at 3000 \AA ($z = 0$) where the u' filter begins and ends at $11,500 \text{ \AA}$ ($z = 2.833$) where the z' filter ends. The four curves are $u'-g'$, $g'-r'$, $r'-i'$, and $i'-z'$, respectively, with $u'-g'$ being the curve in the lower left. These features are similar to the effect that the Lyman- α emission line has on the broad-band colors of quasars. Note the similarity of the dip in u^*-g^* near $z = 1.9$ in Figure 5 to the dip near $z = 0.2$ in Figure 7.

A broad feature, such as is characterized by Fe II emission, has a similar profile, although the slope of the color change between bandpasses is less striking. It is particularly interesting that a relatively weak, but broad emission features such as the Fe II complexes can have an equal effect to that of strong, narrow emission feature such as Lyman- α . The total equivalent width within the bandpass matters much more than the manner in which that equivalent width is distributed, since the bandpasses are broad. For example, note the similarity of the r^*-i^* colors from $z = 0.6$ to $z = 2.4$ and the i^*-z^* colors from $z = 0.8$ to $z = 3.0$ in Figure 5 to the $r' - i'$ and $i' - z'$ shapes, respectively, in Figure 7. These features are produced by a combination of the $\lambda 3000$ bump and Mg II emission.

One of the most powerful uses of this analysis is the refinement of the simulated quasar spectrum, which, in turn, tells us about the empirical properties (spectral indices, emission line equivalent widths, etc.) of quasars. Fan (1999) calculated theoretical colors of quasars in the SDSS filter system as a function of redshift. Although these simulated colors are correct to first order (they correctly reproduce the colors of quasars on the ensemble average), there are deviations from the average that have a significant impact upon the colors of quasars as a function of redshift. The simulated quasar color-redshift track shown in Figure 5 is similar to that of Fan (1999), but uses a larger equivalent width for the Fe II features, and the updated filter curves. This theoretical color-redshift relation matches the observed color-redshift relation surprisingly well. While the simulation does indeed fit the data quite well, there are still regions of color-redshift space where the simulations and the data do not agree well.

4.4.1. The $\lambda 3000$ Bump

One piece of information that we can glean from a comparison of the simulated color-redshift tracks to the observed tracks is the structure of the $\lambda 3000$ bump. The quality of the digital photometry provided by the SDSS allows us to determine the structure of this spectral feature without having to examine any spectra. Such an analysis is of particular interest given the role that the $\lambda 3000$ bump plays in the spectra of quasars (Netzer et al. 1985).

Some of the most notable deviations of the empirical colors from the simulated colors occur at $z = 1.0$ and $z = 1.4$ in r^*-i^* and i^*-z^* , respectively. The sharp break in the simulated colors from Figure 5 is caused by the fact that the Fe II emission surrounding the Mg II emission line has been modeled as two distinct features following Francis et al. (1991). However, a comparison with the empirical color-redshift track shows that the two bumps on either side of Mg II actually

combine to form an apparent continuum, such that Mg II lies well above the power-law continuum level. As a result, the regions surrounding Mg II emission are not representative of the power-law continuum spectrum. In addition to the merging of what Francis et al. (1991) call “Fe II feature 2” and “Fe II Feature 3”, it is also quite possible that “Fe II Feature 1” (longward of C IV emission) merges with both of these, and that the dip near 2200 Å in the flux of composite quasar spectra is caused by dust (Richstone & Schmidt 1980, but see Oke et al. 1984 for a counter-argument).

The effect of the $\lambda 3000$ bump at $z \leq 0.6$ is also quite evident. For r^*-i^* and i^*-z^* the colors of quasars are very tight at $z \leq 0.6$. There is considerable variation as a function of redshift, but very little scatter at a given redshift. This is not the case for u^*-g^* and g^*-r^* , where there is a large range of colors. A possible explanation is that quasars can exhibit a broad range of strength in the $\lambda 3000$ bump at low redshifts. A closer examination of the definition of a quasar at low redshift is warranted (see § 5.5 for more details and another possible explanation).

4.4.2. C IV

There are significant differences between the simulated and measured colors of quasars in the redshift ranges affected by C IV. Note in particular the $z \sim 1.3$ region in the u^*-g^* panel and the $z \sim 2.1$ region in the g^*-r^* panel of Figure 5 and Figure 6. A possible explanation for these discrepancies is that the assumed equivalent width for C IV is considerably smaller than the average equivalent width of C IV in our sample. This is surprising because the C IV equivalent width in the simulation is taken from the LBQS composite quasar spectrum (Francis et al. 1991), and LBQS quasars contribute significantly to our sample. However, as with Mg II and the $\lambda 3000$ bump, C IV may be influenced by other emission, in particular lines of Fe II ($\lambda 1700$ to 2200 Å), He II $\lambda 1640$, and O III] $\lambda 1663$. To the extent that these lines are missing from the simulations, the simulations will deviate from the empirical colors.

4.4.3. H α

A particularly useful diagnostic can be made from the effect of H α on the broad-band colors of SDSS quasars. That this is the case can be seen at $z \sim 0.2$ in the i^*-z^* of Figure 5. The deviation of the simulated colors of Fan (1999) from the observed colors is caused by the fact that the simulations used the original transmission curves. It is now known that the true transmission curves deviate somewhat from those originally reported (Fan et al. 2001). The sharpness of the color-redshift feature in i^*-z^* due to H α can be used as a diagnostic throughout the course of the Survey. Small changes in the transmission curves can be monitored as a function of time and as a function of CCD chip in the camera.

5. Discussion

The primary purpose of this investigation of the empirical colors of quasars in the SDSS photometric system is to aid in the selection of quasars for spectroscopic observations during the course of the Sloan Digital Sky Survey. There are a number of complex issues involved in the selection of quasars in the most complete and efficient manner. The data presented herein provides a wealth of information that can be used to address a number of topics. We now turn to a discussion of some of the more important issues.

5.1. Reddening

Although the photometry presented herein has been corrected for Galactic reddening using the reddening maps of Schlegel et al. (1998), it is important to understand how much effect Galactic reddening has on the colors of quasars. The average Galactic reddening vector for the quasars in our sample is $(0.055, 0.042, 0.027, 0.024)$ in $(u^*-g^*, g^*-r^*, r^*-i^*, i^*-z^*)$ coordinates. These vectors are plotted to scale as the left-most of the two vectors in the lower right-hand corner of the color-redshift curves in Figure 5 and the upper-most of the two vectors in the lower-right hand corner of the color-color plots in Figure 4. At low Galactic latitudes, Galactic reddening can be considerably more significant (c.f., Fan 1999, Figure 5).

In contrast to Galactic reddening, little is known about inter-galactic reddening and reddening internal to quasars. Although it has been suggested that a significant fraction of quasars may be reddened, and therefore missed in flux-limited surveys (e.g., Fall & Pei 1993; Francis et al. 1999), it is difficult to know exactly how prevalent internal reddening is and to what extent it effects the broad-band colors of quasars. Close examination of the color-redshift relations in Figure 5 reveals that the spread in colors around the median color as a function of redshift is much larger for u^*-g^* than for the other colors. Moreover, the scatter is asymmetric, in the sense expected for reddening.

To quantify this effect, we subtract the median colors given in Table 3 at each redshift from the colors of the quasars shown in Figure 5 (i.e., those with small photometric errors) with $0.4 < z < 3.0$, and examine the residual colors. Quasars that are classified as extended (as opposed to point sources) are excluded to avoid contamination from the host galaxy. Low-redshift objects are excluded to avoid confusion with Seyfert galaxies. High-redshift objects are excluded due to a relative paucity of data. Histograms of the residual colors are given in Figure 8. Note the red tail in the distribution of u^*-g^* , and, to a lesser extent, g^*-r^* . In order to determine the cause of this tail, we have created additional diagnostic plots.

The residual colors are plotted as a function of magnitude in the four panels of Figure 9, as a function of redshift in the four panels of Figure 10, and as a function of absolute magnitude ($q_0 = 0.5$, $H_0 = 65 \text{ km sec}^{-1} \text{ Mpc}^{-1}$) in Figure 11. Except for Figure 10 and Figure 11, Figures 8 to 12 exclude all quasars with $z < 0.4$. Two-sigma error bars for objects with magnitude 20 (in

the bandpass given) are plotted in Figure 9. Note that the scatter blueward of the median colors ($\equiv 0$) for each pair of filters is less than the amount of scatter redward of the median colors. This scatter increases towards the red with fainter magnitudes, is more pronounced in the bluer colors, and is independent of redshift.

Such an effect is quite likely the result of reddening of the quasars, either external or internal, but certainly extra-Galactic; the fact that the reddening is independent of redshift points towards internal reddening over external reddening, since external reddening would depend on the volume of space enclosed at a given redshift. Table 5 gives the blue and the red one-sided 95% confidence deviations in each of the median-corrected colors for those objects brighter than $i^* = 21$ and whose errors in each band are less than 0.1 mag. Also given are the corresponding values of spectral index.

We further demonstrate the reddening of some objects in Figure 12 where we plot the corrected colors against each other; typical errors are given in the upper right hand corner of each panel. The vector in each of the panels is the absolute value of the *blue* 95% confidence limit from Table 5. Objects whose red color excess is comparable to or larger than the absolute value of the blue 95% confidence limit given in Table 5 show signs of reddening beyond what is expected from Galactic dust. The difference between the absolute value of the blue 95% confidence limit given in Table 5 and the red 95% confidence limit given in Table 5 yields an estimate of the amount of extra-Galactic reddening. The resulting vector, (0.193, 0.129, 0.037, 0.038), is the extra-Galactic reddening vector used in Figure 4 and Figure 5. This vector is similar in direction to the Galactic reddening vector.

We have defined a sample of 26 “reddened” quasars, which are those quasars whose red color excess in u^*-g^* , g^*-r^* , and r^*-i^* lie outside the blue 95% confidence interval. Nearly half of these are radio sources, as we discuss below in Section 5.3. Some examples of these “red” quasars are given in Figure 13, which presents 10 of the 20 red quasars for which we have SDSS spectra. We show these spectra in order to demonstrate that these objects are truly redder than the average and are not simply the result of photometric errors, etc. Note that these spectra contain some Broad Absorption Line (BAL) quasars and many have strong, narrow absorption lines. These spectra can be compared to those presented in Figure 1, which shows the spectra of 10 more normal SDSS quasars spanning a range in redshift from $z \sim 0$ to $z \sim 5$.

The extent of the reddening in these quasars is a function of the assumed reddening curve. Whether the reddening is internal or external, features such as the 2200 Å bump (Mathis 1994) which is typically associated with reddening from dust grains, may influence the colors in a non-linear manner. If the reddening is internal, it may come from depletion by material associated with the torus of gas and dust that is thought to surround the central quasar engine; if this is the case, reddening might be used as an orientation indicator for quasars that are not radio-detected. Reddening might also arise in the quasar host galaxy or in other galaxies along the line of sight.

Reddened quasars can have colors that can be well removed from the predicted location of quasars in color-color space. Color-selected surveys may select against such quasars. Note in particular the dearth of faint red quasars in the upper right-hand panel of Figure 9. If there is

a significant population of reddened quasars, they may constitute the optical counterparts of the remainder of the hard X-ray background that have hitherto gone undetected (Brandt et al. 2000; Mushotzky et al. 2000).

5.2. Spectral Index Distribution

Table 5 gives the blue and red one-sided range in spectral index (95% confidence) needed to produce the observed range of colors. If the blueward scatter in the colors is representative of the true (unreddened) scatter in optical spectral index, the spectral index distribution of the sample is approximately $\alpha_\nu = \pm 0.65$ (95% confidence), where the error gives the range of values that includes 95% of sources with colors bluer than zero. Note that we have not determined the average spectral index from the data, but instead use $\alpha_\nu = -0.5$, which is typically used for the optical spectral indices of quasars and is not a bad fit to the data (Vanden Berk et al. 2001). A determination of the exact value of the average spectral index would require a large region of quasar spectra to be devoid of emission lines, which is not the case in the UV/optical part of the spectrum.

Another conclusion that may be drawn from Figure 10 is that the scatter in the colors of quasars at a given redshift must be primarily due to the range of optical spectral indices of the individual quasars. If the scatter in the colors was instead dominated by the strength of emission lines, then we would expect that this scatter would be a stronger function of redshift. In addition, as noted by Warren et al. (1994), a large intrinsic range of quasar spectral indices will blur the calculations of the luminosity function. Extrapolation of a magnitude to a different band using the wrong spectral index will give the wrong magnitude in the new band. For the observed range of spectral indices, the range of absolute g^* magnitudes at $z = 2$ given a selection function based on observed i^* magnitudes is $\Delta M_{g'} = 0.89$.

5.3. Radio Sources

Although the vast majority of the quasars that the SDSS finds will be color-selected quasars, many will be radio-selected. All FIRST sources with point-like optical counterparts and $i^* < 19$ will be targeted as quasar candidates. Targeting these radio-detected sources will assist in the determination of the completeness of our color-selected sample; using these objects, we will be able to test whether a significant fraction of quasars is being missed. At the present time, however, our sample of radio-detected quasars is not large enough to determine if the color-redshift distribution of these quasars are significantly different from that of color-selected objects.

We can, however, comment on the ensemble average of the colors of these quasars. For radio sources only, the blue scatter in the median corrected colors is consistent with scatter of ± 0.64 in the spectral index (95% confidence). The scatter of the colors to the blue is not significantly different from the distribution of the sample as a whole. On the other hand, the 95% confidence

limit in the red scatter requires spectral indices redder than $\alpha_\nu = -1.5$, which is considerably redder than the sample as a whole. This result is consistent with the fact that many (12 of 26) of the reddened quasars discussed above are FIRST radio sources.

5.4. UVX Color Selection

Since the colors of $z < 2.2$ quasars are dominated by the continuum power-law spectrum, it is expected that the UVX selection technique for these quasars should be relatively complete, i.e. their median colors are generally significantly bluer than the $u'-g'$ selection criterion. However, from Figure 5 we see that the u^*-g^* color of $z \leq 2.2$ quasars can, in fact, be as red as or redder than $u^*-g^* \sim 0.6$. Quasars with $z \sim 0.1, 0.6, 1.6$, and 2.2 can have colors close to the UVX cutoff. As such, it is *not* possible to assume that the UVX technique is complete. Flux-limited samples will indeed be incomplete near the flux limit as a result of larger scatter in the colors at the faint end of the distribution, and this incompleteness is a function of redshift. For example, Hawkins & Veron (1993) have suggested that the fall-off in the number density of faint quasars as found by UVX quasar surveys such as Boyle et al. (1988) could be a result of this effect. One way to test this is to conduct a survey of faint quasar candidates to a limiting g' magnitude of ~ 22 (comparable to previous surveys) and compare the luminosity function of quasars in redshift regimes where median $u'-g'$ colors are much bluer than the UVX cutoff to those quasars in redshift regimes where median $u'-g'$ colors are very close to the UVX cutoff. Such a project would have to be conducted as a follow-up study to the SDSS using the data from the SDSS equatorial region in the South Galactic Cap which will be imaged multiple times.

Additional problems with UVX quasar selection arise as a result of the colors of stars. At very bright magnitudes ($g^* \sim 16$) there is very little stellar contamination in the UVX regime. However, at fainter limits, there is significant contamination of UVX quasars by stars, due to the metal-poor halo population. Figure 14 plots a color-magnitude diagram of blue stellar sources (as black contours and black points) from run 756, camera column 3. At the bright end, the majority of the blue objects will be quasars, with some contamination from white dwarfs. As g^* gets fainter, there are more and more stars that have blue colors. This is partly due to increasing photometric error at fainter magnitudes, but it is also likely to be the result of shifts in the stellar locus as a function of magnitude (and therefore metallicity) as discussed by Newberg et al. (1999) and Finlator et al. (2000). The blue extension of the contours would only be half as large if the observed effect was purely due to larger photometric errors at fainter magnitudes. The horizontal line in Figure 14 gives the g^* magnitude for a limiting magnitude of $i^* = 19$ assuming a power-law spectrum of $\alpha_\nu = -0.5$. The vertical line gives an approximate cutoff for UVX color selection (the actual SDSS color selection is done in 3-D color space and does not use this cut explicitly). To the limiting magnitude of the low- z SDSS quasar survey ($i^* \sim 19$), the shifting of the stellar locus as a function of metallicity should have little effect upon the efficiency of quasar target selection at $z \leq 2.2$.

Futhermore, it is important to realize that the limiting magnitude of a sample is a function of

the color of the sources. For example, note the decrease in faint, red sources in Figure 14. This dearth is a result of the fact that objects selected to $g^* = 22$, must be bluer than $u^*-g^* = 0.3$ in order to be brighter than the u^* “plate limit” of $u^* \sim 22.3$. Thus a sample that includes objects as red as $u^*-g^* = 0.8$ can only be considered to be complete to $g^* = 21.5$.

5.5. Extended Objects

One of the many interesting questions that we can address with the SDSS quasar sample is whether quasars and Seyferts form a continuum, or whether they represent physically distinct classes of objects. To address this issue it is necessary to target both point sources and extended sources when looking for quasars; the SDSS quasar target selection algorithm will not explicitly distinguish between quasars and Seyferts. However, it is equally important that we not target too many normal galaxies during the process of looking for quasars. As such, we must understand what regions of color space are populated by quasars with unresolved image profiles.

In our sample, extended source quasars are typically redder than point source quasars by ~ 0.2 in both u^*-g^* and g^*-r^* . In r^*-i^* and i^*-z^* the colors of extended and point sources are more similar. That this is the case can be seen in Figure 5, where we plot as magenta points those $z \leq 0.6$ “quasars” that are flagged as extended objects in the SDSS database. The discrepancy in colors could have a number of origins, the most likely is that the extended sources are redder in the blue colors because of contamination from starlight from the quasar host galaxies. Such an effect could also be due to the strength of the small blue bump in low-redshift AGN; we intend to investigate this possibility in future spectroscopic samples. Another possibility is that high-luminosity AGN are more able to blow away dust in their vicinity and are therefore not as reddened. The SDSS sample will eventually cover enough area to assemble a large sample of high-luminosity low-redshift quasars, for comparison with the far more numerous low-luminosity low-redshift quasars. This will allow us to directly test the hypotheses of host galaxy contamination and luminosity- or redshift-dependent reddening.

We further investigate these possibilities by studying the colors of the objects in our sample as a function of absolute g^* magnitude. Seyferts are typically defined as AGN that are fainter than $M_B = -23$ and have broad emission lines. Whether or not this definition represents a distinction between two physically separate classes of objects is not at all clear (Schmidt & Green 1983). Furthermore, Seyfert 2s, like Seyfert 1s have $M_B > -23$, but relatively narrow emission lines. It is an open question whether a population of “Quasar 2s” exists with space density relative to normal quasars comparable to the relative space density of Seyfert 2s and Seyfert 1s. If not, this may represent a physical, luminosity-dependent difference between these classes of objects. Throughout, we refer to Seyfert 1s simply as Seyfert galaxies.

The problem with using $M_B = -23$ as the dividing line between quasars and Seyferts is that in any single survey with an optical flux limit, it is predominantly a division in redshift. At high

redshift, the limiting magnitude of a sample causes a selection effect such that only quasars that are intrinsically bright are found. At low redshift, intrinsically faint objects are bright enough to make it into the sample; however, the volume of space sampled is so small that very few intrinsically bright objects are found. A selection criterion based on absolute magnitude is therefore essentially a redshift cut.

We test to see if the traditional dividing line between quasars and Seyferts is appropriate, and if so, physical. If there exists a correlation between the absolute magnitude and the median-corrected colors, then it might be possible to use colors to discriminate quasars from Seyferts. We ask if there is any such evidence that the colors of quasars are a function of absolute magnitude.

The average absolute magnitude of quasars in our sample is a steep function of redshift for $z < 1$, so we cannot simply ask if the colors of all $z < 1$ quasars are a function of absolute magnitude. However, if we limit ourselves to small regions of redshift space, then we can assume that the average absolute magnitude is not changing across the (small) redshift bin. We have broken our low-redshift data set into redshift slices of $\Delta z = 0.1$ from $z = 0.1$ to $z = 0.6$. We find that within these redshift slices there is a correlation between the color and the absolute magnitude.

Since the average M_{g^*} changes significantly from bin to bin, we cannot simply make a plot of M_{g^*} versus color for the entire redshift range. Instead we have chosen to subtract the average M_{g^*} in each redshift bin and then stack the results for each of the six redshift slices. The result is Figure 15. Here we plot the *residual* color versus the *normalized* absolute magnitude for objects with $0.1 \leq z \leq 0.6$. If the colors of these objects were *not* a function of absolute magnitude, then the colors would be scattered around a color of zero. Instead we see that there is a strong correlation as a function of absolute magnitude in the sense that brighter objects (more negative normalized absolute magnitude) tend to be bluer. Furthermore, the redder objects have a tendency to be extended sources as might be expected if the fainter sources have a larger fraction of their light coming from the stars of the host galaxy. No such color-magnitude correlation is seen for a control sample of higher luminosity objects at higher redshift, again as expected if host galaxy contamination is the cause.

We conclude the following from Figure 15. Quasars and Seyfert galaxies form a continuum of properties. There is no apparent break in the color properties of quasars as function of absolute magnitude that would suggest a real physical difference between quasars and Seyfert galaxies. However, we do find that a cut in absolute magnitude at or near $M_{g^*} \approx -23$ does exclude most of the extended sources from the quasar sample and that extended sources are significantly redder than point sources (in the blue colors). This distinction might be due to a physical difference in the strength of the 3000Å bump between Seyferts and quasars, or due to the fact that the former have a larger contribution from their host galaxies. Arguing against the latter is the fact that the correlation between color and absolute magnitude holds for unresolved objects as well. More work is required to fully understand Figure 15 and what it says about the differences between low- and high-luminosity AGN.

6. Conclusions

We have presented an empirical investigation of the colors of 2625 quasars ($0.04 \leq z \leq 5.28$) in the SDSS photometric system. The number of quasars with accurate photometry that will result from the Sloan Digital Sky Survey will spur significant advances in quasar science in the coming years. The quality of the photometry allows for investigations that have hitherto been reserved for spectroscopic analysis. The combination of SDSS photometry and spectroscopy together will enable the resolution of a number of issues that currently perplex the quasar community. We have addressed some of those issues herein and have drawn the following conclusions.

Quasar colors vary significantly as a function of redshift, yet at a given redshift, the distribution of colors is surprisingly narrow. In four dimensional color space, the colors of quasars are largely non-degenerate as a function of redshift. As a result, it may be possible to determine photometric redshifts for quasars, even at low redshifts.

Typical colors of quasars are consistent with a distribution of spectral indices centered on $\alpha = -0.5$ with a spread of ± 0.65 (95% confidence). We find that the scatter in the colors of quasars at a given redshift must largely be due to a range of spectral indices as opposed to a range of emission line strengths, since the scatter is mostly independent of redshift for $z > 0.5$. However, strong emission lines such as Lyman- α , C IV, Mg II, H β , H α , and even the $\lambda 3000$ bump can have a significant affect upon the broad-band colors of quasars. At low redshift, there is a larger scatter in the colors of quasars in the blue colors. This scatter may result from a wider range of strengths of the $\lambda 3000$ bump in low-redshift, low-luminosity quasars, and/or the low-redshift sample may be significantly contaminated by stellar light from the host galaxies.

Our sample shows no significant break in the colors of lower luminosity quasars (Seyfert galaxies) as compared to higher luminosity objects. However, we do find that lower luminosity quasars are redder than their higher luminosity counterparts for $0.05 < z < 0.65$. We find that the effect of using the traditional dividing line of $M_B = -23$ to separate the populations is to exclude all of the lowest redshift AGN and most of those that are contaminated by stellar light from the host galaxy. However, it is unclear if this division is physical or simply observational.

Finally, we have discovered a statistical sample of reddened quasars. We find that the number of quasars with colors appreciably redder than the median is larger than might be expected in the absence of reddening. This reddening is probably not the result of stellar light from the host galaxy or absorption from intervening galaxies, since the reddening is not a function of redshift. Instead the observed reddening is probably internal to the quasars. Further examination of these quasars on an individual and on a group basis is in progress.

The Sloan Digital Sky Survey²⁹ (SDSS) is a joint project of The University of Chicago, Fermi-

²⁹The SDSS Web site is <http://www.sdss.org/>.

lab, the Institute for Advanced Study, the Japan Participation Group, The Johns Hopkins University, the Max-Planck-Institute for Astronomy, New Mexico State University, Princeton University, the United States Naval Observatory, and the University of Washington. Apache Point Observatory, site of the SDSS, is operated by the Astrophysical Research Consortium (ARC). Funding for the project has been provided by the Alfred P. Sloan Foundation, the SDSS member institutions, the National Aeronautics and Space Administration, the National Science Foundation, the U.S. Department of Energy, Monbusho, and the Max Planck Society. The Hobby-Eberly Telescope (HET) is a joint project of the University of Texas at Austin, the Pennsylvania State University, Stanford University, Ludwig-Maximilians-Universität München, and Georg-August-Universität Göttingen. The HET is named in honor of its principal benefactors, William P. Hobby and Robert E. Eberly. This research has made use of the NASA/IPAC Extragalactic Database (NED) which is operated by the Jet Propulsion Laboratory, California Institute of Technology, under contract with the National Aeronautics and Space Administration. DPS and GTR acknowledge support from NSF grant AST99-00703. XF and MAS acknowledge support from Research Corporation, NSF grants AST96-16901 and AST-0071091, the Princeton University Research Board, and a Porter O. Jacobus Fellowship. We thank Sofia Kirhakos and Emily Leibacher for their assistance in an early stage of this project. We thank Bob Becker for providing data in advance of publication. We thank Pat Hall and David Weinberg for critical readings of the manuscript and for the resulting improvements.

REFERENCES

- Annis, J. A., et al. 2001, in preparation
- Becker, R. H., White, R. L., & Helfand, D. J. 1995, *ApJ*, 450, 559
- Becker, R. H., et al. 1998, *BAAS*, 192, 11.01
- . 2001, in preparation
- Boyle, B. J., Fong, R., Shanks, T., & Peterson, B. A. 1990, *MNRAS*, 243, 1
- Boyle, B. J., Shanks, T., & Peterson, B. A. 1988, *MNRAS*, 235, 935
- Brandt, W. N., et al. 2000, *AJ*, 119, 2349
- Budavári, T., Szalay, A. S., Connolly, A. J., Csabai, I., & Dickinson, M. 2000, *AJ*, 120, 1588
- Crampton, D., Janson, T., Durrell, P., Cowley, A. P., & Schmidtke, P. C. 1988, *AJ*, 96, 816
- Doi, M., et al. 2001, in preparation
- Fall, S. M. & Pei, Y. C. 1993, *ApJ*, 402, 479
- Fan, X. 1999, *AJ*, 117, 2528
- Fan, X. & Chen, J. 1994, *Chinese Astron. Astrophys.*, 277, L5
- Fan, X., et al. 1999, *AJ*, 118, 1
- . 2000, *AJ*, 119, 1
- . 2001, *AJ*, in press
- Finlator, K., et al. 2000, *AJ*, 120, 2615
- Francis, P., Whiting, M., & Webster, R. 1999, *BAAS*, 194, 113.01
- Francis, P. J. 1996, *Publications of the Astronomical Society of Australia*, 13, 212
- Francis, P. J., Hewett, P. C., Foltz, C. B., Chaffee, F. H., Weymann, R. J., & Morris, S. L. 1991, *ApJ*, 373, 465
- Frieman, J., et al. 2001, in preparation
- Fukugita, M., Ichikawa, T., Gunn, J. E., Doi, M., Shimasaku, K., & Schneider, D. P. 1996, *AJ*, 111, 1748
- Grandi, S. A. 1982, *ApJ*, 255, 25

- Green, R. F., Schmidt, M., & Liebert, J. 1986, *ApJS*, 61, 305
- Gregg, M. D., Becker, R. H., White, R. L., Helfand, D. J., McMahon, R. G., & Hook, I. M. 1996, *AJ*, 112, 407
- Gunn, J. E., et al. 1998, *AJ*, 116, 3040
- Hawkins, M. R. S. & Veron, P. 1993, *MNRAS*, 260, 202
- Hewett, P. C., Foltz, C. B., & Chaffee, F. H. 1995, *AJ*, 109, 1498
- Hewitt, A. & Burbidge, G. 1989, *ApJS*, 69, 1
- Irwin, M., McMahon, R. G., & Hazard, C. 1991, in *ASP Conf. Ser. 21: The Space Distribution of Quasars*, ed. D. Crampton (San Francisco: ASP), 117
- Kent, S., et al. 2001, in preparation
- Lupton, R. H., Gunn, J. E., & Szalay, A. S. 1999, *AJ*, 118, 1406
- Lupton, R. H., et al. 2001, in preparation
- Mathis, J. S. 1994, *ApJ*, 422, 176
- Mushotzky, R. F., Cowie, L. L., Barger, A. J., & Arnaud, K. A. 2000, *Nature*, 404, 459
- Netzer, H., Wamsteker, W., Wills, B. J., & Wills, D. 1985, *ApJ*, 292, 143
- Newberg, H. J., Richards, G. T., Richmond, M., & Fan, X. 1999, *ApJS*, 123, 377
- Newberg, H., et al. 2001, in preparation
- Oke, J. B. & Gunn, J. E. 1983, *ApJ*, 266, 713
- Oke, J. B., Shields, G. A., & Korycansky, D. G. 1984, *ApJ*, 277, 64
- Peterson, B. M., ed. 1997, *An Introduction to Active Galactic Nuclei* (Cambridge, New York: Cambridge University Press)
- Petravick, D., et al. 1994, *Proc. SPIE*, 2198, 935
- Pier, J., et al. 2001, in preparation
- Richards, G. T., Fan, X., Schneider, D. P., Strauss, M. A., Vanden Berk, D. E., & SDSS Collaboration. 2000, *BAAS*, 196, 53.04
- Richards, G. T., Yanny, B., Annis, J., Newberg, H. J. M., McKay, T. A., York, D. G., & Fan, X. 1997, *PASP*, 109, 39
- Richards, G. T., et al. 2001, in preparation

- Richstone, D. O. & Schmidt, M. 1980, *ApJ*, 235, 361
- Sandage, A. 1965, *ApJ*, 141, 1560
- Schlegel, D. J., Finkbeiner, D. P., & Davis, M. 1998, *ApJ*, 500, 525
- Schmidt, M. & Green, R. F. 1983, *ApJ*, 269, 352
- Schneider, D. P., Schmidt, M., & Gunn, J. E. 1994, *AJ*, 107, 1245
- . 1999, *AJ*, 117, 40
- Schneider, D., et al. 2001, in preparation
- Schneider, D. P., et al. 2000, *PASP*, 112, 6
- Siegmund, W., et al. 2001, in preparation
- Smith, A., et al. 2001, in preparation
- Spinrad, H., Marr, J., Aguilar, L., & Djorgovski, S. 1985, *PASP*, 97, 932
- Stepanian, J. A., Lipovetsky, V. A., Chavushian, V. H., Erastova, L. K., & Balayan, S. K. 1993, *Bull. Special Astrophys. Obs.*, 36, 5
- Szalay, A., et al. 2001, in preparation
- Tucker, D., et al. 2001, in preparation
- Uomoto, A., et al. 2001a, in preparation
- . 2001b, in preparation
- Vanden Berk, D. E., Richards, G. T., & SDSS Collaboration. 2000, *BAAS*, 196, 50.03
- Vanden Berk, D. E., et al. 2001, in preparation
- Véron-Cetty, M. & Véron, P. 1996, "A Catalogue of Quasars and Active Nuclei" (ESO Scientific Report, Garching: European Southern Observatory (ESO), —c1996, 7th ed.)
- Warren, S. J., Hewett, P. C., Irwin, M. J., & Osmer, P. S. 1991a, *ApJS*, 76, 1
- Warren, S. J., Hewett, P. C., & Osmer, P. S. 1991b, *ApJS*, 76, 23
- . 1994, *ApJ*, 421, 412
- White, R. L., et al. 2000, *ApJS*, 126, 133
- Wolf, C., Meisenheimer, K., & Röser, H.-J. 2000, *astroph/0010092*

Yanny, B., et al. 2001, in preparation

York, D. G., et al. 2000, AJ, 120, 1579

Zheng, W., et al. 2000, AJ, 120, 1607

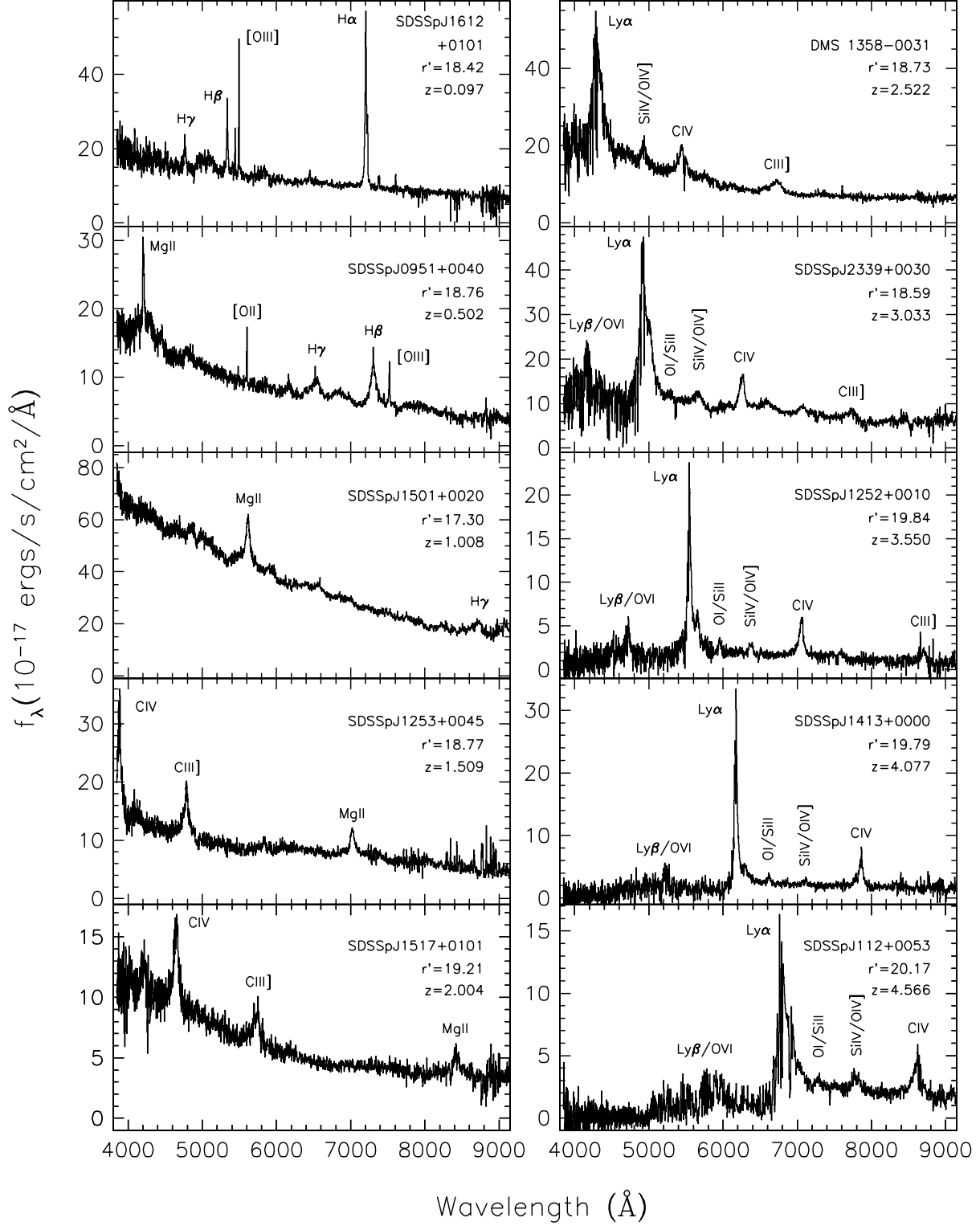


Fig. 1.— Sample SDSS quasars. These quasars are representative of the quasars found in the SDSS sample from $z \sim 0$ to $z \sim 5$.

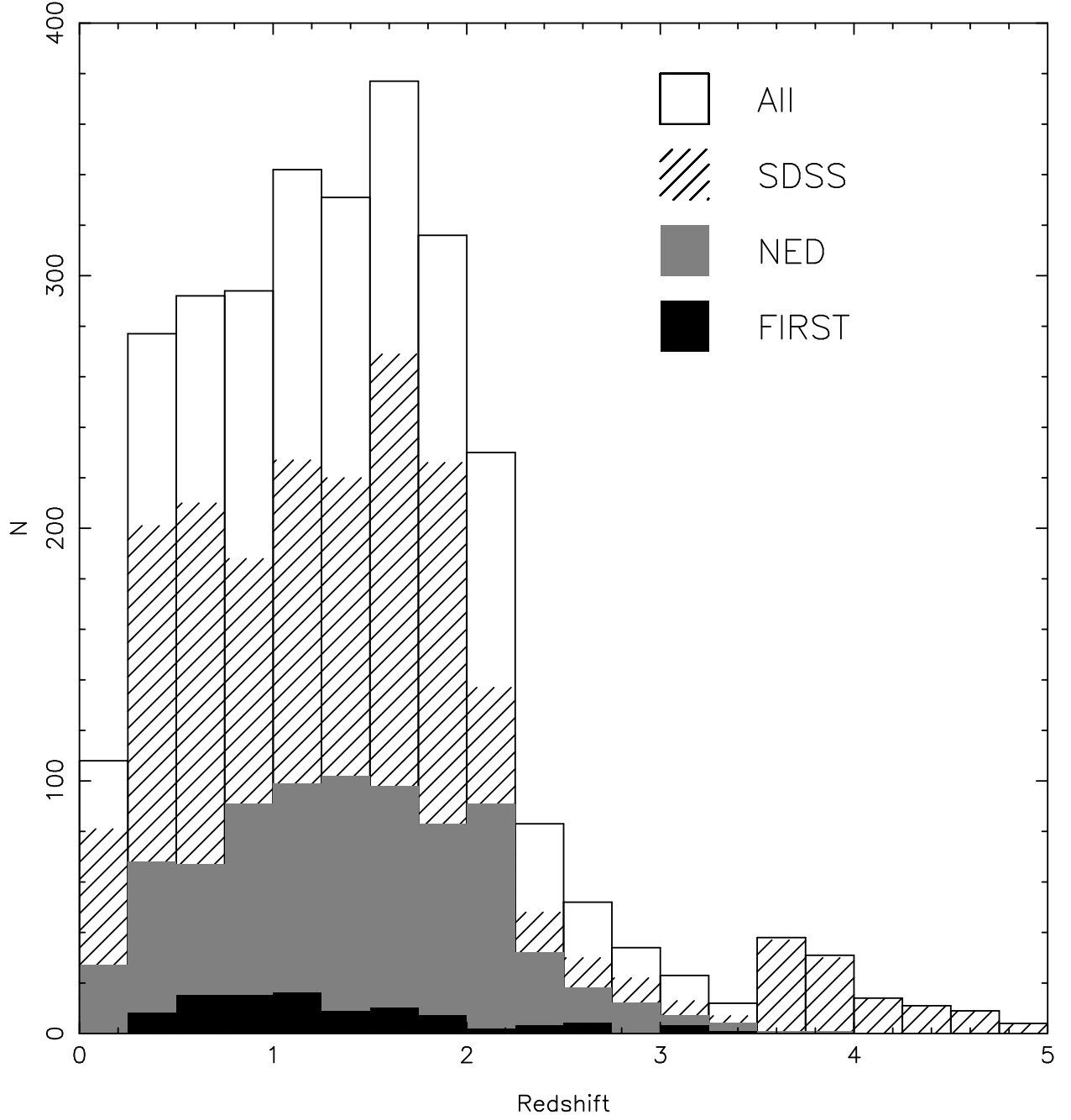


Fig. 2.— Redshift distribution for 801 NED quasars, 92 FIRST quasars, and 1983 SDSS quasars. Some quasars appear in more than one sample. There are 2625 quasars in total.

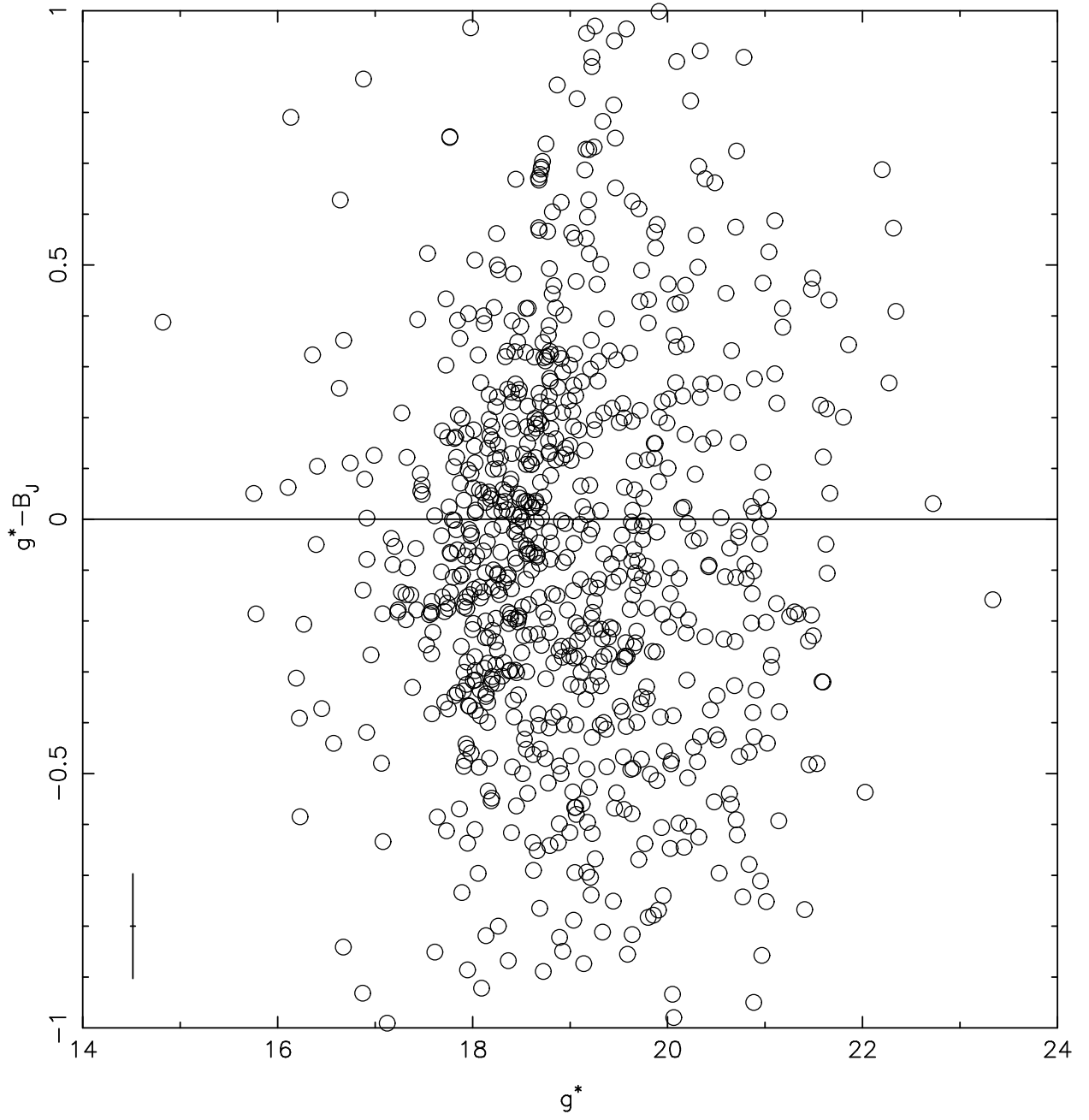


Fig. 3.— Magnitude difference versus magnitude for 867 NED and FIRST quasars. For NED quasars the cataloged magnitude is typically, but not always, B_J ; for FIRST quasars B_J is replaced by O . The cross in the lower left-hand corner shows a 3% error in g^* and the error in $g^* - B_J$ given a 10% error in B_J .

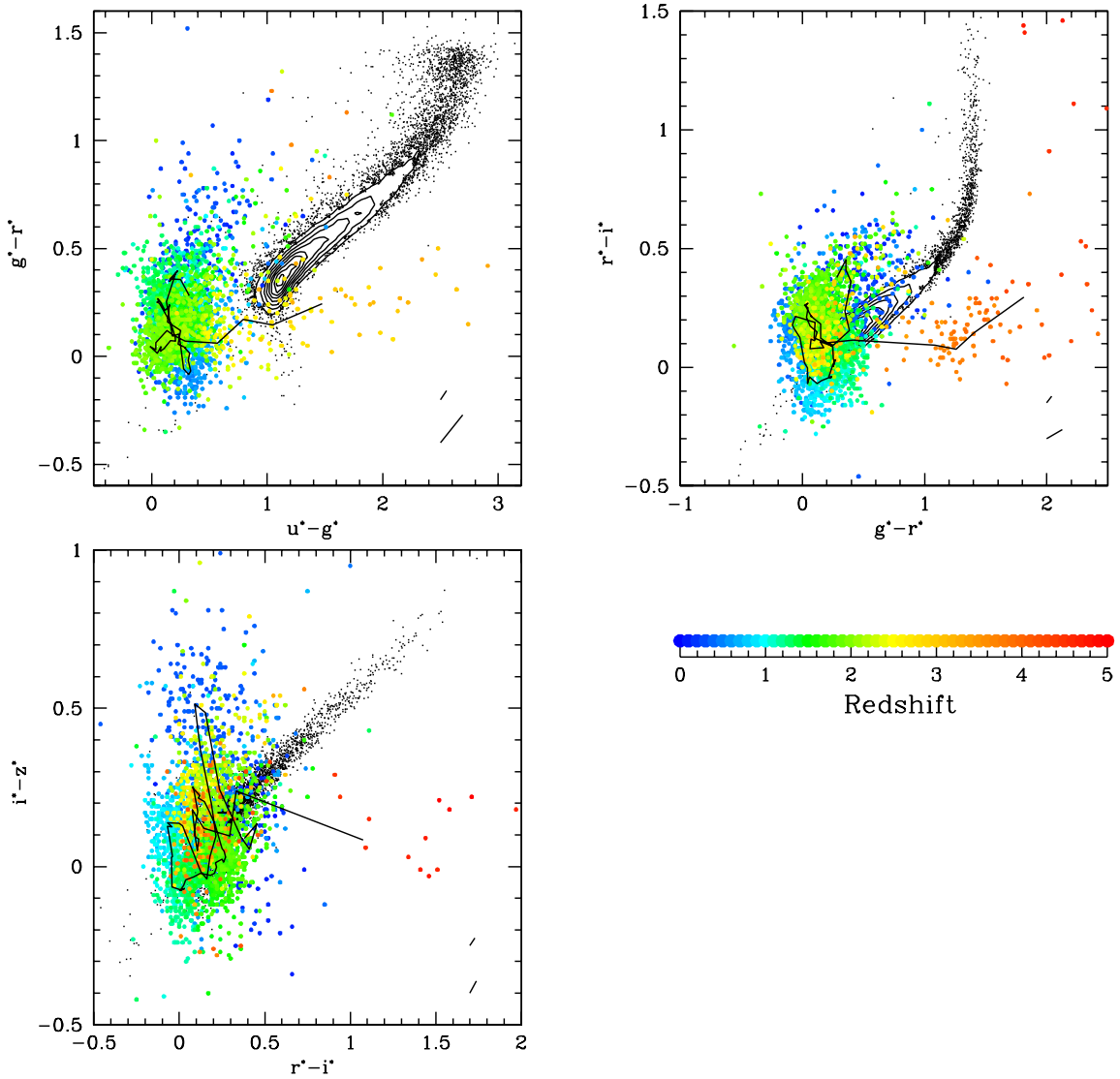


Fig. 4.— SDSS color-color diagrams for 2625 quasars (color points) and 10,000 stars (black points and black contours). Only objects with errors less than 0.2 mag in each band are shown. Quasar points are coded as a function of redshift, where the redshift is given by the color as indicated in the legend. The long solid black lines are the median color-color tracks of the quasars. Galactic (upper) and extra-Galactic (lower) reddening vectors are given in the lower right-hand corner of each panel, where the Galactic reddening vector is the mean over the whole sample.

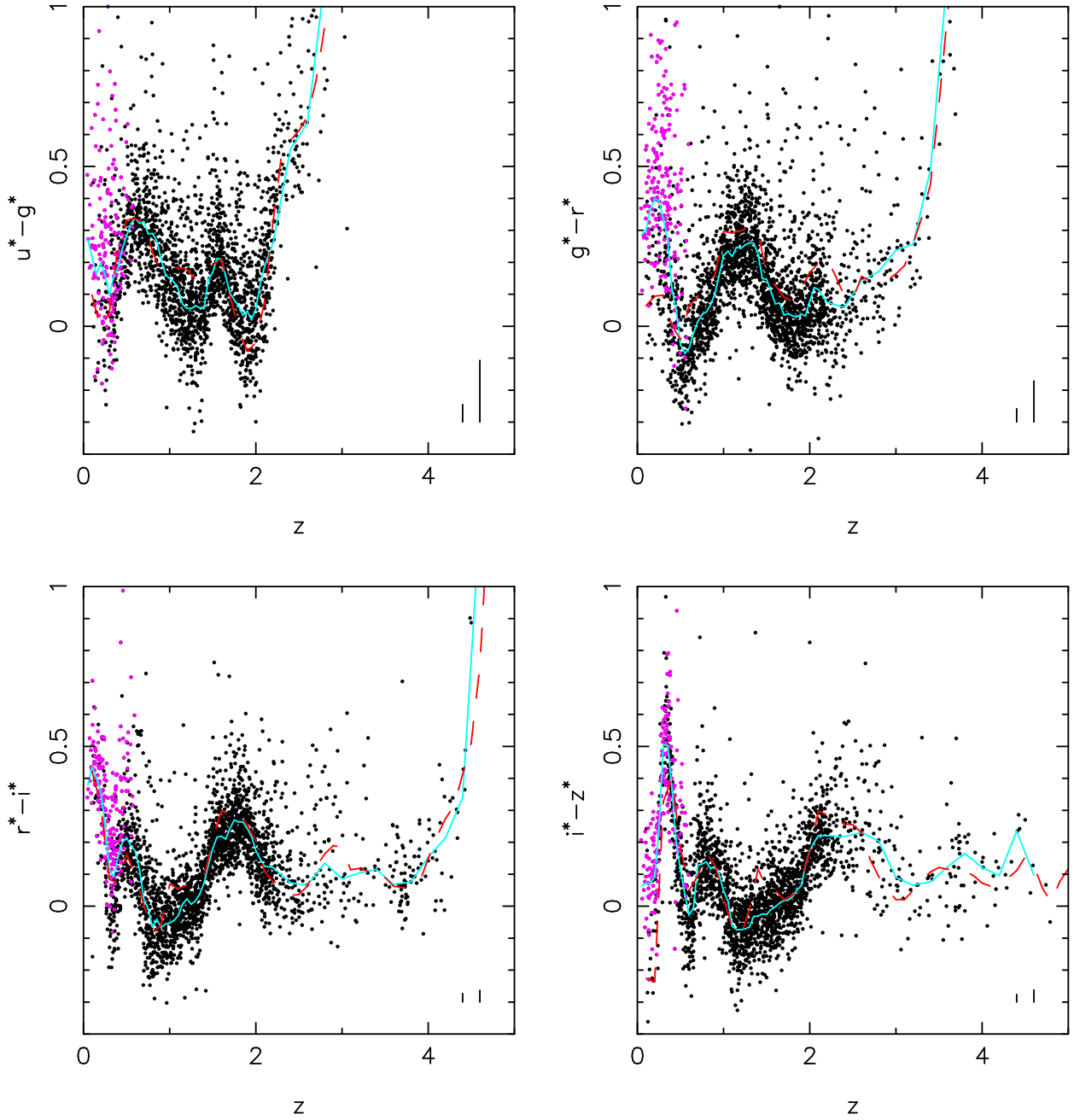


Fig. 5.— The SDSS color versus redshift relation for 2625 quasars (black dots are point sources, magenta dots are extended sources with $z \leq 0.6$). Only objects with errors less than 0.1 mag in all bands are shown. The median in redshift bins of 0.05 ($z \leq 2.2$) and 0.2 ($z > 2.2$) is given by the solid light blue line (smoothed by 50% of the bin size). The dashed red line is a modified version of the simulated median quasar color-redshift relation from Figure 12 of Fan (1999). Galactic (leftmost) and extra-Galactic (rightmost) reddening vectors are given in the lower right-hand corner of each panel.

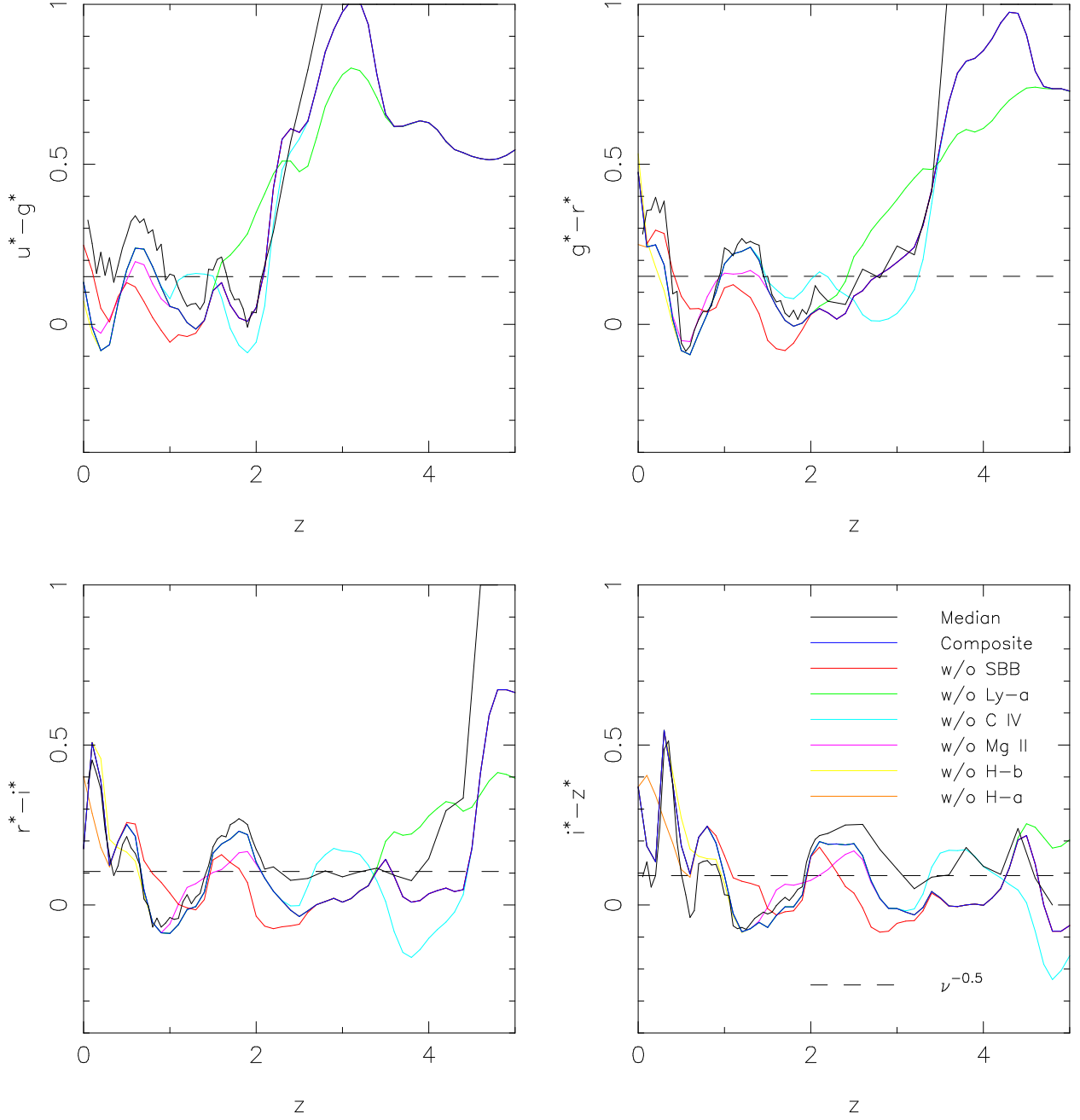


Fig. 6.— Simulated color versus redshift. The solid black line is the observed median color-redshift relation from Table 3. The dashed black line is the color for a power-law spectrum of the form $f_\nu \propto \nu^{-0.5}$. The solid blue line is color-redshift track of the SDSS quasar composite spectrum (Vanden Berk et al. 2000; Vanden Berk et al. 2001). The remaining lines show the colors as a function of redshift when specific emission features are removed from the composite spectrum.

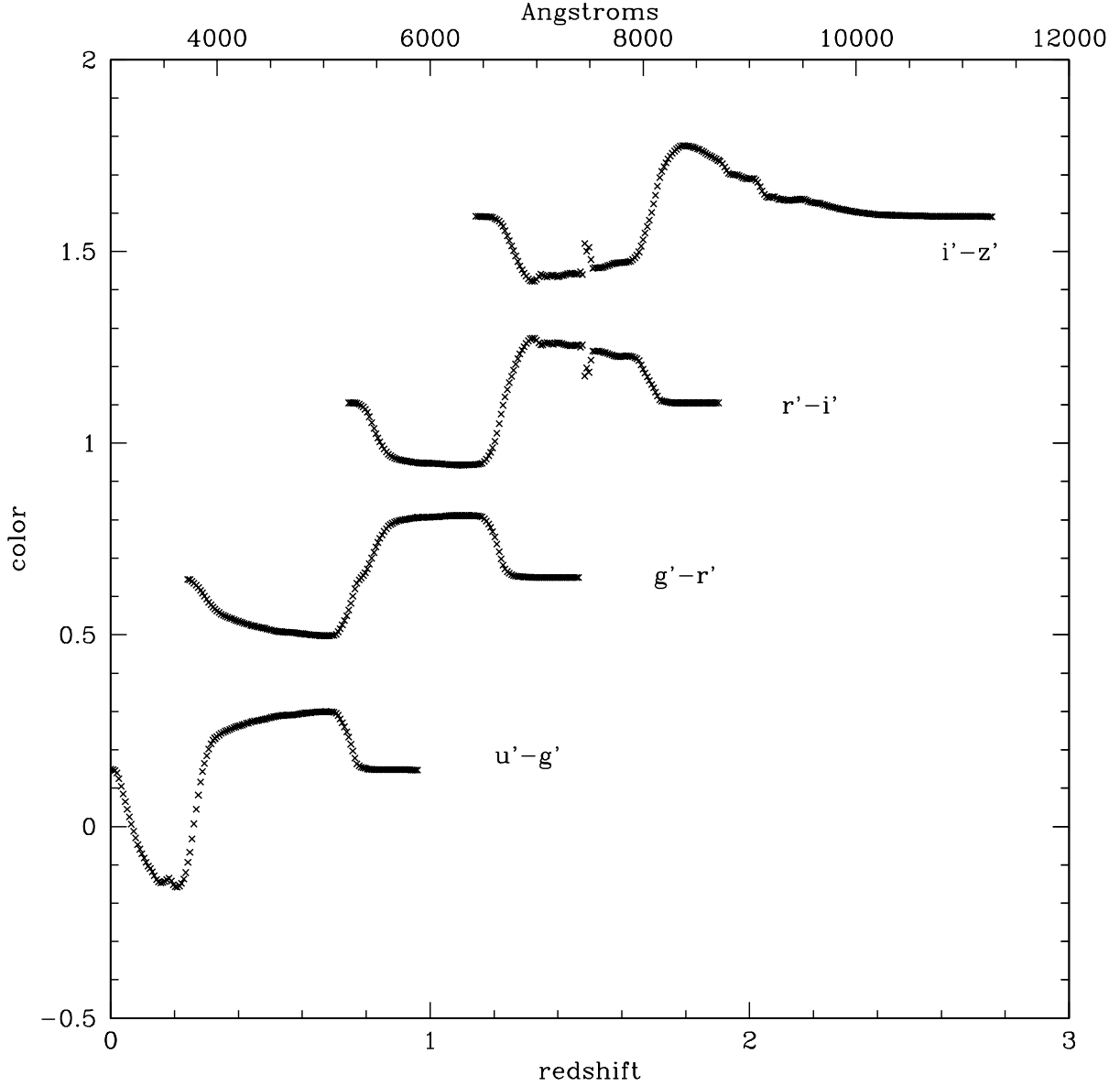


Fig. 7.— Color versus redshift for a top hat emission line superimposed upon a power-law continuum ($\alpha_\nu = -0.5$). The line center of the top hat begins at 3000 Å and is redshifted through each of the transmission curves. The lower axis gives the redshift of the line, whereas the upper axis gives the wavelength of the line. The top hat has an observed equivalent width of 200 Å and is 20 Å wide. The bottom, left-hand curve is the $u' - g'$ curve. The other colors are shifted in the y-direction by 0.5 each.

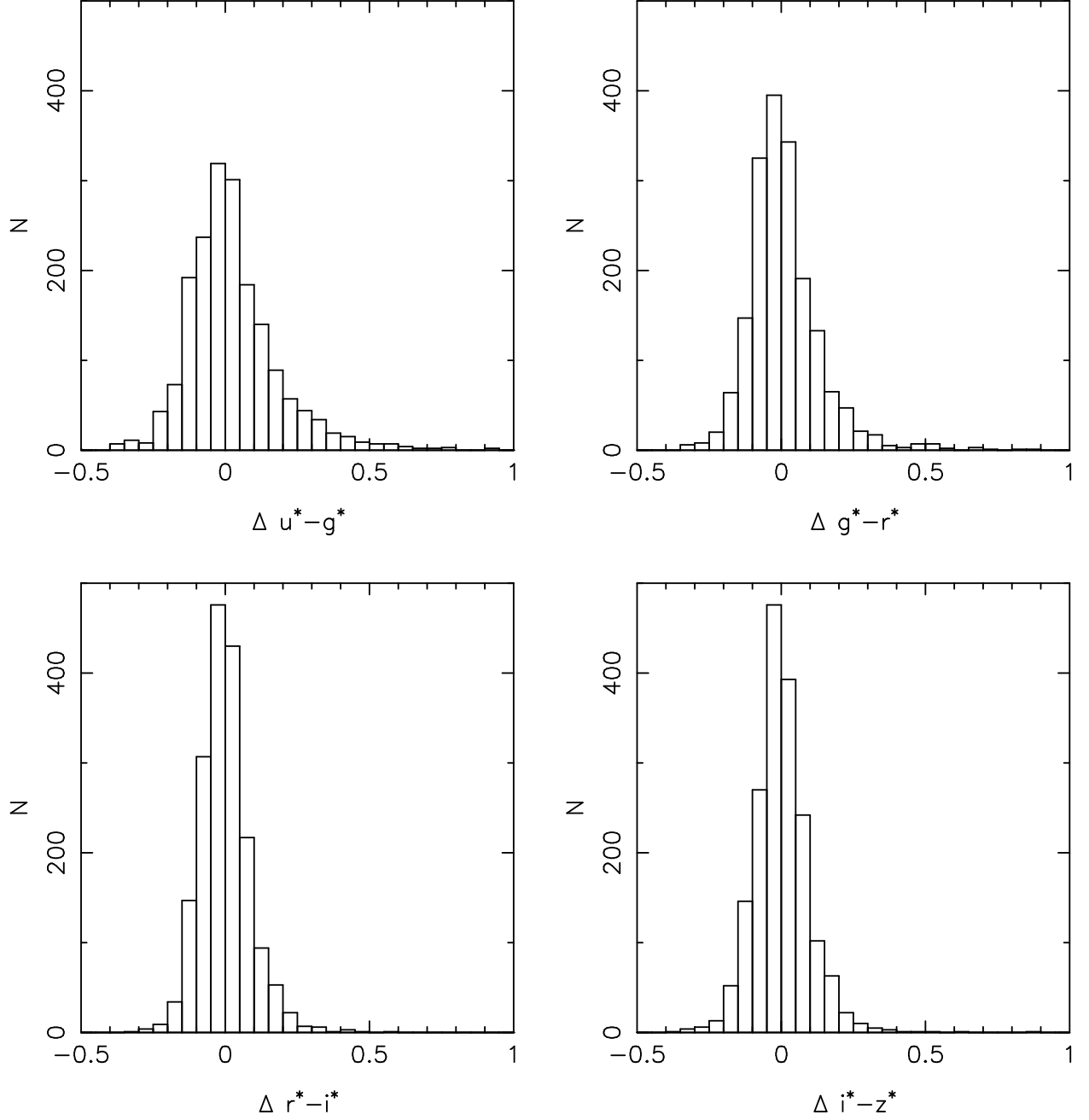


Fig. 8.— Histograms of observed quasar colors corrected by the median colors as a function of redshift.

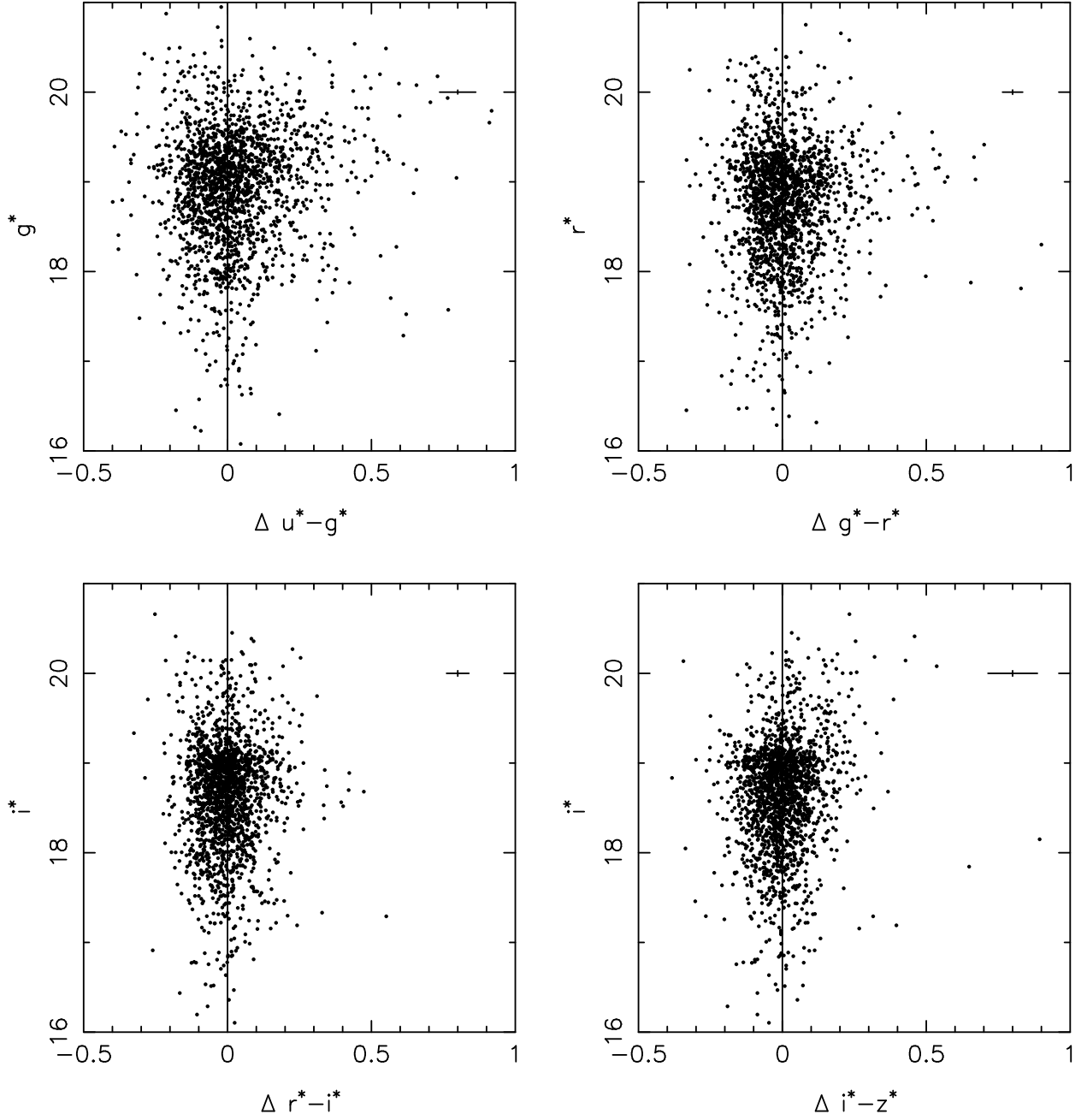


Fig. 9.— Observed quasar colors corrected by the median colors as a function of redshift, plotted as a function of magnitude. Two-sigma error bars in color and magnitude are given for the average 20th magnitude object.

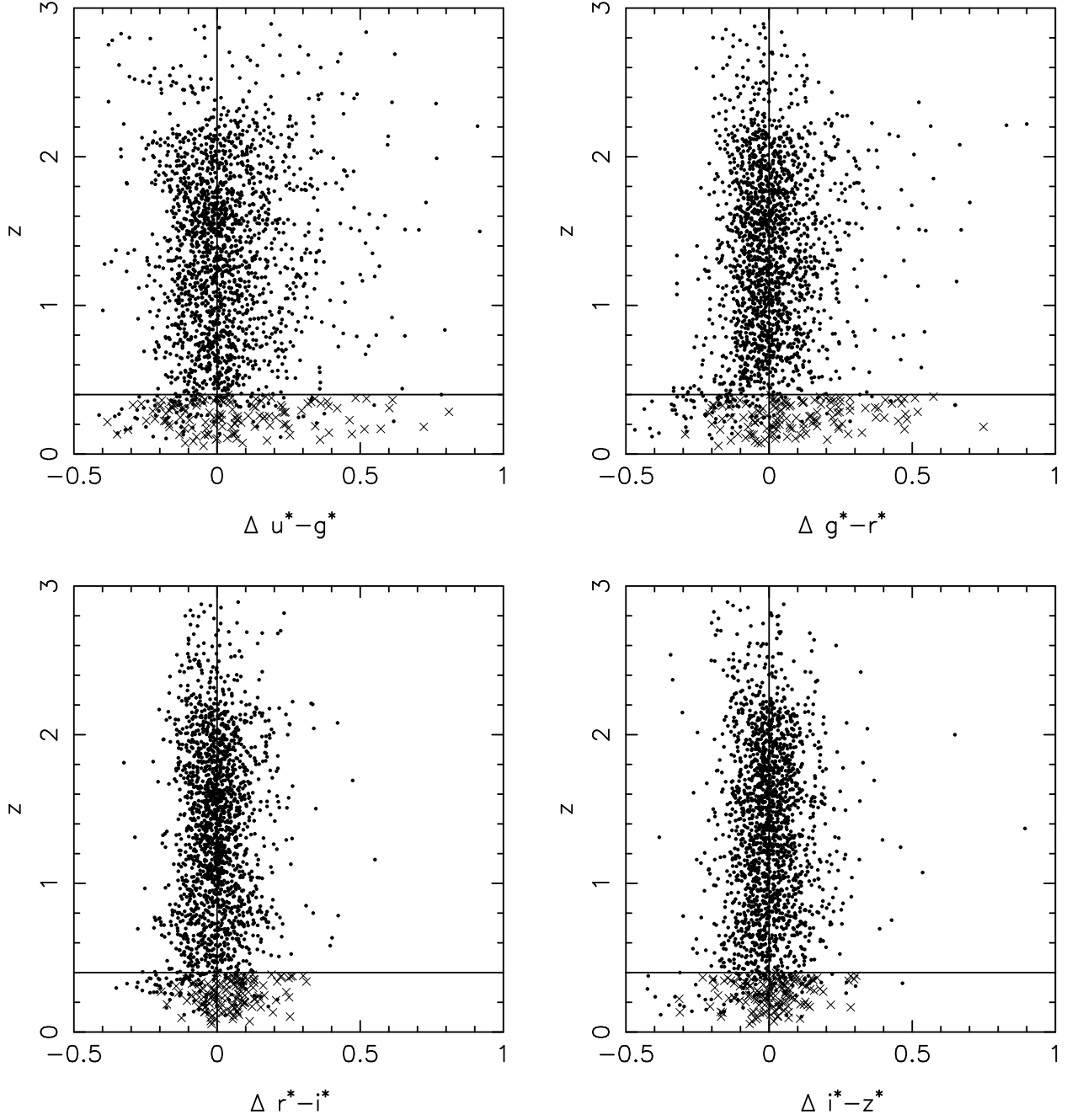


Fig. 10.— Quasar colors (corrected by the median colors as a function of redshift), plotted versus redshift. Objects with $z \leq 0.4$ (horizontal line) are not used in the reddening analysis. Crosses mark extended sources with $z \leq 0.4$.

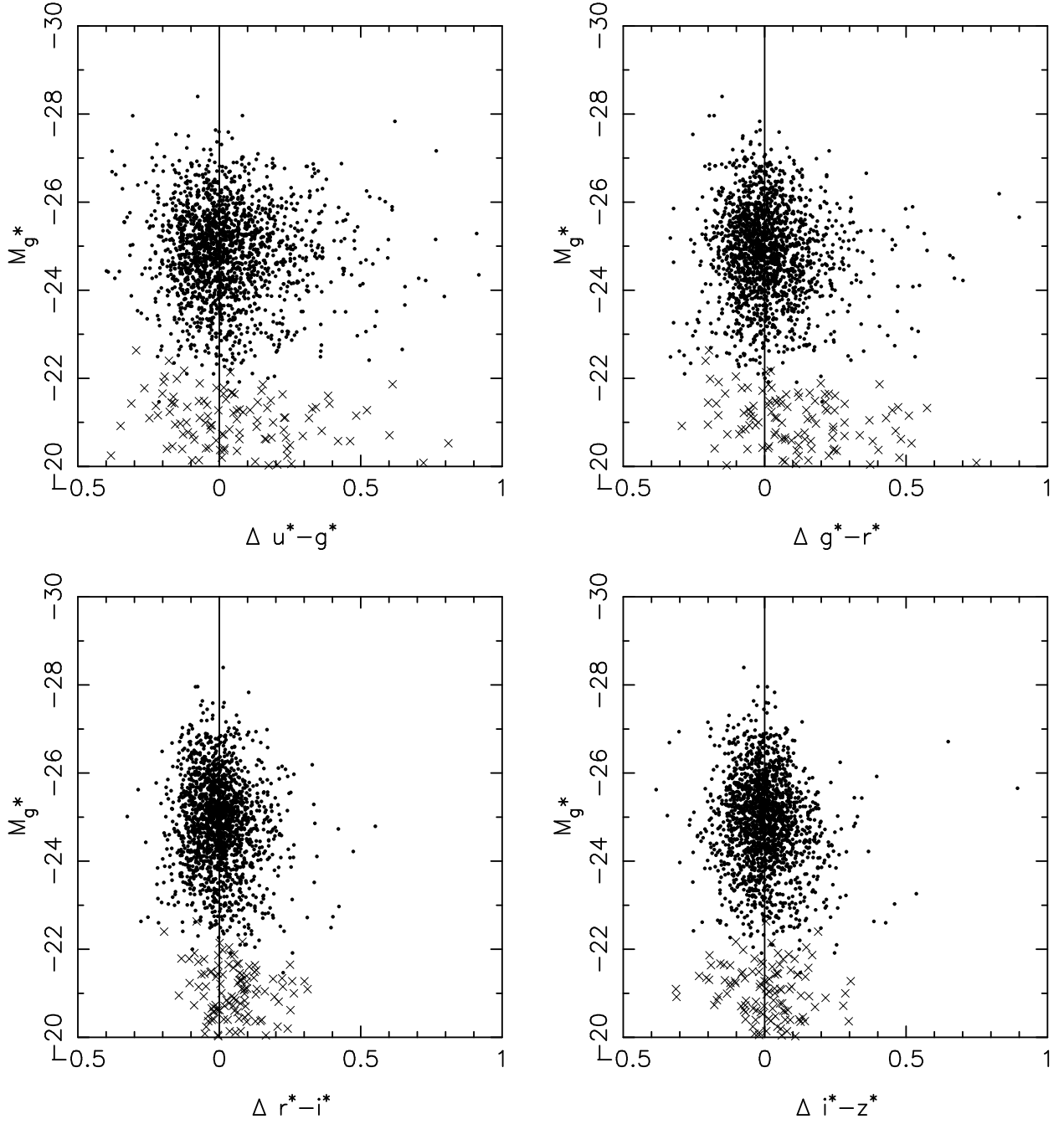


Fig. 11.— Quasar colors (corrected by the median colors as a function of redshift), plotted versus absolute magnitude. Extended sources with $z \leq 0.4$ are plotted as crosses.

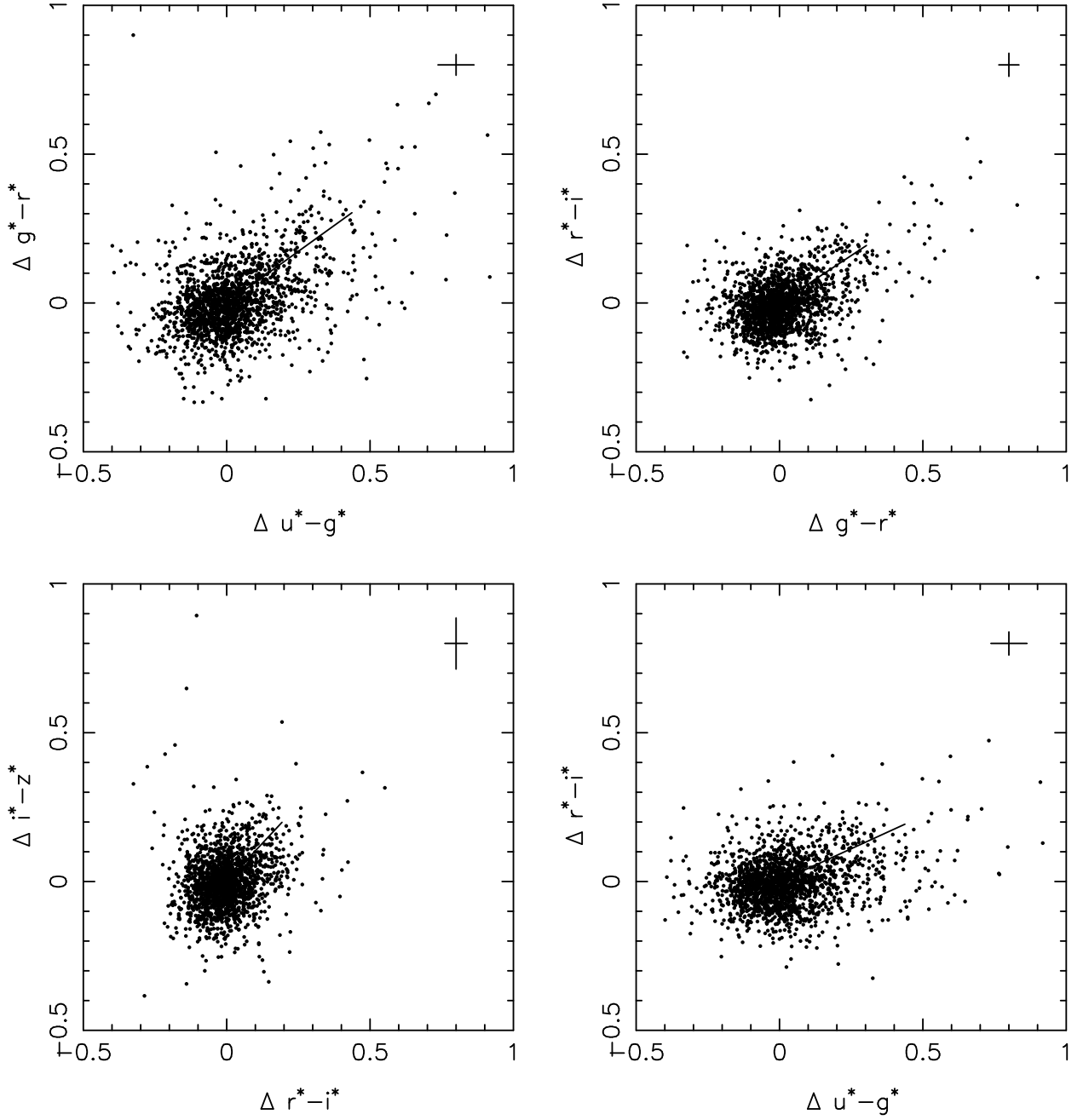


Fig. 12.— Quasar colors (corrected by the median colors as a function of redshift), plotted against each other. Typical errors are given in the upper right hand corner of each panel. The vector in each panel is the absolute value of the blue 95% confidence limit from Table 5.

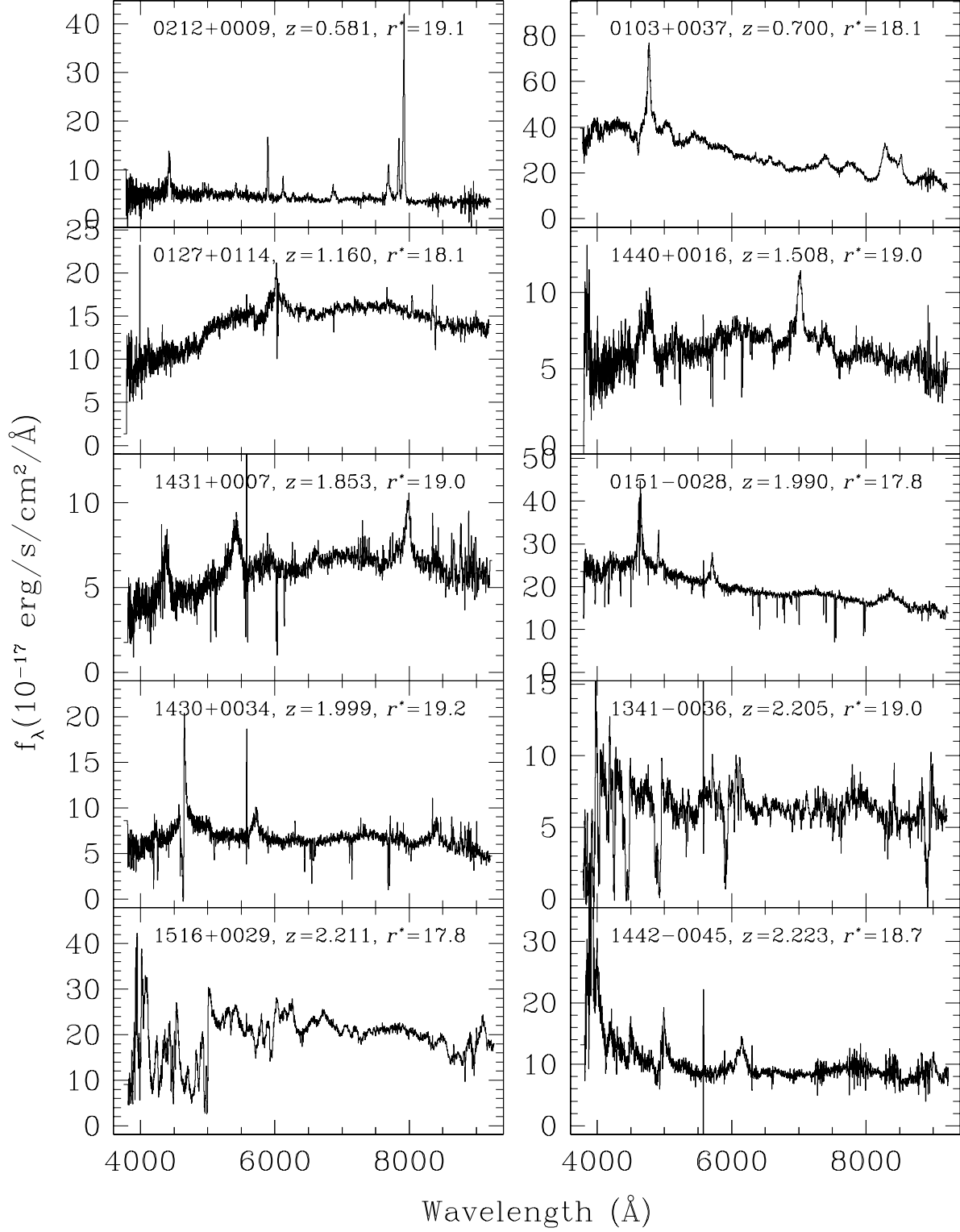


Fig. 13.— Sample “red” quasars (SDSSp J####±#####). That these quasars are anomalously red can be seen by comparing them to the more “normal” quasars at the same redshift shown in Figure 1.

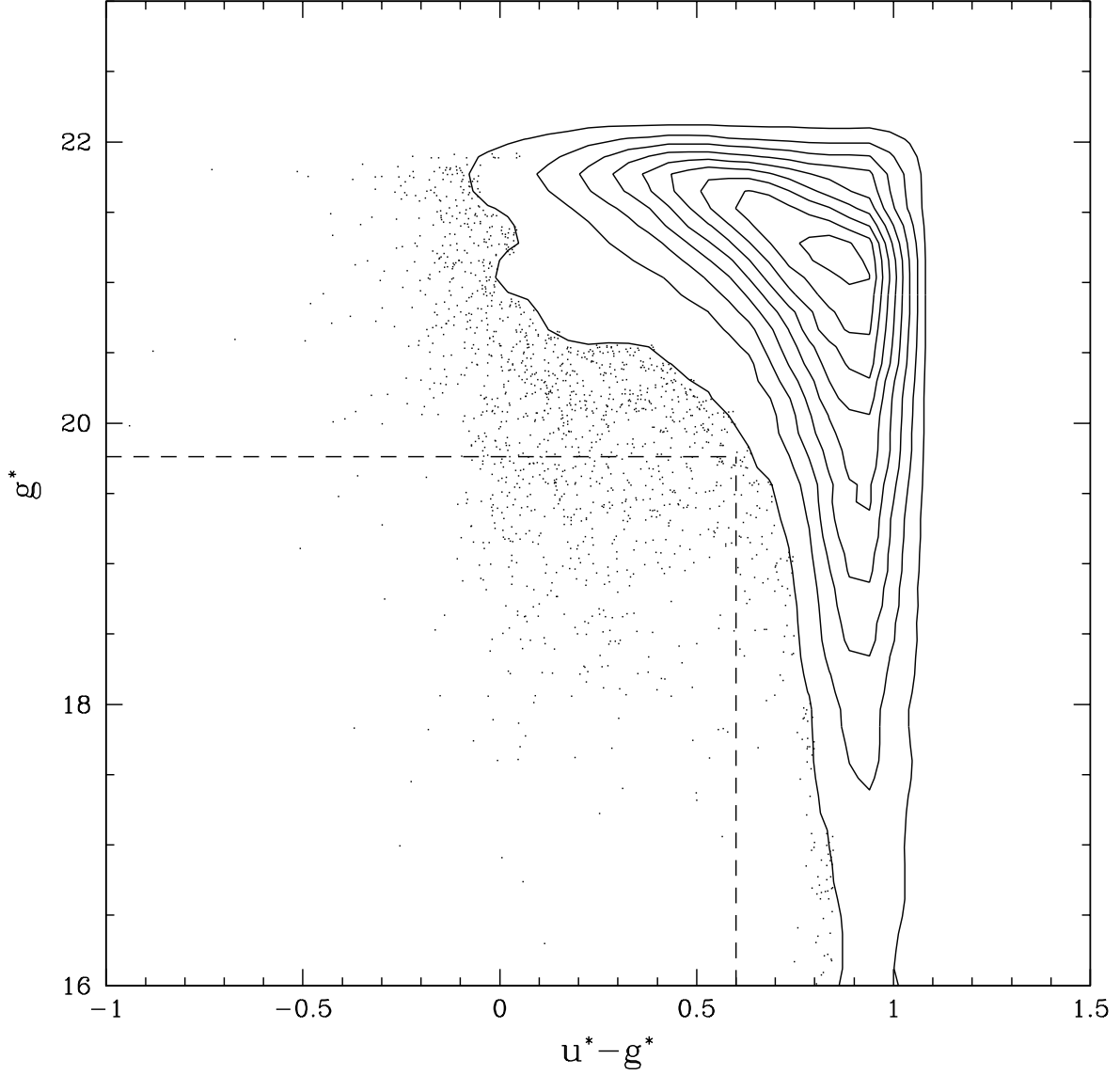


Fig. 14.— Stellar UVX Sources. Stellar objects from camera column 3 of run 756 with $u^*-g^* \leq 1.0$ and $g^* \leq 22.0$. The steep fall-off of the red sources is artificial: it results from the red color-cut on the data. The vertical dashed lines shows an appropriate color-cut for UVX quasars in the SDSS system. The horizontal dashed line shows the average g^* magnitude for a low-redshift quasar with $i^* = 19.0$. Note the shifting of the stellar locus as a function of magnitude and the fall-off of faint, red sources.

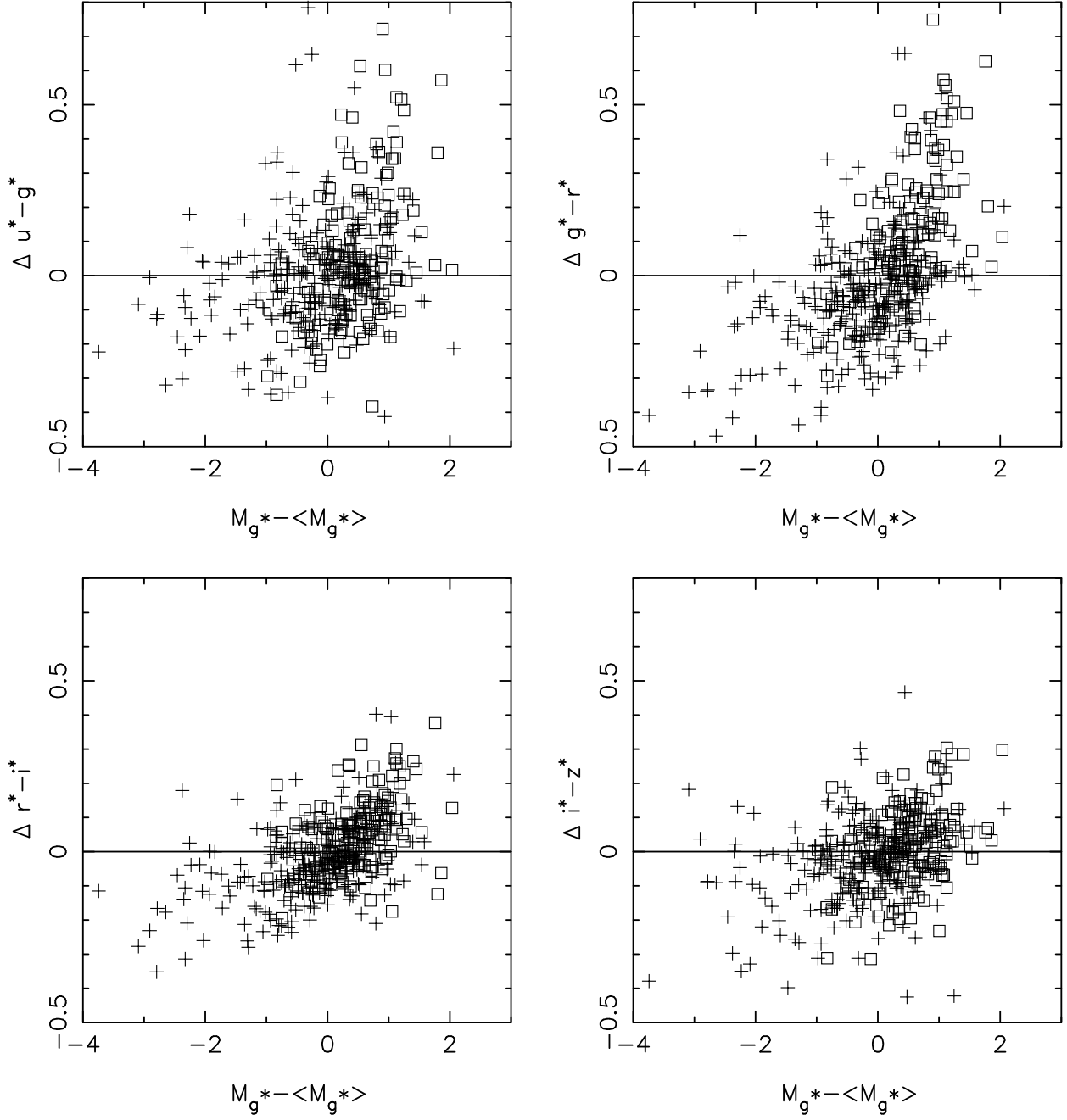


Fig. 15.— Quasar colors (corrected by the median colors as a function of redshift), plotted versus normalized absolute magnitude. The absolute magnitude of the objects is normalized in redshift bins of $\Delta z = 0.1$ from $z = 0.1$ to $z = 0.6$. Crosses are point sources, whereas squares represent extended sources. The lines show the median corrected color around which the points would be evenly distributed if there were not a correlation between color and luminosity. The mean absolute magnitude ranges from $M_{g^*} = -20.1$ in the $z = 0.1$ bin to $M_{g^*} = -23.5$ in the $z = 0.6$ bin.

Table 1. Summary of Observations

Run	UT Date	Strip	RA Range (J2000)	Seeing (")
94	1998 Sep 19	North	22:16 - 03:49	1.5
125	1998 Sep 25	South	23:18 - 05:17	1.5
752	1999 Mar 21	South	08:21 - 15:41	1.5-1.8
756	1999 Mar 22	North	08:21 - 16:34	1.2-1.5

Table 2. SDSS Quasar Photometry

Name	z_{em}	RA(2000)	DEC(2000)	Δ''	u^*	g^*	r^*	i^*	z^*	$E(g^*-r^*)$	source
LBQS 2357-0014	0.479	00 : 00 : 11.96	+00 : 02 : 25.3	0.11	17.83±0.011	17.58±0.01	17.70±0.01	17.65±0.01	17.66±0.024	0.03	1 2
LBQS 2358+0038	0.954	00 : 00 : 42.91	+00 : 55 : 39.7	0.25	18.34±0.016	18.19±0.01	17.93±0.01	17.88±0.01	17.69±0.023	0.03	1 2
ZC 2358-010B	1.890	00 : 00 : 58.24	-00 : 46 : 46.3	0.39	18.55±0.018	18.68±0.01	18.71±0.011	18.40±0.010	18.32±0.036	0.04	1 2
UM 194	0.780	00 : 01 : 16.53	+00 : 02 : 05.4	1.67	18.94±0.025	18.79±0.01	18.94±0.012	19.04±0.017	19.18±0.087	0.03	1
[HB89] 2359-000	2.120	00 : 01 : 46.95	+00 : 14 : 28.9	2.03	20.92±0.087	20.70±0.029	20.66±0.038	20.53±0.057	20.14±0.189	0.03	1
[HB89] 2359+002	2.670	00 : 02 : 12.01	+00 : 32 : 53.5	2.47	20.50±0.084	19.48±0.015	19.42±0.018	19.31±0.026	19.26±0.081	0.03	1
LBQS 2359-0021	0.812	00 : 02 : 22.48	-00 : 04 : 43.4	0.13	18.84±0.017	18.39±0.01	18.19±0.01	18.16±0.01	17.86±0.023	0.03	1 2
CFRS 00.0207	1.352	00 : 02 : 24.50	-00 : 41 : 28.7	0.73	24.05±1.127	23.10±0.341	22.14±0.209	22.49±0.423	20.68±0.298	0.03	1
[HB89] 0001-011	2.010	00 : 04 : 16.47	-00 : 53 : 00.6	1.45	19.78±0.032	19.80±0.016	19.74±0.019	19.56±0.026	19.54±0.102	0.03	1
LBQS 0001-0050	1.458	00 : 04 : 21.03	-00 : 34 : 03.0	0.14	19.09±0.022	18.99±0.01	18.85±0.010	18.65±0.011	18.75±0.047	0.03	1 2
FIRST J000442.1+000023	1.000	00 : 04 : 42.19	+00 : 00 : 23.5	0.12	19.40±0.025	19.17±0.010	18.88±0.01	18.95±0.014	19.02±0.061	0.04	2
UM 197	2.210	00 : 05 : 00.42	-00 : 33 : 48.4	1.37	18.97±0.020	18.75±0.01	18.63±0.01	18.51±0.010	18.25±0.030	0.03	1
[HB89] 0002-010	2.220	00 : 05 : 02.87	-00 : 44 : 48.6	0.57	20.61±0.096	20.38±0.031	20.53±0.052	20.34±0.059	20.16±0.166	0.04	1
[HB89] 0002-008NED02	0.440	00 : 05 : 19.58	-00 : 35 : 17.5	0.60	19.80±0.037	18.87±0.01	18.63±0.01	18.50±0.010	18.41±0.035	0.04	1
[HB89] 0002-011	2.160	00 : 05 : 29.13	-00 : 50 : 01.7	1.15	20.41±0.053	20.16±0.027	20.11±0.027	20.08±0.040	20.09±0.160	0.04	1
[HB89] 0003-009	1.990	00 : 05 : 43.16	-00 : 43 : 00.7	2.49	20.58±0.100	20.42±0.029	20.44±0.047	20.20±0.052	19.88±0.137	0.03	1
[HB89] 0003-006	1.760	00 : 05 : 46.49	-00 : 24 : 14.0	1.03	19.51±0.037	19.35±0.014	19.47±0.019	19.00±0.019	19.14±0.072	0.03	1
[HB89] 0003-008	1.624	00 : 05 : 49.05	-00 : 34 : 35.6	0.03	19.32±0.026	19.17±0.010	19.10±0.011	18.84±0.013	18.82±0.050	0.04	1 2
LBQS 0003+0011	0.259	00 : 05 : 57.25	+00 : 28 : 37.7	0.14	18.52±0.018	18.49±0.01	18.30±0.011	18.17±0.014	17.79±0.023	0.06	1 2
[HB89] 0003-011	1.858	00 : 06 : 02.17	-00 : 53 : 58.2	0.20	19.34±0.024	19.32±0.012	19.24±0.013	18.85±0.014	18.90±0.056	0.03	1 2
3C 002	1.038	00 : 06 : 22.60	-00 : 04 : 24.4	0.08	19.66±0.029	19.54±0.012	19.26±0.012	19.12±0.017	19.15±0.070	0.05	1 2
LBQS 0004-0032	1.720	00 : 06 : 54.11	-00 : 15 : 33.3	0.10	18.23±0.014	18.16±0.01	18.04±0.01	17.72±0.01	17.70±0.020	0.04	1 2
LBQS 0004+0005	0.889	00 : 07 : 01.33	+00 : 22 : 42.5	0.18	17.85±0.010	17.53±0.01	17.32±0.01	17.33±0.01	17.23±0.016	0.07	1 2
LBQS 0004+0036	0.317	00 : 07 : 10.02	+00 : 53 : 29.0	0.16	17.18±0.01	16.87±0.01	16.64±0.01	16.69±0.01	16.05±0.01	0.03	1 2
UM 203	1.472	00 : 08 : 07.54	+00 : 16 : 18.9	1.32	19.35±0.025	19.18±0.01	18.91±0.010	18.69±0.012	18.77±0.058	0.07	1
LBQS 0006+0015	0.265	00 : 08 : 34.72	+00 : 31 : 56.2	0.21	17.86±0.011	17.73±0.01	17.55±0.01	17.55±0.01	17.28±0.014	0.04	1 2
LBQS 0007-0003	0.699	00 : 09 : 45.46	+00 : 13 : 37.1	0.17	18.84±0.018	18.52±0.01	18.44±0.01	18.44±0.010	18.37±0.039	0.03	1 2
FIRST J0010002.9-0101006	0.556	00 : 10 : 02.97	-01 : 01 : 07.1	0.10	19.64±0.027	19.03±0.01	18.85±0.010	18.54±0.011	18.65±0.045	0.03	2
LBQS 0007-0004	2.273	00 : 10 : 16.52	+00 : 12 : 27.7	1.40	19.74±0.044	19.05±0.010	18.69±0.010	18.65±0.013	18.51±0.045	0.03	1
UM 210	2.051	00 : 10 : 50.96	-00 : 31 : 33.2	0.13	19.11±0.022	19.25±0.010	19.23±0.012	18.98±0.015	18.73±0.045	0.05	1 2
[HB89] 0008+008	3.084	00 : 10 : 57.61	+01 : 10 : 11.4	0.61	22.31±0.278	19.20±0.010	18.58±0.01	18.49±0.012	18.45±0.039	0.03	1
ZC 0008+005	0.290	00 : 11 : 31.42	+00 : 47 : 18.2	2.11	19.49±0.026	19.45±0.012	19.57±0.016	19.28±0.020	19.25±0.074	0.03	1
LBQS 0010+0011	1.614	00 : 12 : 52.47	+00 : 28 : 31.9	0.08	18.95±0.020	18.78±0.01	18.63±0.01	18.42±0.011	18.37±0.034	0.04	1 2
LBQS 0010+0049	1.062	00 : 12 : 57.76	+01 : 06 : 03.3	0.21	18.64±0.017	18.47±0.01	18.19±0.01	18.21±0.01	18.08±0.033	0.03	1 2
LBQS 0010-0012	2.164	00 : 13 : 06.15	+00 : 04 : 31.8	0.06	19.13±0.027	18.80±0.01	18.63±0.01	18.56±0.012	18.43±0.042	0.03	1 2
LBQS 0010+0035	0.362	00 : 13 : 27.31	+00 : 52 : 32.0	0.08	18.20±0.014	17.69±0.01	17.41±0.01	17.47±0.01	16.96±0.012	0.03	1 2
[HB89] 0010+008	3.079	00 : 13 : 27.53	+01 : 06 : 46.5	0.12	20.71±0.079	19.25±0.010	18.98±0.011	18.95±0.016	18.79±0.053	0.02	1 2
LBQS 0011+0026	1.704	00 : 14 : 00.45	+00 : 42 : 55.5	0.87	18.77±0.017	18.66±0.01	18.62±0.01	18.35±0.010	18.34±0.035	0.03	1
LBQS 0012-0016	1.552	00 : 14 : 44.03	-00 : 00 : 18.4	0.10	18.19±0.012	17.94±0.01	17.79±0.01	17.61±0.01	17.58±0.018	0.03	1 2
LBQS 0012+0040	1.464	00 : 14 : 51.55	+00 : 56 : 55.5	0.89	19.02±0.026	18.80±0.01	18.69±0.010	18.52±0.013	18.68±0.045	0.03	1
LBQS 0012-0111	0.649	00 : 15 : 04.34	-00 : 54 : 39.1	0.08	18.45±0.015	18.07±0.01	18.15±0.01	18.06±0.01	18.06±0.027	0.04	1 2
LBQS 0012-0024	1.700	00 : 15 : 07.00	-00 : 08 : 00.8	0.11	18.62±0.015	18.55±0.01	18.22±0.01	17.80±0.01	17.71±0.020	0.03	1 2
LBQS 0013-0029	2.081	00 : 16 : 02.40	-00 : 12 : 25.0	0.05	18.41±0.015	18.08±0.01	17.82±0.01	17.55±0.01	17.23±0.014	0.03	1 2
[HB89] 0013-005	1.576	00 : 16 : 11.09	-00 : 15 : 12.4	0.21	20.38±0.071	20.17±0.024	19.90±0.026	19.42±0.024	19.21±0.076	0.03	1 2
LBQS 0016+0045	2.306	00 : 19 : 19.31	+01 : 01 : 52.3	0.04	19.32±0.031	18.78±0.01	18.77±0.011	18.62±0.014	18.28±0.032	0.02	1 2
SDSSp J001950.06-004040.9	4.340	00 : 19 : 50.05	-00 : 40 : 40.8	0.15	24.17±0.919	21.49±0.067	19.82±0.024	19.50±0.024	19.35±0.066	0.03	2
LBQS 0017+0055	1.134	00 : 19 : 57.81	+01 : 11 : 53.6	0.18	18.08±0.012	17.88±0.01	17.65±0.01	17.66±0.01	17.73±0.024	0.03	1 2
LBQS 0018-0004	1.111	00 : 20 : 56.81	+00 : 11 : 47.6	0.15	19.16±0.026	18.68±0.01	18.24±0.01	18.17±0.01	18.19±0.032	0.03	1 2
LBQS 0018+0047	1.819	00 : 21 : 27.88	+01 : 04 : 20.4	0.23	18.51±0.016	18.03±0.01	18.05±0.01	17.90±0.01	17.78±0.024	0.02	1 2
LBQS 0018+0026	1.247	00 : 21 : 33.27	+00 : 43 : 01.1	0.23	17.90±0.010	17.82±0.01	17.55±0.01	17.51±0.01	17.49±0.021	0.03	1 2
LBQS 0019+0022A	0.308	00 : 21 : 41.01	+00 : 38 : 41.8	0.14	18.69±0.016	18.59±0.01	18.18±0.01	17.94±0.01	17.53±0.017	0.03	1 2

Table 2—Continued

Name	z_{em}	RA(2000)	DEC(2000)	Δ''	u^*	g^*	r^*	i^*	z^*	$E(g^*-r^*)$	source
LBQS 0019+0022B	0.661	00 : 21 : 46.36	+00 : 39 : 00.2	0.94	18.86±0.018	18.57±0.01	18.72±0.01	18.66±0.013	18.66±0.043	0.03	1
LBQS 0019-0000	0.576	00 : 22 : 09.95	+00 : 16 : 29.4	0.01	18.34±0.013	18.03±0.01	18.07±0.01	17.95±0.01	17.92±0.028	0.03	1 2
LBQS 0020+0058	0.727	00 : 23 : 03.15	+01 : 15 : 33.6	0.97	18.43±0.014	17.93±0.01	17.91±0.01	17.96±0.01	17.70±0.024	0.02	1
LBQS 0020+0018	0.423	00 : 23 : 11.06	+00 : 35 : 17.5	1.00	19.87±0.041	19.58±0.014	19.34±0.015	19.02±0.016	18.68±0.038	0.02	1
LBQS 0021+0046	1.633	00 : 23 : 42.98	+01 : 02 : 43.0	1.21	18.89±0.022	18.75±0.01	18.61±0.01	18.31±0.010	18.29±0.031	0.03	1
LBQS 0021-0100	0.771	00 : 24 : 11.66	−00 : 43 : 48.1	0.08	18.31±0.015	18.15±0.01	17.98±0.01	17.78±0.01	17.86±0.021	0.03	1
LBQS 0022-0120	1.088	00 : 24 : 42.39	−01 : 03 : 45.9	0.16	19.41±0.029	19.06±0.012	18.88±0.010	18.89±0.015	18.95±0.055	0.03	1 2
LBQS 0022+0015	0.404	00 : 24 : 44.11	+00 : 32 : 21.4	0.40	17.18±0.01	16.92±0.01	16.80±0.01	16.91±0.01	16.43±0.01	0.02	1
LBQS 0023+0010	1.902	00 : 25 : 37.30	+00 : 27 : 24.4	0.37	19.05±0.023	18.79±0.01	18.67±0.01	18.35±0.010	18.32±0.029	0.02	1
LBQS 0023-0032	1.352	00 : 25 : 40.19	−00 : 15 : 31.3	0.12	18.23±0.013	18.15±0.01	17.95±0.01	17.84±0.01	17.96±0.024	0.03	1 2
LBQS 0024+0020	1.228	00 : 27 : 17.37	+00 : 37 : 23.6	0.17	17.74±0.010	17.96±0.01	17.55±0.01	17.52±0.01	17.61±0.017	0.03	1
LBQS 0026-0002	1.604	00 : 28 : 55.94	+00 : 14 : 00.2	0.65	18.70±0.015	18.40±0.01	18.32±0.01	18.05±0.01	18.16±0.032	0.02	1
UM 248	1.970	00 : 30 : 05.06	+00 : 28 : 48.1	0.66	19.12±0.024	19.19±0.010	18.82±0.010	18.79±0.013	18.81±0.043	0.03	1
LBQS 0027+0057	1.468	00 : 30 : 13.92	+01 : 14 : 05.1	0.36	18.05±0.011	17.81±0.01	17.68±0.01	17.63±0.01	17.59±0.018	0.03	1
LBQS 0028-0101	0.542	00 : 31 : 00.84	−00 : 44 : 31.0	0.11	18.84±0.020	18.49±0.01	18.63±0.01	18.37±0.01	18.24±0.027	0.02	1 2
LBQS 0028+0026	0.963	00 : 31 : 01.33	+00 : 43 : 30.6	0.75	18.93±0.022	18.64±0.01	18.31±0.01	18.30±0.01	18.24±0.028	0.03	1
FIRST J003111.3-001121	1.511	00 : 31 : 11.32	−00 : 11 : 21.2	0.20	19.35±0.023	19.09±0.01	18.98±0.01	18.75±0.012	18.80±0.045	0.02	2
LBQS 0028+0017	1.728	00 : 31 : 31.44	+00 : 34 : 20.2	0.99	18.72±0.018	18.65±0.01	18.67±0.01	18.36±0.010	18.33±0.027	0.02	1
FIRST J003443.9-005413	0.655	00 : 34 : 43.92	−00 : 54 : 13.0	0.06	19.69±0.029	19.13±0.010	19.22±0.012	19.15±0.017	19.09±0.061	0.03	2
UM 259	1.835	00 : 34 : 51.86	−01 : 11 : 25.7	0.18	18.43±0.014	18.36±0.01	18.43±0.01	18.13±0.01	18.12±0.026	0.03	1 2
UM 261	1.606	00 : 38 : 23.81	−00 : 00 : 25.0	0.16	18.34±0.013	18.15±0.01	18.04±0.01	17.81±0.01	17.85±0.022	0.02	1 2
UM 265	2.130	00 : 40 : 41.39	−00 : 55 : 37.3	1.89	18.46±0.014	18.18±0.01	18.06±0.01	17.93±0.01	17.72±0.020	0.02	1
SDSSp J004154.38-002955.9	3.800	00 : 41 : 54.37	−00 : 29 : 55.8	0.13	24.04±0.726	21.66±0.065	20.42±0.030	20.33±0.043	20.23±0.161	0.02	2
UM 269	2.000	00 : 43 : 19.75	+00 : 51 : 15.3	1.08	17.98±0.012	18.03±0.01	17.89±0.01	17.85±0.01	17.01±0.011	0.03	1
UM 275	2.137	00 : 46 : 13.54	+01 : 04 : 25.7	0.16	18.60±0.016	18.02±0.01	17.80±0.01	17.57±0.01	17.32±0.017	0.03	1
UM 278	2.530	00 : 48 : 06.06	−01 : 03 : 21.5	0.10	19.09±0.021	18.25±0.01	18.17±0.01	18.01±0.01	17.77±0.019	0.03	1
[HB89] 0045-000	1.536	00 : 48 : 19.12	+00 : 14 : 57.0	1.14	20.44±0.054	20.24±0.019	20.09±0.022	19.85±0.028	20.12±0.176	0.02	1
LBQS 0048+0029	0.727	00 : 51 : 21.25	+00 : 45 : 21.5	0.93	18.74±0.016	18.37±0.01	18.20±0.01	18.12±0.01	17.91±0.021	0.02	1
SDSSp J005129.39-003644.7	3.710	00 : 51 : 29.38	−00 : 36 : 44.9	0.20	23.55±0.625	21.81±0.069	20.43±0.028	20.21±0.037	20.49±0.195	0.05	2
LBQS 0048+0025	1.188	00 : 51 : 30.49	+00 : 41 : 49.9	0.10	18.69±0.015	18.44±0.01	18.25±0.01	18.19±0.01	18.19±0.027	0.02	1
LBQS 0049-0123	1.560	00 : 51 : 35.28	−01 : 07 : 09.1	0.29	18.20±0.012	17.83±0.01	17.73±0.01	17.52±0.01	17.57±0.017	0.04	1
LBQS 0049-0104	2.096	00 : 51 : 38.33	−00 : 48 : 12.0	2.74	19.98±0.048	19.91±0.019	19.84±0.020	19.51±0.024	19.23±0.065	0.05	1
LBQS 0049-0012	1.966	00 : 51 : 57.24	+00 : 03 : 54.9	0.66	18.24±0.013	17.94±0.01	17.84±0.01	17.63±0.01	17.58±0.020	0.03	1
LBQS 0049+0045	2.265	00 : 52 : 02.41	+01 : 01 : 29.3	0.27	17.77±0.011	17.37±0.01	17.28±0.01	17.22±0.01	17.01±0.011	0.03	1
LBQS 0049-0053	1.402	00 : 52 : 25.23	−00 : 37 : 04.8	0.51	18.65±0.019	18.45±0.01	18.23±0.01	18.02±0.01	18.03±0.023	0.04	1
LBQS 0049+0003	1.324	00 : 52 : 25.33	+00 : 20 : 06.7	0.57	19.24±0.022	19.30±0.010	19.05±0.010	18.93±0.013	18.99±0.066	0.02	1
LBQS 0049+0019	0.400	00 : 52 : 26.84	+00 : 35 : 38.9	0.62	19.61±0.035	18.60±0.01	18.17±0.01	17.96±0.01	17.89±0.020	0.02	1
LBQS 0050-0033	1.676	00 : 52 : 56.92	−00 : 17 : 09.2	0.40	19.19±0.026	19.04±0.01	18.83±0.010	18.46±0.010	18.33±0.032	0.03	1
SDSSp J005348.66-002157.2	3.740	00 : 53 : 48.66	−00 : 21 : 57.2	0.09	24.59±0.715	22.16±0.119	20.46±0.034	20.31±0.046	20.63±0.224	0.03	2
LBQS 0051-0019	1.713	00 : 53 : 55.15	−00 : 03 : 09.3	0.84	18.86±0.017	18.51±0.01	18.31±0.01	17.98±0.01	17.87±0.021	0.02	1
LBQS 0051-0035	0.940	00 : 54 : 08.98	−00 : 19 : 09.5	1.27	18.82±0.020	18.71±0.01	18.50±0.01	18.53±0.010	18.48±0.035	0.02	1
LBQS 0052-0015	0.648	00 : 54 : 41.19	+00 : 01 : 10.7	0.71	18.46±0.016	18.06±0.01	17.99±0.012	17.70±0.013	17.68±0.025	0.03	1
SDSSp J005452.86-001344.6	3.740	00 : 54 : 52.86	−00 : 13 : 44.6	0.04	23.73±0.850	21.31±0.056	20.18±0.029	20.14±0.041	20.17±0.149	0.03	2
LBQS 0052-0058	2.212	00 : 54 : 54.85	−00 : 42 : 44.2	0.71	18.32±0.015	18.01±0.01	18.00±0.01	17.83±0.01	17.65±0.018	0.03	1
LBQS 0052+0040	1.450	00 : 55 : 00.38	+00 : 56 : 37.4	0.70	19.02±0.025	18.86±0.01	18.67±0.01	18.56±0.012	18.76±0.039	0.03	1
[KB98] J0056-010	0.170	00 : 56 : 07.08	−01 : 03 : 40.4	0.62	20.41±0.065	19.10±0.011	18.45±0.01	18.07±0.01	17.84±0.021	0.03	1
LBQS 0053-0015	1.175	00 : 56 : 29.32	+00 : 01 : 09.3	0.44	18.76±0.020	18.58±0.01	18.54±0.01	18.51±0.011	18.51±0.044	0.02	1
[HB89] 0054-006	2.795	00 : 57 : 17.00	−00 : 24 : 33.2	0.22	20.05±0.044	19.19±0.010	19.17±0.010	19.10±0.014	18.87±0.052	0.03	1
LBQS 0055+0025	1.914	00 : 58 : 24.74	+00 : 41 : 13.4	1.04	17.14±0.01	17.06±0.01	16.94±0.01	16.71±0.01	16.60±0.01	0.03	1
LBQS 0056-0009	0.717	00 : 59 : 05.51	+00 : 06 : 51.6	0.22	17.86±0.010	17.56±0.01	17.52±0.01	17.52±0.01	17.40±0.016	0.03	1
LBQS 0056+0009	0.613	00 : 59 : 18.22	+00 : 25 : 19.8	0.40	18.55±0.014	18.17±0.01	18.12±0.01	18.03±0.01	17.85±0.026	0.03	1

Table 2—Continued

Name	z_{em}	RA(2000)	DEC(2000)	Δ''	u^*	g^*	r^*	i^*	z^*	$E(g^*-r^*)$	source
SDSSp J005922.65+000301.4	4.160	00 : 59 : 22.65	+00 : 03 : 01.4	0.02	23.68±0.776	22.45±0.156	19.26±0.014	19.14±0.017	19.07±0.066	0.03	2
LBQS 0057+0000	0.776	01 : 00 : 02.31	+00 : 16 : 42.7	0.70	17.62±0.01	17.33±0.01	17.26±0.01	17.32±0.01	17.08±0.014	0.03	1
DMS 0059-0051	0.840	01 : 01 : 37.67	-00 : 35 : 23.3	1.74	20.72±0.069	20.21±0.020	19.92±0.019	19.75±0.025	19.58±0.088	0.05	1
DMS 0059-0056	2.630	01 : 01 : 42.96	-00 : 40 : 02.3	1.54	21.69±0.230	21.63±0.078	21.49±0.089	21.36±0.120	20.76±0.241	0.04	1
DMS 0059-0103	0.710	01 : 01 : 45.67	-00 : 47 : 03.2	1.23	21.15±0.147	20.89±0.041	20.88±0.052	20.88±0.076	20.99±0.249	0.04	1
LBQS 0059+0004	0.323	01 : 01 : 51.07	+00 : 20 : 29.0	0.38	19.22±0.022	18.80±0.01	18.56±0.01	18.53±0.010	17.90±0.026	0.03	1
DMS 0059-0059	1.920	01 : 02 : 11.34	-00 : 43 : 43.1	0.55	20.61±0.081	20.98±0.044	20.94±0.055	20.68±0.067	20.35±0.162	0.04	1
DMS 0059-0104	1.050	01 : 02 : 11.84	-00 : 48 : 13.5	0.81	23.45±0.770	23.05±0.258	22.21±0.171	21.68±0.165	21.39±0.372	0.04	1
DMS 0059-0055	0.296	01 : 02 : 26.31	-00 : 39 : 04.6	0.66	16.36±0.01	16.23±0.01	16.15±0.01	16.31±0.01	15.91±0.01	0.04	1
LBQS 0059+0035	2.545	01 : 02 : 27.51	+00 : 51 : 36.9	0.23	19.07±0.025	18.53±0.01	18.24±0.01	18.25±0.010	18.10±0.021	0.03	1
DMS 0100.1-0058	1.730	01 : 02 : 41.04	-00 : 42 : 08.9	1.06	19.52±0.034	19.23±0.012	19.10±0.012	18.72±0.014	18.72±0.041	0.03	1
DMS 0100.3-0058	1.170	01 : 02 : 52.27	-00 : 42 : 04.5	1.22	20.25±0.065	20.21±0.021	19.92±0.023	19.86±0.035	19.94±0.119	0.03	1
DMS 0100-0057	0.770	01 : 03 : 11.64	-00 : 41 : 38.9	1.09	21.15±0.130	20.89±0.041	20.59±0.044	20.17±0.043	20.04±0.128	0.04	1
LBQS 0101+0009	0.394	01 : 03 : 42.73	+00 : 25 : 37.4	0.59	17.75±0.01	17.47±0.01	17.45±0.01	17.35±0.01	16.98±0.013	0.04	1
LBQS 0101-0130	1.156	01 : 04 : 30.58	-01 : 14 : 30.3	1.42	18.50±0.016	18.37±0.01	18.11±0.01	18.14±0.01	18.27±0.031	0.05	1
LBQS 0102-0106	1.588	01 : 05 : 08.14	-00 : 50 : 41.3	0.66	18.39±0.013	18.01±0.01	17.86±0.01	17.61±0.01	17.64±0.018	0.03	1
LBQS 0102+0036	0.649	01 : 05 : 09.30	+00 : 52 : 58.8	0.16	18.59±0.018	18.21±0.01	18.16±0.01	18.11±0.01	18.26±0.029	0.03	1
LBQS 0103-0014	1.629	01 : 06 : 29.60	+00 : 01 : 22.3	0.30	18.69±0.019	18.49±0.01	18.38±0.01	18.15±0.01	18.06±0.030	0.02	1
LBQS 0104+0001	0.910	01 : 06 : 36.55	+00 : 17 : 13.6	0.88	18.36±0.013	18.03±0.01	17.91±0.01	18.00±0.01	17.87±0.026	0.03	1
LBQS 0104+0030	1.874	01 : 06 : 48.02	+00 : 46 : 27.9	0.35	18.44±0.013	18.46±0.01	18.45±0.01	18.22±0.01	18.10±0.025	0.03	1
LBQS 0105-0035	0.737	01 : 07 : 37.01	-00 : 19 : 11.5	0.49	18.70±0.018	18.36±0.01	18.25±0.01	18.22±0.01	18.12±0.027	0.03	1
SDSSp J010822.70+001147.9	3.700	01 : 08 : 22.70	+00 : 11 : 48.0	0.08	23.36±0.720	20.71±0.034	19.42±0.038	19.47±0.043	19.50±0.105	0.03	2
UM 305	1.378	01 : 08 : 26.85	-00 : 37 : 24.2	0.25	17.88±0.012	17.69±0.01	17.41±0.01	17.24±0.01	17.20±0.012	0.03	1
LBQS 0106-0026	1.243	01 : 08 : 41.38	-00 : 10 : 03.0	0.27	18.60±0.014	18.58±0.01	18.31±0.01	18.25±0.01	18.31±0.030	0.03	1
LBQS 0106-0113	1.668	01 : 08 : 55.02	-00 : 57 : 47.2	0.29	18.12±0.010	17.92±0.01	17.79±0.01	17.53±0.01	17.49±0.016	0.08	1
SDSSp J010905.81+001617.1	3.690	01 : 09 : 05.81	+00 : 16 : 17.2	0.06	24.29±0.605	22.03±0.075	20.78±0.038	20.66±0.056	21.24±0.430	0.03	2
LBQS 0107+0051	0.966	01 : 09 : 47.43	+01 : 07 : 50.6	1.16	18.62±0.014	18.45±0.01	18.19±0.01	18.30±0.01	18.27±0.031	0.03	1
LBQS 0107+0022	1.968	01 : 09 : 54.37	+00 : 38 : 12.9	0.40	18.78±0.019	18.68±0.01	18.52±0.01	18.39±0.011	18.27±0.025	0.03	1
LBQS 0107-0128	1.455	01 : 09 : 54.86	-01 : 12 : 46.8	0.89	18.82±0.019	18.73±0.01	18.58±0.01	18.34±0.010	18.32±0.030	0.07	1
LBQS 0107-0031	1.753	01 : 10 : 24.51	-00 : 15 : 43.8	0.78	19.21±0.025	19.06±0.010	18.95±0.011	18.58±0.011	18.55±0.035	0.03	1
NGC 0450:[GMS97]068	0.468	01 : 10 : 33.46	+00 : 08 : 30.9	0.56	19.33±0.027	19.09±0.01	19.15±0.014	18.95±0.014	18.85±0.055	0.02	1
NGC 0450:[GMS97]101	1.424	01 : 10 : 37.43	-00 : 27 : 42.1	1.12	19.54±0.027	19.31±0.010	18.85±0.01	18.61±0.011	18.84±0.045	0.03	1
LBQS 0108+0028	2.005	01 : 10 : 38.09	+00 : 44 : 54.0	0.97	18.37±0.012	18.30±0.01	18.27±0.01	18.03±0.01	17.83±0.020	0.03	1
LBQS 0108+0030	0.428	01 : 10 : 52.86	+00 : 46 : 48.7	0.92	19.45±0.024	19.29±0.010	19.38±0.013	19.23±0.018	18.91±0.049	0.03	1
NGC 0450:[GMS97]041	1.003	01 : 11 : 24.43	+00 : 26 : 47.0	0.44	18.64±0.017	18.55±0.01	18.29±0.01	18.28±0.01	18.20±0.024	0.03	1
LBQS 0109-0128	1.758	01 : 12 : 27.61	-01 : 12 : 21.7	0.33	18.46±0.014	18.13±0.01	18.01±0.01	17.71±0.01	17.68±0.017	0.07	1
LBQS 0110-0107	1.896	01 : 12 : 40.24	-00 : 52 : 03.5	1.01	19.33±0.022	19.18±0.010	19.13±0.010	18.89±0.013	18.84±0.051	0.03	1
PB 06317	1.230	01 : 12 : 54.92	+00 : 03 : 13.1	0.35	17.64±0.01	17.61±0.01	17.54±0.01	17.30±0.01	17.31±0.016	0.04	1
NGC 0450:[GMS97]030	0.910	01 : 12 : 55.87	+00 : 44 : 09.6	1.14	20.10±0.038	19.95±0.016	19.92±0.018	19.59±0.024	19.38±0.074	0.03	1
LBQS 0110-0015	0.976	01 : 13 : 01.74	-00 : 00 : 04.0	0.61	18.99±0.018	18.68±0.01	18.30±0.01	18.28±0.01	18.02±0.026	0.03	1
LBQS 0110-0009	1.686	01 : 13 : 01.84	+00 : 06 : 33.5	0.78	18.09±0.012	17.93±0.01	17.91±0.01	17.79±0.01	17.77±0.023	0.03	1
LBQS 0110-0047	0.412	01 : 13 : 10.39	-00 : 31 : 33.3	0.76	19.33±0.024	19.00±0.01	19.02±0.010	18.80±0.011	18.48±0.035	0.03	1
NGC 0450:[GMS97]105	0.935	01 : 13 : 26.64	-00 : 26 : 02.9	0.58	20.27±0.049	19.86±0.015	19.73±0.015	19.78±0.025	19.64±0.096	0.03	1
NGC 0450:[GMS97]106	0.995	01 : 13 : 39.39	-00 : 30 : 09.3	0.36	18.60±0.015	18.53±0.01	18.43±0.01	18.57±0.010	18.50±0.036	0.03	1
NGC 0450:[GMS97]107	0.181	01 : 13 : 59.54	-00 : 32 : 48.7	0.96	19.22±0.023	19.15±0.010	18.72±0.01	18.23±0.01	18.00±0.023	0.03	1
NGC 0450:[GMS97]129	0.350	01 : 14 : 02.36	-00 : 47 : 50.9	0.67	18.79±0.020	18.77±0.01	18.62±0.01	18.57±0.011	18.08±0.025	0.03	1
NGC 0450:[GMS97]093	1.908	01 : 14 : 30.61	-00 : 15 : 50.6	1.46	20.12±0.050	20.15±0.022	20.03±0.023	19.84±0.027	19.99±0.131	0.03	1
[HB89] 0112-014	2.200	01 : 14 : 39.86	-01 : 10 : 53.8	0.62	20.65±0.081	20.47±0.033	20.56±0.033	20.31±0.047	20.03±0.143	0.10	1
NGC 0450:[GMS97]245	1.585	01 : 15 : 29.46	-00 : 57 : 23.7	0.59	20.20±0.042	19.91±0.017	19.82±0.018	19.63±0.025	19.65±0.103	0.04	1
NGC 0450:[GMS97]058	1.279	01 : 15 : 37.72	+00 : 20 : 28.7	1.28	19.19±0.022	19.17±0.01	18.93±0.01	18.89±0.013	18.99±0.069	0.03	1
NGC 0450:[GMS97]131	1.968	01 : 15 : 47.94	-00 : 47 : 13.7	0.91	19.80±0.046	19.76±0.016	19.64±0.018	19.38±0.019	19.28±0.068	0.04	1

Table 2—Continued

Name	z_{em}	RA(2000)	DEC(2000)	Δ''	u^*	g^*	r^*	i^*	z^*	$E(g^*-r^*)$	source
NGC 0450:[GMS97]142	2.055	01 : 16 : 11.94	-01 : 02 : 24.6	0.97	19.33±0.029	19.39±0.013	19.40±0.015	19.20±0.020	19.00±0.054	0.04	1
NGC 0450:[GMS97]119	1.263	01 : 16 : 15.51	-00 : 43 : 34.8	1.35	19.09±0.026	18.80±0.01	18.52±0.01	18.48±0.012	18.45±0.032	0.04	1
NGC 0450:[GMS97]073	1.316	01 : 16 : 33.69	+00 : 06 : 25.4	1.71	18.84±0.020	18.73±0.01	18.49±0.01	18.44±0.010	18.45±0.041	0.03	1
UM 314	2.175	01 : 18 : 27.98	-00 : 52 : 39.9	0.27	18.62±0.014	18.21±0.01	18.12±0.01	18.00±0.01	17.72±0.020	0.04	1
NGC 0450:[GMS97]120	1.052	01 : 19 : 22.86	-00 : 44 : 19.8	0.67	18.57±0.018	18.42±0.01	18.18±0.01	18.12±0.01	18.02±0.022	0.04	1
1RXS J011929.1-000834	0.090	01 : 19 : 29.06	-00 : 08 : 39.7	0.89	18.57±0.014	18.08±0.01	17.83±0.01	17.38±0.01	17.12±0.013	0.04	1
NGC 0450:[GMS97]044	0.648	01 : 20 : 12.14	+00 : 27 : 03.3	1.16	19.27±0.024	19.03±0.01	19.02±0.011	18.92±0.016	18.93±0.047	0.03	1
NGC 0450:[GMS97]146	0.203	01 : 20 : 15.13	-00 : 58 : 38.7	0.82	19.83±0.032	19.50±0.012	18.82±0.01	18.35±0.01	18.10±0.026	0.04	1
SDSSp J012019.99+000735.5	4.080	01 : 20 : 19.99	+00 : 07 : 35.6	0.06	23.77±0.820	21.51±0.064	20.02±0.025	19.82±0.030	20.08±0.162	0.04	2
NGC 0450:[GMS97]045	0.328	01 : 21 : 28.09	+00 : 34 : 50.6	0.18	18.97±0.022	18.89±0.01	18.72±0.01	18.64±0.012	17.97±0.022	0.03	1 2
MRK 1503	0.054	01 : 21 : 59.82	-01 : 02 : 24.4	0.48	16.92±0.01	16.59±0.01	16.43±0.01	16.03±0.01	15.98±0.01	0.04	1
NGC 0450:[GMS97]122	1.949	01 : 22 : 01.23	-00 : 39 : 40.5	0.09	19.01±0.025	19.00±0.010	18.95±0.011	18.80±0.013	18.65±0.039	0.05	1 2
NGC 0450:[GMS97]076	0.909	01 : 22 : 39.10	+00 : 05 : 30.0	0.19	19.31±0.028	19.00±0.01	18.76±0.01	18.85±0.013	18.75±0.050	0.03	1 2
FIRST J012240.1-003239	0.887	01 : 22 : 40.12	-00 : 32 : 39.7	0.03	18.96±0.019	18.28±0.01	18.15±0.01	18.09±0.01	17.88±0.021	0.05	2
NGC 0450:[GMS97]077	1.355	01 : 23 : 01.79	+00 : 03 : 23.4	0.37	18.97±0.020	18.92±0.01	18.53±0.01	18.58±0.011	18.71±0.048	0.04	1
NGC 0450:[GMS97]047	0.770	01 : 23 : 09.04	+00 : 33 : 05.5	0.02	19.26±0.027	18.89±0.01	18.89±0.010	19.11±0.018	18.76±0.041	0.03	1 2
NGC 0450:[GMS97]018	1.310	01 : 23 : 40.08	+01 : 03 : 32.0	0.34	19.62±0.038	19.50±0.013	19.29±0.015	19.26±0.021	19.29±0.076	0.03	1
NGC 0450:[GMS97]020	1.554	01 : 24 : 14.50	+01 : 11 : 15.1	0.20	19.04±0.021	18.78±0.01	18.68±0.01	18.49±0.011	18.18±0.033	0.03	1 2
NGC 0450:[GMS97]123	2.252	01 : 24 : 15.53	-00 : 33 : 18.6	0.66	19.32±0.024	18.66±0.01	18.71±0.01	18.64±0.013	18.34±0.032	0.04	1
NGC 0450:[GMS97]022	2.041	01 : 24 : 18.19	+01 : 08 : 39.5	0.07	19.43±0.027	19.35±0.010	19.32±0.013	19.11±0.018	18.55±0.046	0.03	1 2
UM 320	2.271	01 : 25 : 17.15	-00 : 18 : 28.9	0.15	19.02±0.023	18.26±0.01	18.36±0.01	18.21±0.01	18.02±0.023	0.03	1 2
UM 321	1.070	01 : 25 : 28.84	-00 : 05 : 55.9	0.27	16.66±0.01	16.57±0.01	16.47±0.01	16.47±0.01	16.47±0.01	0.03	1
NGC 0450:[GMS97]097	1.889	01 : 25 : 44.01	-00 : 15 : 43.7	0.32	19.54±0.033	19.64±0.015	19.70±0.018	19.33±0.020	19.37±0.069	0.03	1
NGC 0450:[GMS97]099	1.761	01 : 26 : 02.20	-00 : 19 : 24.1	0.12	18.68±0.018	18.69±0.01	18.56±0.01	18.18±0.01	18.15±0.025	0.03	1 2
SDSSp J012700.69-004559.1	4.060	01 : 27 : 00.69	-00 : 45 : 59.0	0.05	24.86±0.643	19.79±0.017	18.28±0.01	18.04±0.01	18.08±0.024	0.04	2
UM 327	2.070	01 : 27 : 48.32	-00 : 13 : 33.1	0.31	18.09±0.012	17.91±0.01	17.71±0.01	17.50±0.01	17.34±0.014	0.04	1
FIRST J012841.8-003316	1.657	01 : 28 : 41.87	-00 : 33 : 17.2	0.07	19.69±0.031	19.01±0.01	18.57±0.01	18.24±0.01	18.20±0.027	0.03	2
FIRST J0129005.3-005450	0.706	01 : 29 : 05.33	-00 : 54 : 50.7	0.18	19.26±0.021	18.68±0.01	18.53±0.01	18.53±0.010	18.40±0.033	0.03	2
SDSSp J013108.19+005248.2	4.190	01 : 31 : 08.18	+00 : 52 : 48.2	0.08	22.95±0.522	22.11±0.106	20.39±0.035	20.03±0.039	20.28±0.151	0.02	2
UM 338	1.370	01 : 33 : 52.65	+01 : 13 : 45.4	0.94	18.26±0.013	18.30±0.01	18.12±0.01	18.15±0.01	17.28±0.016	0.03	1
UM 339	1.310	01 : 33 : 58.25	-00 : 03 : 33.1	2.23	18.36±0.013	18.24±0.01	18.59±0.01	18.84±0.012	19.26±0.067	0.03	1
UM 341	0.400	01 : 34 : 18.19	+00 : 15 : 36.8	0.31	16.74±0.01	16.57±0.01	16.60±0.01	16.60±0.01	16.21±0.01	0.02	1
[HB89] 0133+004NED02	1.460	01 : 35 : 55.46	+00 : 39 : 24.4	0.68	19.20±0.021	19.01±0.010	18.92±0.016	18.76±0.050	18.90±0.061	0.04	1
[HB89] 0133+004NED01	0.910	01 : 35 : 55.88	+00 : 40 : 16.9	0.37	18.84±0.016	18.44±0.01	18.21±0.01	18.20±0.01	17.98±0.022	0.03	1
UM 349	2.150	01 : 38 : 14.53	+00 : 00 : 03.6	0.60	19.36±0.023	19.07±0.01	18.94±0.01	18.80±0.011	18.49±0.034	0.05	1
SDSSp J013932.68-010115.2	3.687	01 : 39 : 32.68	-01 : 01 : 15.2	0.06	25.36±0.868	22.12±0.097	21.03±0.047	20.95±0.078	20.64±0.233	0.04	2
UM 357	0.334	01 : 40 : 17.07	-00 : 50 : 03.0	1.09	16.31±0.01	16.19±0.01	16.20±0.01	16.35±0.01	15.64±0.01	0.04	1
UM 359	1.650	01 : 40 : 54.47	+01 : 00 : 59.8	1.28	21.87±0.227	19.46±0.012	18.43±0.01	17.99±0.01	17.84±0.019	0.03	1
UM 365	1.930	01 : 45 : 01.51	+01 : 00 : 01.5	0.52	18.44±0.016	18.39±0.01	18.22±0.01	17.97±0.01	17.83±0.019	0.03	1
UM 368	3.159	01 : 46 : 19.98	-00 : 46 : 28.9	1.23	21.04±0.113	19.15±0.010	18.91±0.010	18.93±0.013	18.95±0.042	0.04	1
SDSSp J015015.58+004555.7	3.900	01 : 50 : 15.58	+00 : 45 : 55.6	0.07	24.63±0.553	22.39±0.102	20.80±0.039	20.51±0.054	20.43±0.188	0.03	2
UM 373	0.880	01 : 52 : 50.84	-00 : 54 : 19.6	1.82	19.08±0.018	18.79±0.01	18.64±0.01	18.66±0.011	18.59±0.039	0.02	1
MRK 1014	0.163	01 : 59 : 50.24	+00 : 23 : 40.9	0.63	15.65±0.01	15.76±0.01	15.83±0.01	15.59±0.01	15.59±0.01	0.03	1
NVSS J020106+003402	0.299	02 : 01 : 06.18	+00 : 34 : 00.2	1.19	19.35±0.026	19.06±0.01	18.43±0.01	18.14±0.01	17.83±0.018	0.02	1
SDSSp J020427.81-011239.6	3.920	02 : 04 : 27.80	-01 : 12 : 39.6	0.13	22.58±0.318	21.01±0.044	19.75±0.018	19.65±0.024	19.46±0.069	0.03	2
SDSSp J020731.68+010348.9	3.900	02 : 07 : 31.69	+01 : 03 : 48.9	0.11	23.16±0.486	21.33±0.047	20.23±0.027	20.04±0.035	19.92±0.110	0.03	2
UM 400	1.887	02 : 08 : 45.53	+00 : 22 : 36.1	0.09	17.06±0.01	17.12±0.01	17.13±0.01	16.85±0.01	16.74±0.011	0.02	1 2
UM 402	2.856	02 : 09 : 50.71	-00 : 05 : 06.4	0.46	18.21±0.012	17.08±0.01	17.03±0.01	16.90±0.01	16.80±0.010	0.03	1
UM 403	2.186	02 : 09 : 53.16	+00 : 55 : 11.1	0.31	18.86±0.020	18.70±0.01	18.67±0.01	18.56±0.011	18.33±0.028	0.03	1 2
SDSSp J021043.17-001818.4	4.790	02 : 10 : 43.16	-00 : 18 : 18.3	0.21	23.59±0.668	22.87±0.156	20.74±0.041	19.28±0.015	19.31±0.060	0.03	2
SDSSp J021102.72-000910.3	4.900	02 : 11 : 02.72	-00 : 09 : 10.2	0.08	23.19±0.450	23.54±0.290	21.54±0.079	19.96±0.036	19.78±0.121	0.03	2

Table 2—Continued

Name	z_{em}	RA(2000)	DEC(2000)	Δ''	u^*	g^*	r^*	i^*	z^*	$E(g^*-r^*)$	source
FIRST J021225.5+010056	0.512	02 : 12 : 25.57	+01 : 00 : 56.1	0.31	18.46±0.016	18.26±0.01	18.38±0.01	18.20±0.01	18.17±0.023	0.03	2
FIRST J021229.8+000934	0.581	02 : 12 : 29.82	+00 : 09 : 34.0	0.07	20.37±0.058	19.64±0.013	19.15±0.012	18.56±0.010	18.61±0.043	0.03	2
FIRST J0213009.3-004734	1.513	02 : 13 : 09.33	−00 : 47 : 35.3	0.18	19.20±0.026	18.78±0.01	18.45±0.01	18.17±0.01	18.18±0.024	0.03	2
UM 414	2.370	02 : 15 : 58.51	−00 : 51 : 20.4	1.40	18.60±0.015	18.40±0.01	18.30±0.01	18.05±0.01	18.12±0.031	0.04	1
UM 416	2.150	02 : 16 : 12.20	−01 : 05 : 18.8	0.25	18.10±0.012	17.95±0.01	17.73±0.01	17.46±0.01	17.52±0.015	0.03	1
SDSSp J022239.42-005806.3	3.634	02 : 22 : 39.42	−00 : 58 : 06.4	0.11	24.48±0.596	21.34±0.052	20.23±0.027	20.06±0.039	19.96±0.138	0.04	2
[HB89] 0222+000	0.523	02 : 25 : 08.08	+00 : 17 : 07.3	0.49	18.81±0.016	18.45±0.01	18.51±0.01	18.26±0.01	18.20±0.034	0.04	1
NGC 0936 UB1	1.130	02 : 28 : 27.89	−01 : 10 : 45.9	0.11	18.95±0.019	19.05±0.010	18.81±0.01	18.80±0.013	18.95±0.045	0.03	1
SDSSp J023446.58-001415.9	3.603	02 : 34 : 46.58	−00 : 14 : 16.0	0.08	23.99±0.666	21.48±0.056	20.27±0.026	20.15±0.031	20.42±0.151	0.02	2
SDSSp J023749.33+005715.6	3.570	02 : 37 : 49.34	+00 : 57 : 15.6	0.10	23.04±0.498	21.70±0.071	20.65±0.038	20.62±0.058	20.60±0.193	0.03	2
SDSSp J023908.98-002121.5	3.731	02 : 39 : 08.99	−00 : 21 : 21.4	0.16	24.79±0.652	21.06±0.039	19.66±0.016	19.57±0.018	19.38±0.066	0.03	2
SDSSp J023935.25+010256.9	4.050	02 : 39 : 35.27	+01 : 02 : 56.8	0.28	23.11±0.515	22.50±0.140	20.72±0.043	20.55±0.057	20.52±0.190	0.04	2
[CLA95] 023803.96-000130.1	0.468	02 : 40 : 37.89	+00 : 11 : 18.9	1.72	19.27±0.025	19.00±0.01	18.88±0.01	18.68±0.011	18.49±0.037	0.03	1
[CLA95] 023853.53-005813.7	0.726	02 : 41 : 26.71	−00 : 45 : 26.2	1.67	18.56±0.016	18.36±0.01	18.27±0.01	18.29±0.01	18.18±0.023	0.03	1
[CLA95] 023907.70-000829.6	0.649	02 : 41 : 41.52	+00 : 04 : 16.6	1.88	18.67±0.017	18.49±0.01	18.55±0.01	18.46±0.01	18.64±0.042	0.03	1
[CLA95] 023921.95+002156.7	1.054	02 : 41 : 56.15	+00 : 34 : 42.0	2.47	18.85±0.018	18.83±0.01	18.59±0.01	18.72±0.012	18.81±0.037	0.03	1
[CLA95] 023923.29-000541.8	1.552	02 : 41 : 57.15	+00 : 07 : 03.6	2.31	19.15±0.023	18.85±0.01	18.68±0.01	18.46±0.010	18.49±0.036	0.03	1
[CLA95] 023927.14-001224.2	1.112	02 : 42 : 00.92	+00 : 00 : 21.0	2.03	19.08±0.020	18.99±0.01	18.60±0.01	18.74±0.011	18.85±0.047	0.04	1
[B99] J024207.2+000038	0.385	02 : 42 : 07.28	+00 : 00 : 38.7	1.32	19.91±0.034	19.75±0.013	19.40±0.012	19.14±0.015	18.73±0.042	0.03	1
E 0240+007	0.569	02 : 42 : 40.31	+00 : 57 : 27.2	0.53	16.50±0.01	16.22±0.01	16.29±0.01	16.20±0.01	16.26±0.01	0.04	1
[CLA95] 024030.91-001237.0	2.018	02 : 43 : 04.68	+00 : 00 : 05.5	1.36	18.57±0.015	18.43±0.01	18.28±0.01	18.03±0.01	17.84±0.020	0.03	1
SDSSp J024347.37-010611.7	3.890	02 : 43 : 47.37	−01 : 06 : 11.6	0.10	22.84±0.372	22.04±0.112	20.42±0.031	20.24±0.041	20.05±0.122	0.03	2
[CLA95] 024139.85+000554.5	0.684	02 : 44 : 13.83	+00 : 18 : 33.6	2.06	19.00±0.019	18.81±0.01	18.84±0.01	18.76±0.012	18.67±0.049	0.03	1
SDSSp J024434.87+000124.9	3.760	02 : 44 : 34.87	+00 : 01 : 24.9	0.04	23.34±0.634	21.93±0.081	20.52±0.033	20.47±0.042	20.43±0.202	0.04	2
SDSSp J024452.33-003318.0	3.970	02 : 44 : 52.33	−00 : 33 : 17.9	0.11	23.75±0.614	21.96±0.075	20.40±0.027	20.29±0.039	20.06±0.126	0.03	2
SDSSp J024457.19-010809.9	4.010	02 : 44 : 57.18	−01 : 08 : 09.9	0.09	22.81±0.377	20.04±0.020	18.62±0.01	18.33±0.01	18.16±0.024	0.03	2
4C +00.09	1.520	02 : 45 : 34.06	+01 : 08 : 13.8	0.22	20.05±0.042	19.25±0.010	18.63±0.01	18.31±0.010	18.24±0.030	0.04	1
[CLA95] 024328.29-011211.7	0.201	02 : 46 : 01.26	−00 : 59 : 37.3	0.93	18.48±0.013	18.39±0.01	18.16±0.01	17.79±0.01	17.76±0.020	0.03	1
US 3133	1.596	02 : 46 : 03.68	−00 : 32 : 11.8	0.30	19.00±0.019	18.68±0.01	18.54±0.01	18.25±0.01	18.19±0.026	0.03	1
[CTL96] 024333.27-010806.2	1.422	02 : 46 : 06.21	−00 : 55 : 31.9	0.22	20.10±0.038	20.06±0.018	19.86±0.019	19.78±0.028	19.89±0.119	0.03	1
US 3137	1.139	02 : 46 : 17.09	−00 : 06 : 02.6	0.43	18.49±0.014	18.45±0.01	18.19±0.01	18.15±0.01	18.24±0.028	0.03	1
US 3139	1.292	02 : 46 : 21.11	−00 : 01 : 52.0	0.20	18.88±0.017	18.82±0.01	18.43±0.01	18.33±0.01	18.37±0.031	0.03	1
[CTL96] 024355.42-005730.5	2.103	02 : 46 : 28.49	−00 : 44 : 57.3	0.70	19.85±0.042	19.58±0.014	19.60±0.017	19.47±0.021	19.16±0.055	0.03	1
[HB89] 0243-007	2.147	02 : 46 : 32.45	−00 : 32 : 14.3	1.08	19.38±0.024	19.03±0.01	18.92±0.01	18.76±0.011	18.57±0.036	0.03	1
[CLB91] 024358.7-000704	1.305	02 : 46 : 32.55	+00 : 05 : 29.0	0.72	19.62±0.033	19.48±0.011	19.19±0.012	19.08±0.014	19.14±0.064	0.03	1
[CTL96] 024359.35-004712.2	1.726	02 : 46 : 32.56	−00 : 34 : 39.2	0.58	20.17±0.043	19.91±0.015	19.93±0.018	19.64±0.022	19.85±0.108	0.04	1
[HB89] 0244-003	1.815	02 : 46 : 35.63	−00 : 08 : 50.5	0.60	18.45±0.017	18.55±0.01	18.50±0.01	18.25±0.01	18.20±0.028	0.04	1
[CTL96] 024404.84-005338.2	0.859	02 : 46 : 37.95	−00 : 41 : 05.4	0.98	19.93±0.046	19.59±0.014	19.50±0.016	19.62±0.025	19.52±0.074	0.03	1
[CTL96] 024406.25-001509.7	2.315	02 : 46 : 39.89	−00 : 02 : 37.1	0.22	21.90±0.162	20.71±0.026	20.70±0.033	20.56±0.048	19.92±0.121	0.03	1
[CTL96] 024417.87-005729.3	2.172	02 : 46 : 50.94	−00 : 44 : 57.3	0.72	19.67±0.038	19.44±0.012	19.19±0.012	19.04±0.014	18.89±0.042	0.04	1
[HB89] 0244-012	0.467	02 : 46 : 51.91	−00 : 59 : 31.0	0.20	17.23±0.01	16.89±0.01	16.91±0.01	16.76±0.01	16.73±0.01	0.04	1
[CTL96] 024427.45-000901.2	2.137	02 : 47 : 01.19	+00 : 03 : 30.3	1.40	20.61±0.071	19.73±0.013	19.16±0.012	18.78±0.011	18.45±0.036	0.04	1
[CTL96] 024506.14-010450.9	2.125	02 : 47 : 39.12	−00 : 52 : 21.2	0.30	20.44±0.050	20.34±0.023	20.08±0.022	19.94±0.030	19.64±0.096	0.05	1
[CTL96] 024514.58-010039.2	1.918	02 : 47 : 47.60	−00 : 48 : 10.1	0.10	19.64±0.032	19.62±0.014	19.53±0.016	19.27±0.018	19.12±0.054	0.04	1
[CTL96] 024515.22-001416.8	1.859	02 : 47 : 48.87	−00 : 01 : 47.6	0.61	19.43±0.025	19.33±0.010	19.30±0.011	18.97±0.015	18.90±0.049	0.04	1
[HB89] 0245-004	2.118	02 : 47 : 56.35	−00 : 15 : 56.1	0.68	18.41±0.014	18.16±0.01	18.03±0.01	18.00±0.01	17.76±0.018	0.04	1
[CTL96] 024527.96-005244.3	0.812	02 : 48 : 01.10	−00 : 40 : 15.8	0.17	19.42±0.030	19.20±0.010	19.17±0.012	19.32±0.018	19.15±0.054	0.04	1
[CTL96] 024533.58+002323.9	0.835	02 : 48 : 07.72	+00 : 35 : 52.1	0.27	19.84±0.037	19.56±0.013	19.46±0.015	19.44±0.021	19.28±0.060	0.05	1
[CTL96] 024541.80+001649.0	1.030	02 : 48 : 15.85	+00 : 29 : 16.7	0.87	20.21±0.049	20.03±0.018	19.77±0.018	19.85±0.029	19.84±0.095	0.04	1
[CTL96] 024547.58-003814.4	1.450	02 : 48 : 20.91	−00 : 25 : 46.9	0.18	20.16±0.044	19.78±0.014	19.55±0.014	19.38±0.018	19.23±0.063	0.04	1
[CTL96] 024549.38+002325.5	1.015	02 : 48 : 23.52	+00 : 35 : 52.7	0.43	19.81±0.036	19.72±0.015	19.53±0.015	19.55±0.024	19.55±0.074	0.05	1

Table 2—Continued

Name	z_{em}	RA(2000)	DEC(2000)	Δ''	u^*	g^*	r^*	i^*	z^*	$E(g^*-r^*)$	source
[CTL96] 024557.55+003706.0	1.598	02 : 48 : 31.85	+00 : 49 : 33.1	0.81	19.74±0.030	19.50±0.011	19.46±0.013	19.23±0.018	19.21±0.062	0.06	1
US 3182	1.822	02 : 48 : 33.89	−00 : 46 : 16.4	0.47	18.60±0.017	18.50±0.01	18.33±0.01	17.95±0.01	17.90±0.019	0.06	1
US 3187	2.239	02 : 48 : 40.78	−00 : 35 : 48.3	0.41	19.37±0.024	18.89±0.01	18.79±0.01	18.68±0.012	18.51±0.035	0.04	1
US 3186	1.684	02 : 48 : 40.98	−00 : 12 : 29.0	0.24	19.24±0.025	19.08±0.01	18.65±0.01	18.58±0.010	18.69±0.038	0.06	1
[CTL96] 024613.67-005729.4	1.704	02 : 48 : 46.72	−00 : 45 : 03.2	0.38	20.39±0.066	20.33±0.022	20.36±0.030	20.22±0.037	20.25±0.141	0.05	1
[CTL96] 024621.63+001040.8	1.017	02 : 48 : 55.61	+00 : 23 : 06.4	0.61	19.61±0.029	19.55±0.012	19.35±0.012	19.49±0.021	19.54±0.111	0.06	1
US 3193	1.709	02 : 48 : 56.53	−00 : 56 : 04.4	0.60	18.92±0.017	18.78±0.01	18.76±0.01	18.57±0.014	18.53±0.037	0.05	1
[CTL96] 024633.65-001914.8	2.249	02 : 49 : 07.30	−00 : 06 : 49.5	1.64	20.30±0.045	19.74±0.013	19.69±0.015	19.62±0.022	19.22±0.070	0.05	1
[CTL96] 024652.63-003213.1	2.475	02 : 49 : 26.03	−00 : 19 : 48.9	0.44	20.32±0.057	19.68±0.014	19.61±0.016	19.56±0.021	19.29±0.061	0.05	1
[HB89] 0246+009	0.953	02 : 49 : 28.85	+01 : 09 : 24.7	0.83	18.56±0.016	18.44±0.01	18.33±0.01	18.45±0.011	18.28±0.035	0.05	1
US 3205	1.419	02 : 49 : 29.20	−00 : 21 : 04.3	0.32	20.04±0.046	19.34±0.011	18.89±0.01	18.55±0.010	18.49±0.031	0.05	1
[CTL96] 024709.99+002054.1	1.480	02 : 49 : 44.10	+00 : 33 : 17.3	0.68	20.05±0.044	19.88±0.017	19.69±0.017	19.47±0.022	19.45±0.067	0.06	1
US 3213	0.584	02 : 49 : 54.50	+01 : 01 : 48.1	0.11	19.63±0.037	19.25±0.011	19.30±0.014	19.02±0.016	19.12±0.056	0.06	1
[LCB92] 0247+0018	2.015	02 : 50 : 19.27	+00 : 31 : 00.7	0.47	19.66±0.033	19.65±0.014	19.64±0.017	19.52±0.023	19.55±0.075	0.06	1
SDSSp J025019.78+004650.3	4.740	02 : 50 : 19.78	+00 : 46 : 50.2	0.08	23.76±0.648	22.88±0.164	21.07±0.050	19.63±0.026	19.54±0.091	0.06	2
[HB89] 0247-003	1.458	02 : 50 : 30.78	−00 : 08 : 01.9	0.35	18.23±0.012	18.11±0.01	17.96±0.01	17.84±0.01	17.82±0.022	0.07	1
[HB89] 0248-009	1.845	02 : 50 : 38.68	−00 : 47 : 39.1	0.32	18.34±0.015	18.38±0.01	18.31±0.01	18.14±0.01	18.09±0.023	0.06	1
[CTL96] 024806.79-010010.3	2.422	02 : 50 : 39.82	−00 : 47 : 49.5	0.58	20.88±0.100	20.28±0.025	20.19±0.027	20.18±0.039	19.58±0.081	0.06	1
87GB[BWE91] 0248-0010	0.766	02 : 50 : 48.67	+00 : 02 : 07.6	0.27	19.13±0.024	18.67±0.01	18.45±0.01	18.63±0.011	18.40±0.038	0.08	1
[LCB92] 0248+0054	1.708	02 : 50 : 57.73	+01 : 06 : 54.8	0.52	19.72±0.036	19.47±0.011	19.36±0.014	19.18±0.019	18.96±0.065	0.06	1
[LCB92] 0248+0035	0.828	02 : 51 : 01.01	+00 : 48 : 02.9	0.13	19.55±0.027	19.28±0.010	19.17±0.011	19.27±0.019	19.09±0.060	0.06	1
[WB92] 0248-0005	1.435	02 : 51 : 02.70	+00 : 06 : 00.6	0.39	19.11±0.023	18.79±0.01	18.66±0.01	18.51±0.010	18.46±0.041	0.07	1
[LCB92] 0248-0039	2.329	02 : 51 : 28.74	−00 : 26 : 50.8	0.56	20.07±0.042	19.51±0.012	19.51±0.014	19.51±0.021	19.18±0.061	0.05	1
[LCB92] 0249-0058B	1.383	02 : 51 : 45.10	−00 : 46 : 39.8	0.17	19.64±0.039	19.66±0.015	19.32±0.014	19.28±0.018	19.13±0.059	0.06	1
[LCB92] 0249-0052	0.817	02 : 51 : 46.79	−00 : 40 : 35.7	0.74	19.45±0.033	19.21±0.010	19.22±0.013	19.21±0.017	19.09±0.057	0.06	1
[CLB91] 024915.5-005855	1.569	02 : 51 : 48.54	−00 : 46 : 37.8	0.95	19.48±0.034	19.28±0.011	19.26±0.013	19.02±0.014	18.95±0.051	0.06	1
[LCB92] 0249+0045	1.824	02 : 51 : 51.28	+00 : 57 : 39.1	0.33	19.60±0.037	19.76±0.016	19.75±0.020	19.40±0.022	19.28±0.073	0.07	1
LBQS 0249+0044	0.470	02 : 51 : 56.31	+00 : 57 : 06.3	0.25	18.98±0.024	18.65±0.01	18.72±0.01	18.46±0.011	18.17±0.028	0.07	1
[LCB92] 0249-0006B	2.099	02 : 52 : 09.80	+00 : 05 : 48.9	0.07	20.37±0.066	20.32±0.023	20.34±0.031	20.14±0.035	19.99±0.162	0.08	1
[LCB92] 0249+0015	1.678	02 : 52 : 20.55	+00 : 27 : 35.0	0.76	20.13±0.050	19.74±0.015	19.49±0.016	19.30±0.019	19.22±0.064	0.10	1
[VCV96] PB 6909	0.175	02 : 52 : 20.89	+00 : 43 : 31.3	1.40	19.14±0.022	18.93±0.01	18.40±0.01	17.90±0.01	17.72±0.019	0.08	1
LBQS 0249-0006	0.811	02 : 52 : 21.03	+00 : 05 : 59.2	0.92	17.54±0.01	17.17±0.01	17.03±0.01	17.13±0.01	16.96±0.012	0.07	1
[LCB92] 0249+0018	1.106	02 : 52 : 28.56	+00 : 31 : 09.0	0.95	18.82±0.018	18.71±0.01	18.48±0.01	18.44±0.010	18.35±0.030	0.10	1
[CLB91] 024955.2+004833	2.010	02 : 52 : 29.77	+01 : 00 : 49.1	0.51	19.59±0.038	19.61±0.014	19.51±0.016	19.29±0.020	19.07±0.086	0.07	1
[LCB92] 0250-0058	1.007	02 : 52 : 37.81	−00 : 46 : 28.0	0.12	19.82±0.045	19.67±0.015	19.36±0.014	19.31±0.019	19.25±0.062	0.07	1
[LCB92] 0250-0106	0.846	02 : 52 : 37.92	−00 : 54 : 06.5	0.58	20.12±0.041	19.72±0.014	19.56±0.016	19.48±0.023	19.37±0.077	0.07	1
US 3268	1.251	02 : 52 : 57.18	−01 : 02 : 20.9	0.39	19.68±0.038	19.43±0.014	19.02±0.011	18.96±0.016	18.99±0.051	0.07	1
[LCB92] 0250-0051	0.889	02 : 53 : 14.00	−00 : 39 : 02.5	0.50	20.09±0.058	19.69±0.015	19.36±0.014	19.40±0.021	19.22±0.059	0.07	1
[LCB92] 0250+0055	1.030	02 : 53 : 16.45	+01 : 07 : 59.8	0.70	19.19±0.024	18.87±0.01	18.62±0.01	18.63±0.012	18.38±0.041	0.07	1
[LCB92] 0250-0009	1.214	02 : 53 : 23.62	+00 : 02 : 30.5	0.59	19.80±0.042	19.65±0.014	19.34±0.013	19.26±0.018	19.35±0.085	0.07	1
[LCB92] 0250-0039	1.363	02 : 53 : 24.70	−00 : 26 : 55.8	0.25	19.81±0.035	19.65±0.012	19.20±0.011	19.10±0.015	19.03±0.053	0.07	1
[LCB92] 0250+0004	1.810	02 : 53 : 31.93	+00 : 16 : 24.8	0.55	19.27±0.023	19.06±0.01	19.00±0.01	18.73±0.011	18.58±0.045	0.09	1
LBQS 0251-0001	1.682	02 : 53 : 40.94	+00 : 11 : 10.1	0.30	18.94±0.022	18.72±0.01	18.42±0.01	18.05±0.01	18.01±0.026	0.08	1
[CLB91] 025112.1-005918	2.449	02 : 53 : 45.20	−00 : 47 : 06.1	0.10	19.34±0.031	18.74±0.01	18.57±0.01	18.54±0.011	18.34±0.028	0.07	1
[LCB92] 0251-0001B	1.688	02 : 53 : 56.08	+00 : 10 : 57.5	0.66	19.48±0.032	19.32±0.011	19.23±0.012	19.03±0.015	19.09±0.067	0.08	1
[LCB92] 0251-0023	0.757	02 : 53 : 56.81	−00 : 11 : 23.8	0.28	19.42±0.025	19.05±0.01	18.82±0.01	18.87±0.013	18.68±0.041	0.08	1
US 3309	1.986	02 : 54 : 01.45	+00 : 29 : 16.2	0.74	19.32±0.027	19.18±0.010	19.15±0.012	18.93±0.015	18.82±0.041	0.10	1
[LCB92] 0251-0004	1.213	02 : 54 : 22.86	+00 : 07 : 58.8	0.89	19.98±0.049	20.01±0.018	19.60±0.017	19.61±0.024	19.77±0.122	0.08	1
[LCB92] 0251-0101	1.955	02 : 54 : 32.32	−00 : 49 : 32.8	0.43	20.68±0.061	20.49±0.026	20.35±0.028	20.03±0.035	19.88±0.120	0.07	1
LBQS 0251-0054	0.433	02 : 54 : 32.52	−00 : 42 : 20.1	0.38	18.71±0.019	18.25±0.01	18.19±0.01	17.93±0.01	17.57±0.016	0.06	1
US 3333	0.354	02 : 55 : 05.67	+00 : 25 : 23.2	0.51	17.73±0.01	17.73±0.01	17.81±0.01	17.86±0.01	17.31±0.016	0.08	1

Table 2—Continued

Name	z_{em}	RA(2000)	DEC(2000)	Δ''	u^*	g^*	r^*	i^*	z^*	$E(g^*-r^*)$	source
[LCB92] 0252-0005	1.885	02 : 55 : 13.03	+00 : 06 : 39.5	0.72	19.13±0.025	19.17±0.011	19.24±0.013	19.01±0.015	18.79±0.053	0.07	1
[LCB92] 0252-0014	1.426	02 : 55 : 28.94	−00 : 02 : 19.1	0.59	19.56±0.027	19.41±0.010	19.17±0.011	19.10±0.015	19.18±0.062	0.07	1
[HB89] 0253+004	0.921	02 : 55 : 47.06	+00 : 38 : 14.9	0.62	19.75±0.037	19.11±0.010	18.78±0.010	18.84±0.015	18.66±0.036	0.09	1
[HB89] 0253+006	0.847	02 : 55 : 59.91	+00 : 53 : 11.4	0.62	18.85±0.021	18.51±0.01	18.44±0.01	18.43±0.011	18.31±0.029	0.10	1
[LCB92] 0253+0040	0.531	02 : 56 : 02.57	+00 : 52 : 55.3	0.87	19.97±0.049	19.52±0.012	19.54±0.017	19.17±0.019	19.31±0.067	0.10	1
[LCB92] 0253+0058	1.347	02 : 56 : 07.24	+01 : 10 : 38.7	0.93	19.23±0.025	18.99±0.01	18.68±0.01	18.52±0.011	18.54±0.040	0.09	1
[LCB92] 0253+0003	2.012	02 : 56 : 13.16	+00 : 15 : 08.3	0.94	20.39±0.050	20.19±0.019	19.97±0.020	19.78±0.026	19.35±0.092	0.07	1
US 3375	0.916	02 : 56 : 14.04	+00 : 39 : 41.2	0.09	19.72±0.030	19.22±0.010	18.99±0.010	19.09±0.016	18.95±0.051	0.10	1
[CLA95] 025345.90-005705.1	0.720	02 : 56 : 19.00	−00 : 45 : 01.3	0.35	18.14±0.012	17.95±0.01	17.86±0.01	18.01±0.01	18.02±0.022	0.06	1
LBQS 0254+0000	2.247	02 : 56 : 44.69	+00 : 12 : 46.1	0.25	18.33±0.014	17.91±0.01	17.77±0.01	17.71±0.01	17.57±0.018	0.07	1
[LCB92] 0254+0042	1.115	02 : 56 : 58.62	+00 : 54 : 47.6	0.53	19.39±0.032	19.22±0.010	18.92±0.011	18.96±0.016	19.09±0.055	0.09	1
[LCB92] 0254-0114	0.876	02 : 57 : 02.08	−01 : 02 : 17.1	0.29	19.31±0.027	19.13±0.011	18.95±0.011	18.98±0.016	18.81±0.042	0.07	1
[LCB92] 0254-0022	1.585	02 : 57 : 05.88	−00 : 10 : 53.5	0.58	19.66±0.028	19.35±0.010	19.14±0.010	18.91±0.013	18.91±0.054	0.07	1
[CLB91] 025440.2-011359	1.866	02 : 57 : 13.07	−01 : 01 : 57.6	0.56	19.47±0.024	19.31±0.011	19.31±0.012	18.96±0.015	19.00±0.061	0.07	1
[LCB92] 0254-0057	1.032	02 : 57 : 16.87	−00 : 45 : 36.0	0.51	20.11±0.055	20.01±0.018	19.70±0.018	19.69±0.026	19.45±0.072	0.07	1
[LCB92] 0254-0010B	1.250	02 : 57 : 25.08	+00 : 01 : 14.3	0.41	20.01±0.047	19.99±0.016	19.55±0.015	19.60±0.023	19.81±0.122	0.06	1
[LCB92] 0254+0003	1.601	02 : 57 : 27.26	+00 : 15 : 45.9	0.84	20.12±0.040	19.87±0.015	19.74±0.016	19.57±0.022	19.34±0.094	0.07	1
[HB89] 0255+001	1.498	02 : 57 : 51.55	+00 : 20 : 45.6	0.84	20.08±0.041	19.65±0.013	19.34±0.012	19.03±0.014	18.94±0.067	0.07	1
[LCB92] 0255-0022	1.557	02 : 58 : 04.27	−00 : 10 : 59.9	0.41	19.81±0.034	19.58±0.012	19.46±0.013	19.23±0.016	19.26±0.072	0.08	1
US 3437	1.318	02 : 58 : 15.55	−00 : 03 : 34.1	0.73	19.28±0.023	19.26±0.010	18.89±0.01	18.81±0.012	18.87±0.051	0.08	1
[LCB92] 0255-0020	2.094	02 : 58 : 19.33	−00 : 08 : 06.2	0.47	20.06±0.041	20.00±0.016	19.75±0.016	19.48±0.020	19.22±0.069	0.08	1
[LCB92] 0256-0107	0.905	02 : 58 : 44.25	−00 : 55 : 12.6	0.98	20.24±0.046	19.74±0.015	19.56±0.015	19.58±0.024	19.36±0.080	0.11	1
[LCB92] 0256+0030	1.569	02 : 58 : 54.88	+00 : 42 : 21.8	0.38	20.63±0.061	20.29±0.021	20.07±0.022	19.76±0.029	19.80±0.117	0.08	1
LBQS 0256-0000	3.364	02 : 59 : 05.64	+00 : 11 : 21.9	0.64	20.99±0.107	18.08±0.01	17.66±0.01	17.60±0.01	17.54±0.018	0.08	1
NRRF J025906.8+000758	2.381	02 : 59 : 06.90	+00 : 07 : 57.6	0.39	20.04±0.047	19.40±0.011	19.31±0.014	19.20±0.017	19.03±0.061	0.08	1
LBQS 0256-0034	0.360	02 : 59 : 10.39	−00 : 22 : 39.8	0.23	18.29±0.014	18.11±0.01	17.90±0.01	17.94±0.01	17.41±0.014	0.10	1
US 3461	1.853	02 : 59 : 22.63	+00 : 58 : 29.4	0.78	18.71±0.019	18.68±0.01	18.59±0.01	18.34±0.010	18.22±0.026	0.08	1
LBQS 0256-0031	1.995	02 : 59 : 28.52	−00 : 19 : 60.0	0.01	17.38±0.01	17.43±0.01	17.31±0.01	17.01±0.01	16.83±0.01	0.10	1
US 3468	1.748	02 : 59 : 33.73	−00 : 25 : 17.7	1.26	18.81±0.018	18.69±0.010	18.65±0.031	18.33±0.024	18.35±0.043	0.12	1
[LCB92] 0257-0020	1.298	02 : 59 : 35.82	−00 : 09 : 02.7	0.37	20.01±0.039	19.66±0.013	19.31±0.012	19.31±0.018	19.50±0.090	0.09	1
LBQS 0257+0025	0.532	02 : 59 : 37.47	+00 : 37 : 36.2	0.49	16.70±0.01	16.45±0.01	16.47±0.01	16.29±0.01	16.37±0.01	0.09	1
[VCV96] S 0257+0030	0.197	02 : 59 : 38.15	+00 : 42 : 16.4	0.82	19.25±0.023	18.68±0.01	18.16±0.01	17.65±0.01	17.47±0.016	0.09	1
[LCB92] 0257-0109	0.661	02 : 59 : 39.39	−00 : 57 : 53.2	0.26	20.28±0.046	19.86±0.019	19.81±0.018	19.64±0.027	19.81±0.120	0.12	1
[LCB92] 0257-0010	1.710	02 : 59 : 49.09	+00 : 01 : 39.2	0.77	20.40±0.061	20.18±0.018	20.12±0.025	19.76±0.032	19.94±0.133	0.09	1
[VCV96] S 0257+0051	0.257	02 : 59 : 50.75	+01 : 03 : 04.5	0.93	19.46±0.032	19.09±0.01	18.51±0.01	18.16±0.01	17.84±0.020	0.08	1
[LCB92] 0257+0023B	0.820	02 : 59 : 57.86	+00 : 34 : 54.2	0.91	19.88±0.038	19.32±0.011	19.08±0.012	18.96±0.016	18.81±0.039	0.10	1
SDSSp J030025.23+003224.2	4.190	03 : 00 : 25.23	+00 : 32 : 24.3	0.12	22.76±0.317	22.01±0.087	19.99±0.021	19.94±0.033	19.76±0.085	0.10	2
US 3499	2.006	03 : 00 : 27.12	−00 : 48 : 48.8	0.81	19.11±0.024	19.13±0.01	18.96±0.011	18.73±0.011	18.52±0.030	0.12	1
[LCB92] 0257-0007	0.761	03 : 00 : 29.81	+00 : 04 : 21.0	0.18	19.94±0.042	19.64±0.012	19.61±0.017	19.76±0.025	19.64±0.097	0.11	1
[LCB92] 0257+0031	0.806	03 : 00 : 33.92	+00 : 43 : 24.8	0.38	20.02±0.039	19.63±0.013	19.54±0.015	19.38±0.022	19.20±0.068	0.10	1
[LCB92] 0258-0027	1.435	03 : 00 : 35.97	−00 : 15 : 32.9	1.03	19.03±0.022	18.91±0.01	18.71±0.01	18.55±0.010	18.58±0.032	0.11	1
[LCB92] 0258+0020	1.112	03 : 00 : 41.77	+00 : 32 : 37.6	0.57	19.21±0.024	19.11±0.01	18.87±0.010	18.84±0.013	18.90±0.040	0.10	1
[LCB92] 0258+0005	1.727	03 : 00 : 45.25	+00 : 16 : 56.7	0.78	19.15±0.022	18.91±0.01	18.79±0.01	18.46±0.010	18.32±0.041	0.11	1
[LCB92] 0258+0009	1.497	03 : 00 : 45.48	+00 : 21 : 33.1	0.38	19.78±0.034	19.56±0.012	19.41±0.013	19.16±0.017	19.19±0.087	0.11	1
US 3513	0.661	03 : 00 : 48.94	+00 : 54 : 40.8	0.60	18.89±0.021	18.54±0.01	18.46±0.01	18.41±0.010	18.35±0.028	0.09	1
[LCB92] 0259+0104	1.770	03 : 01 : 40.98	+01 : 15 : 51.1	0.39	19.61±0.034	19.59±0.011	19.14±0.012	18.71±0.014	18.44±0.042	0.10	1
US 3543	0.641	03 : 02 : 06.77	−00 : 01 : 21.1	0.43	19.53±0.033	19.02±0.01	19.03±0.010	18.88±0.013	18.89±0.050	0.11	1
[CTL96] 025941.16-001020.1	1.179	03 : 02 : 14.82	+00 : 01 : 25.3	0.78	19.96±0.041	19.86±0.015	19.57±0.016	19.52±0.020	19.47±0.084	0.11	1
LBQS 0259-0034	0.706	03 : 02 : 20.32	−00 : 22 : 22.8	0.84	19.31±0.025	18.85±0.01	18.71±0.01	18.56±0.010	18.47±0.030	0.12	1
CADIS 03h-0211	3.300	03 : 02 : 22.09	+00 : 06 : 31.0	0.16	23.25±0.579	21.15±0.039	20.46±0.033	20.29±0.038	20.12±0.145	0.10	1
CFRS 03.0106	2.070	03 : 02 : 23.11	+00 : 13 : 12.4	0.65	21.13±0.108	21.07±0.038	20.92±0.050	20.90±0.064	20.22±0.161	0.10	1

Table 2—Continued

Name	z_{em}	RA(2000)	DEC(2000)	Δ''	u^*	g^*	r^*	i^*	z^*	$E(g^*-r^*)$	source
CFRS 03.0603	1.048	03 : 02 : 33.18	+00 : 13 : 31.1	0.30	22.09±0.194	21.86±0.065	21.40±0.066	21.16±0.093	20.33±0.207	0.10	1
CADIS 03h-0238	1.030	03 : 02 : 42.82	+00 : 07 : 15.7	0.45	19.52±0.030	19.22±0.011	18.85±0.01	18.84±0.012	18.78±0.046	0.10	1
CADIS 03h-0224	0.900	03 : 02 : 43.55	+00 : 05 : 08.4	0.85	21.79±0.190	21.18±0.041	21.00±0.051	20.92±0.065	20.35±0.179	0.10	1
[HB89] 0300-004	0.699	03 : 03 : 13.03	-00 : 14 : 57.4	0.10	19.25±0.024	18.82±0.01	18.56±0.01	18.60±0.011	18.27±0.026	0.11	1 2
LBQS 0300-0018	0.703	03 : 03 : 15.67	-00 : 07 : 02.0	0.02	19.00±0.019	18.57±0.01	18.47±0.01	18.38±0.01	18.33±0.030	0.11	1 2
LBQS 0301-0035	3.219	03 : 03 : 41.05	-00 : 23 : 21.8	0.75	20.08±0.042	17.86±0.01	17.61±0.01	17.50±0.01	17.45±0.014	0.11	1
LBQS 0301+0015	1.644	03 : 03 : 42.79	+00 : 27 : 00.6	0.24	18.31±0.013	18.01±0.01	17.79±0.01	17.58±0.01	17.55±0.014	0.09	1 2
LBQS 0301+0010	0.639	03 : 04 : 22.39	+00 : 22 : 31.8	0.10	17.33±0.01	16.96±0.01	16.96±0.01	16.78±0.01	16.89±0.012	0.09	1 2
LBQS 0302-0019	3.281	03 : 04 : 49.86	-00 : 08 : 13.4	1.08	19.01±0.019	17.79±0.01	17.54±0.01	17.48±0.01	17.42±0.015	0.10	1
PMN J0304+0002	0.562	03 : 04 : 58.97	+00 : 02 : 35.7	0.10	18.15±0.012	17.81±0.01	17.87±0.01	17.78±0.01	17.87±0.023	0.09	1 2
SDSSp J030707.46-001601.4	3.690	03 : 07 : 07.46	-00 : 16 : 01.4	0.07	22.91±0.480	21.30±0.050	20.06±0.022	19.96±0.029	20.11±0.127	0.07	2
LBQS 0307-0015	0.770	03 : 09 : 39.45	-00 : 03 : 39.2	0.79	17.75±0.01	17.46±0.01	17.38±0.01	17.44±0.01	17.36±0.014	0.10	1
LBQS 0307-0058	2.106	03 : 10 : 03.02	-00 : 46 : 45.7	0.77	18.07±0.011	18.02±0.01	17.96±0.01	17.79±0.01	17.55±0.015	0.07	1
LBQS 0307+0049	1.386	03 : 10 : 19.95	+01 : 01 : 11.5	0.94	18.11±0.013	17.92±0.01	17.73±0.01	17.61±0.01	17.61±0.017	0.12	1
SDSSp J031036.85+005521.7	3.785	03 : 10 : 36.85	+00 : 55 : 21.6	0.11	23.52±0.579	21.03±0.040	19.51±0.016	19.31±0.021	19.18±0.059	0.12	2
SDSSp J031036.97-001457.0	4.630	03 : 10 : 36.97	-00 : 14 : 57.0	0.07	23.06±0.529	23.32±0.283	21.44±0.076	19.93±0.033	19.94±0.123	0.08	2
SDSSp J031427.92+002339.4	3.680	03 : 14 : 27.93	+00 : 23 : 39.5	0.14	24.39±0.602	21.63±0.062	20.44±0.028	20.36±0.042	20.25±0.209	0.10	2
KUV 03197+0045	0.181	03 : 22 : 13.90	+00 : 55 : 13.5	0.53	16.63±0.01	16.39±0.01	16.18±0.01	15.76±0.01	15.96±0.01	0.12	1
SDSSp J032459.10-005705.1	4.780	03 : 24 : 59.09	-00 : 57 : 05.1	0.15	23.27±0.474	25.01±0.745	22.69±0.213	20.67±0.063	20.32±0.181	0.10	2
SDSSp J033414.10+004056.6	4.330	03 : 34 : 14.09	+00 : 40 : 56.6	0.12	24.37±0.673	23.26±0.236	21.18±0.057	20.79±0.071	20.73±0.257	0.14	2
SDSSp J033505.43+010337.2	3.560	03 : 35 : 05.43	+01 : 03 : 37.0	0.22	24.05±0.560	22.29±0.123	20.78±0.053	20.58±0.067	20.25±0.163	0.11	2
SDSSp J033829.31+002156.3	5.000	03 : 38 : 29.31	+00 : 21 : 56.3	0.06	23.70±0.606	24.92±0.507	21.68±0.085	19.97±0.032	19.75±0.133	0.09	2
SDSSp J033910.53-003009.2	3.740	03 : 39 : 10.52	-00 : 30 : 09.2	0.11	23.34±0.557	21.31±0.044	20.09±0.022	19.95±0.030	19.72±0.099	0.11	2
KUV 03399-0014	0.384	03 : 42 : 26.50	-00 : 04 : 27.1	1.51	17.48±0.01	17.48±0.01	17.57±0.01	17.62±0.01	17.09±0.012	0.08	1
SDSSp J083929.33+003759.0	3.731	08 : 39 : 29.32	+00 : 37 : 59.0	0.08	23.55±0.487	20.52±0.030	19.28±0.016	19.19±0.023	18.95±0.044	0.04	2
PKS 0837+012	1.123	08 : 39 : 49.61	+01 : 04 : 26.7	0.35	18.99±0.067	18.88±0.022	18.66±0.018	18.68±0.018	18.79±0.043	0.05	1
SDSSp J084455.08+001848.5	3.691	08 : 44 : 55.07	+00 : 18 : 48.5	0.13	23.06±0.362	21.34±0.043	19.94±0.019	19.85±0.028	19.85±0.093	0.03	2
[HB89] 0922+005	1.720	09 : 25 : 07.82	+00 : 19 : 14.0	0.28	17.64±0.023	17.41±0.033	17.25±0.018	16.94±0.013	16.82±0.023	0.04	1
SDSSp J093556.92+002255.7	3.727	09 : 35 : 56.92	+00 : 22 : 55.7	0.01	25.03±0.444	19.83±0.029	18.69±0.021	18.55±0.022	18.40±0.037	0.05	2
SDSSp J093931.91+003955.0	4.486	09 : 39 : 31.91	+00 : 39 : 54.9	0.07	22.91±0.376	24.34±0.431	21.59±0.067	20.65±0.053	20.43±0.135	0.07	2
SDSSp J094053.77+010514.4	3.886	09 : 40 : 53.77	+01 : 05 : 14.3	0.05	23.93±0.434	21.70±0.063	20.45±0.035	20.26±0.044	20.17±0.133	0.10	2
PKS 0950+00	1.060	09 : 52 : 45.57	+00 : 00 : 15.6	0.09	19.57±0.033	19.45±0.022	19.07±0.011	18.98±0.016	18.95±0.070	0.05	1 2
RX J0959.8+0049	2.243	09 : 59 : 46.82	+00 : 49 : 18.7	2.90	18.52±0.033	18.08±0.016	17.97±0.017	17.95±0.014	17.70±0.039	0.02	1
[HB89] 0957+003	0.905	10 : 00 : 17.67	+00 : 05 : 23.7	0.04	19.44±0.039	18.93±0.014	18.99±0.014	18.89±0.017	18.53±0.059	0.03	1 2
LBQS 1013-0020	2.504	10 : 15 : 56.31	-00 : 35 : 05.0	1.00	19.13±0.038	18.54±0.023	18.25±0.019	18.22±0.021	18.07±0.032	0.04	1
LBQS 1013+0124	0.779	10 : 15 : 57.05	+01 : 09 : 13.7	0.74	17.07±0.024	16.74±0.025	16.65±0.018	16.77±0.017	16.54±0.046	0.04	1
LBQS 1014+0023	2.291	10 : 16 : 35.99	+00 : 08 : 51.1	1.08	18.87±0.049	18.27±0.010	18.27±0.017	18.13±0.012	17.90±0.031	0.04	1
LBQS 1014+0007	0.337	10 : 16 : 58.65	-00 : 07 : 08.3	1.01	19.12±0.059	19.18±0.017	18.93±0.018	18.85±0.016	18.25±0.045	0.04	1
LBQS 1015-0019	1.508	10 : 18 : 20.88	-00 : 34 : 31.8	1.23	18.17±0.115	17.91±0.018	17.81±0.015	17.62±0.015	17.69±0.031	0.05	1
SDSSp J101832.46+001436.4	3.826	10 : 18 : 32.45	+00 : 14 : 36.5	0.10	24.12±0.511	21.63±0.051	20.23±0.034	20.09±0.030	19.87±0.094	0.04	2
LBQS 1016-0039	2.175	10 : 18 : 59.97	-00 : 54 : 20.4	0.80	18.89±0.068	18.62±0.017	18.67±0.013	18.38±0.015	18.05±0.034	0.05	1
LBQS 1017-0009	1.127	10 : 19 : 56.76	-00 : 24 : 09.8	1.28	16.94±0.025	16.69±0.022	16.39±0.019	16.36±0.01	16.35±0.012	0.05	1
LBQS 1018-0005	2.596	10 : 20 : 59.55	-00 : 20 : 26.1	1.15	18.45±0.052	17.74±0.015	17.78±0.011	17.73±0.014	17.48±0.038	0.05	1
LBQS 1018+0115	0.588	10 : 20 : 59.74	+01 : 00 : 34.5	0.76	18.54±0.017	18.18±0.010	18.23±0.01	18.09±0.018	18.12±0.043	0.04	1
LBQS 1020+0126	1.615	10 : 22 : 47.45	+01 : 10 : 53.2	1.42	18.21±0.039	17.97±0.010	17.84±0.013	17.64±0.013	17.54±0.019	0.06	1
LBQS 1020+0028	1.901	10 : 23 : 29.95	+00 : 13 : 10.1	1.29	18.14±0.051	18.25±0.013	18.18±0.027	17.86±0.013	17.78±0.029	0.05	1
[HB89] 1021-006	2.547	10 : 24 : 29.59	-00 : 52 : 55.4	0.48	19.05±0.021	18.40±0.01	18.31±0.01	18.23±0.035	17.91±0.036	0.06	1
LBQS 1022-0005	0.323	10 : 24 : 50.51	-00 : 21 : 02.4	0.66	19.20±0.071	18.82±0.020	18.46±0.038	18.35±0.023	17.76±0.041	0.07	1
LBQS 1022-0002	1.492	10 : 24 : 57.42	-00 : 17 : 42.1	0.97	17.49±0.049	17.30±0.016	17.07±0.01	16.86±0.014	16.85±0.019	0.06	1
UN J1025-0040	0.634	10 : 25 : 00.81	-00 : 40 : 44.0	1.04	20.03±0.051	19.58±0.015	19.09±0.013	18.52±0.023	18.47±0.031	0.06	1
LBQS 1022+0046	0.363	10 : 25 : 02.74	+00 : 31 : 26.9	1.06	19.69±0.037	19.46±0.014	18.97±0.012	18.59±0.021	18.23±0.029	0.05	1

Table 2—Continued

Name	z_{em}	RA(2000)	DEC(2000)	Δ''	u^*	g^*	r^*	i^*	z^*	$E(g^*-r^*)$	source
LBQS 1022+0051	0.986	10 : 25 : 06.29	+00 : 35 : 53.2	1.21	18.67±0.026	18.44±0.011	18.21±0.010	18.16±0.020	18.27±0.029	0.06	1
LBQS 1023-0040	1.763	10 : 25 : 42.36	−00 : 55 : 44.0	1.38	18.50±0.056	18.39±0.011	18.29±0.021	18.03±0.010	17.91±0.030	0.06	1
LBQS 1024+0030	2.166	10 : 26 : 36.95	+00 : 15 : 30.3	0.83	18.66±0.074	18.54±0.037	18.44±0.025	18.28±0.022	18.11±0.046	0.07	1
LBQS 1024-0057	1.267	10 : 27 : 24.02	−01 : 13 : 00.9	0.28	18.10±0.016	18.07±0.012	17.76±0.012	17.70±0.01	17.66±0.023	0.06	1
LBQS 1025+0046	1.129	10 : 27 : 53.84	+00 : 30 : 55.3	0.73	18.51±0.072	18.34±0.01	18.21±0.01	18.23±0.017	18.33±0.036	0.08	1
LBQS 1025-0030	2.869	10 : 28 : 32.09	−00 : 46 : 07.0	1.00	19.45±0.054	18.18±0.021	17.96±0.012	17.85±0.011	17.79±0.026	0.05	1
LBQS 1026-0045A	1.437	10 : 28 : 35.00	−01 : 00 : 43.8	0.22	18.38±0.045	18.25±0.017	18.20±0.01	18.13±0.010	18.18±0.028	0.06	1
LBQS 1026-0045B	1.530	10 : 28 : 37.02	−01 : 00 : 27.5	0.58	18.39±0.045	18.25±0.017	18.17±0.01	17.95±0.01	17.90±0.025	0.06	1
SDSSp J102846.10-010203.2	3.725	10 : 28 : 46.09	−01 : 02 : 03.0	0.18	23.91±0.504	21.02±0.036	19.69±0.016	19.57±0.023	19.54±0.067	0.06	2
LBQS 1026-0032	0.258	10 : 29 : 20.70	−00 : 47 : 47.5	0.50	19.05±0.076	18.66±0.019	18.25±0.015	18.07±0.014	17.76±0.022	0.05	1
LBQS 1027-0058	1.471	10 : 30 : 16.92	−01 : 13 : 32.2	0.35	18.88±0.022	18.68±0.01	18.48±0.014	18.20±0.01	18.16±0.026	0.05	1
LBQS 1030-0050	1.264	10 : 32 : 36.85	−01 : 06 : 10.9	0.78	17.18±0.015	17.00±0.010	16.78±0.01	16.74±0.01	16.76±0.013	0.06	1
DMS 1034-0040	1.220	10 : 37 : 07.28	−00 : 56 : 35.9	0.94	18.75±0.066	18.67±0.012	18.41±0.010	18.33±0.016	18.36±0.026	0.07	1
DMS 0708 10e	0.940	10 : 37 : 12.46	−01 : 01 : 03.0	0.54	21.37±0.105	20.93±0.035	20.82±0.034	20.74±0.051	20.91±0.208	0.06	1
SDSSp J103848.12+004753.5	3.743	10 : 38 : 48.12	+00 : 47 : 53.4	0.08	22.46±0.185	20.77±0.027	19.64±0.016	19.56±0.024	19.32±0.053	0.06	2
[HB89] 1039+013	1.724	10 : 41 : 56.00	+01 : 06 : 07.7	0.73	21.01±0.112	20.74±0.028	20.62±0.035	20.31±0.040	20.40±0.151	0.05	1
[HB89] 1039+012NED01	1.398	10 : 42 : 30.66	+01 : 00 : 01.7	0.87	18.64±0.092	18.59±0.011	18.31±0.01	18.21±0.016	18.24±0.046	0.05	1
[HB89] 1039+012NED02	2.106	10 : 42 : 33.86	+01 : 02 : 06.3	0.67	19.34±0.094	18.90±0.012	18.68±0.010	18.48±0.017	18.22±0.047	0.06	1
[HB89] 1040+013NED01	0.700	10 : 42 : 48.72	+01 : 07 : 22.3	0.41	20.21±0.054	20.04±0.017	20.06±0.027	20.01±0.038	19.79±0.089	0.04	1
[HB89] 1040+014NED01	1.426	10 : 42 : 51.63	+01 : 13 : 02.6	1.17	19.55±0.044	19.27±0.013	19.03±0.022	18.89±0.029	18.89±0.049	0.05	1
[HB89] 1040+008	2.116	10 : 42 : 53.50	+00 : 33 : 05.9	0.12	20.24±0.042	19.96±0.018	19.85±0.024	19.87±0.030	19.74±0.072	0.06	1
[HB89] 1040+011NED01	0.730	10 : 43 : 03.85	+00 : 54 : 20.5	0.89	20.48±0.069	20.12±0.023	19.69±0.018	19.22±0.020	18.87±0.039	0.05	1
[HB89] 1040+014NED02	2.503	10 : 43 : 06.49	+01 : 08 : 48.8	0.29	21.46±0.112	20.90±0.028	20.80±0.040	20.80±0.063	20.35±0.145	0.05	1
[HB89] 1040+011NED02	1.692	10 : 43 : 09.73	+00 : 50 : 56.5	0.68	20.52±0.070	20.08±0.022	20.07±0.024	19.87±0.030	20.01±0.111	0.05	1
[HB89] 1040+012	1.917	10 : 43 : 14.16	+01 : 02 : 09.4	0.69	19.55±0.047	19.59±0.020	19.56±0.017	19.20±0.020	19.20±0.060	0.05	1
[HB89] 1040+013NED02	1.494	10 : 43 : 14.65	+01 : 05 : 40.4	0.87	20.86±0.073	20.55±0.022	20.29±0.029	20.10±0.040	20.14±0.118	0.05	1
[HB89] 1040+009	0.622	10 : 43 : 21.58	+00 : 43 : 21.4	0.55	19.96±0.034	19.38±0.022	19.23±0.015	18.99±0.025	18.81±0.038	0.05	1
[HB89] 1041+007NED01	1.402	10 : 43 : 40.97	+00 : 30 : 07.5	0.69	19.91±0.035	19.74±0.016	19.58±0.017	19.49±0.027	19.56±0.073	0.05	1
[HB89] 1041+010	1.249	10 : 43 : 47.22	+00 : 50 : 03.4	0.48	18.55±0.023	18.61±0.021	18.10±0.012	18.10±0.023	18.10±0.028	0.05	1
[HB89] 1041+011NED01	0.305	10 : 43 : 50.80	+00 : 55 : 22.8	0.18	21.23±0.108	20.68±0.030	20.03±0.023	19.80±0.030	19.48±0.073	0.04	1
[HB89] 1041+011NED02	1.692	10 : 44 : 00.66	+00 : 50 : 54.1	0.65	18.78±0.031	18.42±0.015	18.39±0.010	18.20±0.015	18.17±0.026	0.04	1
[HB89] 1041+009NED01	1.194	10 : 44 : 02.42	+00 : 41 : 00.1	0.31	21.16±0.071	20.49±0.023	19.77±0.016	19.63±0.029	19.41±0.055	0.05	1
[HB89] 1041+008	0.192	10 : 44 : 17.14	+00 : 37 : 23.9	0.90	19.54±0.037	19.08±0.019	18.57±0.015	18.19±0.017	18.05±0.025	0.05	1
[HB89] 1041+009NED02	1.324	10 : 44 : 23.10	+00 : 40 : 55.7	0.28	19.00±0.029	18.87±0.014	18.64±0.010	18.77±0.024	18.86±0.037	0.04	1
[HB89] 1041+007NED02	0.600	10 : 44 : 23.62	+00 : 27 : 42.2	1.24	20.71±0.065	20.51±0.029	20.15±0.025	20.21±0.039	20.20±0.112	0.05	1
[HB89] 1042+007NED01	1.244	10 : 44 : 33.91	+00 : 32 : 01.1	1.77	20.82±0.070	20.72±0.033	20.27±0.028	20.41±0.046	20.00±0.098	0.05	1
[HB89] 1042+007NED02	0.857	10 : 44 : 53.08	+00 : 28 : 14.5	0.62	20.03±0.051	19.78±0.016	19.72±0.018	19.90±0.029	19.77±0.082	0.05	1
[HB89] 1042+008	1.166	10 : 44 : 55.63	+00 : 37 : 23.1	0.50	20.11±0.052	20.20±0.020	19.92±0.021	19.86±0.030	19.91±0.097	0.05	1
F855:174	1.737	10 : 45 : 15.40	−00 : 20 : 14.9	1.87	21.81±0.158	21.66±0.060	21.55±0.079	21.42±0.098	21.24±0.303	0.04	1
F855:159	1.203	10 : 45 : 42.72	−00 : 05 : 10.8	1.43	20.83±0.105	20.95±0.032	20.63±0.030	20.49±0.041	20.53±0.155	0.05	1
F855:107	1.087	10 : 45 : 46.75	−00 : 15 : 07.5	0.97	20.17±0.063	20.00±0.018	19.75±0.018	19.82±0.028	19.60±0.092	0.05	1
F855:137	1.180	10 : 45 : 58.08	−00 : 11 : 48.9	0.34	20.71±0.103	20.84±0.029	20.48±0.027	20.51±0.042	20.43±0.144	0.05	1
AX J1046.1-0020	1.070	10 : 46 : 05.88	−00 : 20 : 25.3	0.42	20.63±0.067	20.47±0.036	20.16±0.024	20.11±0.038	19.93±0.109	0.05	1
F855:121	2.113	10 : 46 : 11.05	−00 : 38 : 34.8	0.85	21.39±0.130	20.77±0.032	20.49±0.037	20.27±0.042	19.80±0.088	0.05	1
F855:086	0.967	10 : 46 : 11.36	−00 : 43 : 13.0	0.58	18.57±0.020	18.35±0.015	18.16±0.021	18.15±0.019	18.12±0.031	0.05	1
F855:158	2.354	10 : 46 : 11.78	−00 : 13 : 19.9	0.34	22.37±0.256	21.52±0.059	21.69±0.083	21.57±0.110	20.61±0.178	0.04	1
F855:168	1.045	10 : 46 : 13.74	−00 : 19 : 56.0	0.95	21.30±0.107	21.05±0.045	20.57±0.033	20.37±0.045	20.36±0.147	0.05	1
F855:125	1.952	10 : 46 : 14.94	−00 : 22 : 48.5	1.02	20.75±0.073	20.49±0.036	20.29±0.027	20.14±0.039	19.81±0.100	0.05	1
F855:141	1.358	10 : 46 : 18.66	−00 : 35 : 25.7	2.16	20.96±0.077	21.05±0.032	20.75±0.038	20.68±0.046	20.48±0.154	0.05	1
F855:134	1.107	10 : 46 : 19.46	−00 : 12 : 57.8	0.95	20.76±0.075	20.58±0.037	20.35±0.028	20.31±0.042	20.31±0.142	0.04	1
F855:108	1.446	10 : 46 : 25.52	−00 : 30 : 39.7	1.37	20.69±0.067	20.10±0.020	19.80±0.026	19.54±0.020	19.47±0.070	0.05	1

Table 2—Continued

Name	z_{em}	RA(2000)	DEC(2000)	Δ''	u^*	g^*	r^*	i^*	z^*	$E(g^*-r^*)$	source
F855:162	1.256	10 : 46 : 29.57	-00 : 06 : 57.8	0.92	21.57±0.115	21.64±0.046	21.29±0.049	21.35±0.077	21.27±0.281	0.04	1
ARS B104357.69+000215.9	1.999	10 : 46 : 31.35	-00 : 13 : 32.2	1.17	22.41±0.278	22.07±0.085	22.63±0.196	22.54±0.196	21.63±0.366	0.04	1
LDSS 10.12087	2.749	10 : 46 : 32.86	-00 : 09 : 52.5	1.61	22.93±0.305	22.72±0.107	22.15±0.101	22.34±0.183	21.74±0.366	0.04	1
ARS B104402.71+000148.3	1.599	10 : 46 : 36.37	-00 : 13 : 59.8	1.28	23.26±0.502	23.34±0.239	22.71±0.212	22.04±0.161	21.87±0.412	0.04	1
F855:123	2.057	10 : 46 : 37.27	-00 : 16 : 34.3	1.90	20.96±0.122	20.82±0.037	20.97±0.047	20.77±0.065	20.17±0.125	0.04	1
F855:156	1.602	10 : 46 : 40.34	-00 : 07 : 35.0	1.14	21.63±0.120	21.66±0.046	21.61±0.086	21.39±0.080	21.05±0.235	0.04	1
F855:102	2.050	10 : 46 : 46.41	-00 : 26 : 01.4	0.63	19.81±0.046	19.52±0.017	19.39±0.023	19.32±0.018	19.15±0.055	0.04	1
F855:124	1.395	10 : 46 : 56.19	-00 : 11 : 38.7	0.71	21.17±0.122	21.19±0.039	20.90±0.052	20.90±0.055	20.91±0.206	0.04	1
F855:152	2.113	10 : 46 : 56.73	-00 : 33 : 16.6	1.22	21.58±0.126	21.32±0.039	21.15±0.053	20.93±0.059	20.58±0.163	0.04	1
F855:155	1.789	10 : 47 : 02.30	-00 : 20 : 04.1	1.53	22.24±0.401	21.87±0.070	22.00±0.116	21.45±0.102	21.21±0.286	0.04	1
F855:133	1.073	10 : 47 : 06.51	-00 : 15 : 21.8	1.40	22.06±0.203	21.71±0.062	21.21±0.060	21.21±0.071	21.34±0.315	0.04	1
F855:185	1.252	10 : 47 : 09.93	-00 : 26 : 53.0	1.38	21.57±0.126	21.39±0.042	21.07±0.050	21.02±0.065	21.06±0.227	0.04	1
F855:148	2.016	10 : 47 : 11.25	-00 : 17 : 59.4	0.89	21.60±0.149	21.36±0.049	21.28±0.063	21.51±0.108	21.27±0.300	0.04	1
F855:111	0.729	10 : 47 : 11.32	-00 : 13 : 42.2	1.20	20.58±0.100	19.99±0.027	19.94±0.026	19.94±0.029	19.67±0.086	0.04	1
F855:140	1.518	10 : 47 : 13.38	-00 : 11 : 50.8	0.90	20.90±0.115	20.71±0.033	20.51±0.046	20.34±0.036	20.74±0.176	0.04	1
RX J1047.8-0113	0.435	10 : 47 : 50.00	-01 : 12 : 43.6	1.61	18.75±0.020	18.44±0.01	18.54±0.01	18.36±0.016	18.07±0.024	0.05	1
SDSSp J104837.40-002813.7	3.994	10 : 48 : 37.40	-00 : 28 : 13.7	0.06	24.88±0.575	20.87±0.040	19.27±0.019	19.04±0.063	18.97±0.127	0.04	2
PG 1049-005	0.360	10 : 51 : 51.45	-00 : 51 : 17.8	1.13	16.00±0.025	15.79±0.020	15.73±0.01	15.82±0.01	15.26±0.019	0.06	1
UN J1053-0058	1.550	10 : 53 : 52.87	-00 : 58 : 52.5	1.85	19.00±0.048	18.42±0.01	17.98±0.017	17.59±0.010	17.47±0.021	0.04	1
[CCH91] 1055.6+0055	2.827	10 : 58 : 08.48	+00 : 39 : 30.7	1.18	19.45±0.038	18.63±0.014	18.46±0.014	18.37±0.033	18.37±0.029	0.04	1
[CCH91] 1055.7+0054	1.667	10 : 58 : 16.49	+00 : 38 : 23.4	0.39	19.63±0.086	19.56±0.014	19.42±0.013	19.26±0.025	19.23±0.050	0.05	1
[CCH91] 1056.1+0119	1.445	10 : 58 : 37.98	+01 : 03 : 47.8	0.39	19.75±0.094	19.67±0.022	19.43±0.023	19.25±0.025	19.19±0.073	0.03	1
[CCH91] 1056.2+0113	2.322	10 : 58 : 47.19	+00 : 56 : 57.0	0.10	19.66±0.056	19.08±0.014	19.04±0.020	18.98±0.032	18.75±0.062	0.03	1
[CCH91] 1057.2+0052	2.144	10 : 59 : 44.63	+00 : 36 : 43.1	1.01	19.87±0.045	19.66±0.015	19.59±0.021	19.29±0.019	18.99±0.045	0.03	1
[CCH91] 1057.3+0102	2.002	10 : 59 : 54.00	+00 : 46 : 47.9	1.72	18.72±0.033	18.77±0.020	18.66±0.017	18.54±0.025	18.28±0.028	0.03	1
[CCH91] 1057.5+0110	2.017	11 : 00 : 04.28	+00 : 54 : 07.9	0.95	19.10±0.058	18.89±0.015	18.69±0.019	18.55±0.013	18.28±0.062	0.03	1
[CCH91] 1057.6+0106	2.127	11 : 00 : 08.50	+00 : 50 : 27.8	0.84	18.83±0.057	18.60±0.015	18.54±0.019	18.45±0.013	18.27±0.062	0.03	1
[CCH91] 1057.6+0130	1.740	11 : 00 : 09.95	+01 : 14 : 42.5	0.94	19.44±0.052	19.22±0.019	19.11±0.016	18.78±0.025	18.65±0.043	0.04	1
[CCH91] 1058.0+0058	1.531	11 : 00 : 32.84	+00 : 41 : 54.1	0.93	19.32±0.029	19.24±0.030	19.19±0.016	18.94±0.026	19.05±0.043	0.03	1
[CCH91] 1058.1+0052	2.024	11 : 00 : 41.19	+00 : 36 : 32.0	0.15	18.66±0.048	18.58±0.011	18.43±0.017	18.24±0.013	17.97±0.032	0.03	1
[CCH91] 1058.6+0119	2.461	11 : 01 : 09.25	+01 : 03 : 48.5	0.87	20.79±0.098	20.20±0.025	20.18±0.024	20.14±0.033	19.86±0.091	0.03	1
[CCH91] 1059.1+0038	1.714	11 : 01 : 40.54	+00 : 22 : 17.5	1.00	20.45±0.045	20.48±0.026	20.42±0.026	20.08±0.034	20.06±0.110	0.03	1
[CCH91] 1059.2+0043	1.350	11 : 01 : 48.77	+00 : 27 : 22.0	1.42	19.82±0.083	20.05±0.027	19.57±0.018	19.69±0.029	19.68±0.069	0.03	1
UN J1104-0004	1.350	11 : 04 : 40.83	-00 : 04 : 41.7	1.38	19.97±0.096	19.33±0.015	18.99±0.021	18.93±0.017	18.87±0.039	0.04	1
PG 1103-006	0.423	11 : 06 : 31.78	-00 : 52 : 52.4	0.53	16.42±0.01	16.26±0.013	16.45±0.01	16.44±0.037	16.21±0.028	0.04	1
SDSSp J110813.86-005944.5	4.013	11 : 08 : 13.86	-00 : 59 : 44.6	0.06	23.72±0.445	21.01±0.033	19.56±0.014	19.29±0.022	19.14±0.047	0.05	2
BRI 1110+0106	3.920	11 : 12 : 46.30	+00 : 49 : 57.5	0.10	24.57±0.445	20.00±0.024	18.76±0.019	18.61±0.017	18.51±0.036	0.04	1 2
SDSSp J111401.48-005321.1	4.590	11 : 14 : 01.47	-00 : 53 : 21.2	0.16	23.64±0.463	22.94±0.173	20.72±0.029	19.61±0.020	19.46±0.057	0.03	2
SDSSp J112253.51+005329.8	4.560	11 : 22 : 53.50	+00 : 53 : 29.8	0.13	23.39±0.590	22.66±0.169	20.17±0.028	19.08±0.017	19.02±0.058	0.04	2
UM 427	1.691	11 : 25 : 42.29	+00 : 01 : 01.4	1.43	17.85±0.035	17.77±0.01	17.69±0.014	17.44±0.017	17.35±0.040	0.04	1
LBQS 1127+0037	0.999	11 : 30 : 31.58	+00 : 20 : 33.3	0.10	18.24±0.063	18.12±0.028	17.96±0.015	17.92±0.025	17.87±0.056	0.03	1 2
LBQS 1128+0022	1.379	11 : 31 : 06.65	+00 : 05 : 38.1	0.17	18.27±0.051	18.32±0.041	18.10±0.010	17.99±0.022	17.96±0.026	0.03	1 2
LBQS 1129+0009	0.964	11 : 32 : 16.66	-00 : 06 : 52.0	0.02	18.64±0.041	18.36±0.026	18.24±0.015	18.35±0.018	18.20±0.039	0.03	1 2
LBQS 1130+0018	1.251	11 : 32 : 48.27	+00 : 01 : 55.8	0.25	18.50±0.031	18.40±0.013	18.09±0.021	18.13±0.013	18.20±0.046	0.03	1 2
LBQS 1130+0032	1.170	11 : 33 : 03.03	+00 : 15 : 49.0	0.09	18.95±0.092	18.91±0.014	18.64±0.033	18.68±0.018	18.86±0.050	0.02	1 2
LBQS 1131+0114	1.937	11 : 33 : 45.62	+00 : 58 : 13.6	0.23	18.81±0.050	18.57±0.012	18.20±0.013	17.92±0.011	17.88±0.051	0.03	1 2
LBQS 1131-0043	2.157	11 : 34 : 12.91	-00 : 59 : 47.6	0.08	19.12±0.023	18.80±0.013	18.82±0.031	18.75±0.040	18.45±0.029	0.02	1 2
LBQS 1131-0039	0.268	11 : 34 : 32.30	-00 : 55 : 48.2	0.15	18.03±0.018	18.17±0.012	18.11±0.013	18.11±0.021	17.65±0.016	0.02	1 2
LBQS 1132-0054	2.753	11 : 35 : 14.95	-01 : 11 : 13.3	1.08	18.89±0.018	18.25±0.01	18.15±0.010	17.97±0.01	17.96±0.022	0.02	1
LBQS 1132-0013	0.957	11 : 35 : 22.96	-00 : 29 : 57.5	0.20	17.68±0.061	17.74±0.015	17.67±0.016	17.80±0.019	17.75±0.017	0.02	1 2
LBQS 1132-0053	1.357	11 : 35 : 28.42	-01 : 10 : 23.6	0.07	18.35±0.013	18.31±0.01	18.13±0.010	18.09±0.01	18.25±0.028	0.02	1 2

Table 2—Continued

Name	z_{em}	RA(2000)	DEC(2000)	Δ''	u^*	g^*	r^*	i^*	z^*	$E(g^*-r^*)$	source
SDSSp J113559.94+002422.8	4.000	11 : 35 : 59.95	+00 : 24 : 22.7	0.15	23.62±0.351	21.37±0.049	20.03±0.026	19.88±0.031	19.73±0.084	0.02	2
LBQS 1135+0040	0.720	11 : 37 : 41.92	+00 : 23 : 51.2	0.34	18.69±0.088	18.31±0.025	18.38±0.028	18.54±0.030	18.33±0.036	0.03	1
LBQS 1135+0044	0.805	11 : 37 : 49.75	+00 : 27 : 35.3	0.14	17.52±0.028	17.33±0.012	17.30±0.018	17.24±0.01	17.15±0.019	0.02	1 2
[VCV96] Q 1136+0000	0.135	11 : 39 : 09.66	-00 : 16 : 08.6	0.14	18.32±0.030	18.13±0.014	17.82±0.01	17.36±0.013	17.43±0.020	0.02	1 2
LBQS 1137+0051	0.877	11 : 39 : 43.07	+00 : 35 : 21.3	0.03	18.24±0.028	17.98±0.011	18.06±0.01	18.07±0.013	18.06±0.024	0.02	1 2
LBQS 1137+0110	1.136	11 : 40 : 16.68	+00 : 53 : 51.2	0.13	18.25±0.019	18.06±0.011	17.66±0.011	17.77±0.013	17.88±0.047	0.02	1 2
LBQS 1138+0015	1.766	11 : 40 : 43.67	-00 : 01 : 26.3	0.12	18.62±0.016	18.60±0.033	18.57±0.015	18.33±0.027	18.32±0.026	0.03	1 2
LBQS 1138+0003	0.504	11 : 41 : 17.63	-00 : 12 : 50.3	0.11	18.42±0.084	18.04±0.014	18.18±0.011	18.03±0.025	17.95±0.058	0.03	1 2
LBQS 1139+0106	0.462	11 : 41 : 58.52	+00 : 49 : 27.1	0.13	18.46±0.044	18.18±0.016	18.03±0.023	17.91±0.016	17.85±0.042	0.02	1 2
LBQS 1139-0037	1.917	11 : 42 : 11.59	-00 : 53 : 44.2	0.03	18.16±0.050	18.14±0.012	18.09±0.011	17.93±0.013	17.86±0.031	0.02	1 2
LBQS 1141-0038	0.517	11 : 43 : 47.11	-00 : 54 : 48.8	0.07	19.17±0.026	18.94±0.019	19.07±0.014	18.88±0.018	18.78±0.035	0.02	1 2
LBQS 1144+0030	0.940	11 : 46 : 47.72	+00 : 13 : 50.8	0.18	18.06±0.135	17.90±0.046	17.75±0.024	17.78±0.029	17.68±0.026	0.03	1 2
LBQS 1145-0039	1.941	11 : 47 : 45.57	-00 : 56 : 09.3	1.20	18.38±0.029	18.44±0.013	18.43±0.01	18.14±0.014	18.02±0.019	0.02	1
LBQS 1145+0015	1.261	11 : 47 : 49.66	-00 : 01 : 09.4	0.06	18.98±0.076	18.80±0.017	18.50±0.015	18.46±0.026	18.61±0.040	0.03	1 2
LBQS 1145+0121	2.061	11 : 47 : 52.67	+01 : 04 : 30.8	0.06	18.98±0.091	18.68±0.011	18.56±0.023	18.49±0.025	18.24±0.052	0.03	1 2
LBQS 1145-0049	1.256	11 : 47 : 55.56	-01 : 05 : 48.7	0.13	18.63±0.022	18.47±0.010	18.35±0.01	18.33±0.010	18.40±0.035	0.02	1 2
LBQS 1145+0120	1.614	11 : 48 : 16.91	+01 : 03 : 57.5	0.04	18.90±0.132	18.58±0.014	18.50±0.014	18.34±0.065	18.32±0.028	0.03	1 2
[VCV96] Q 1147+0025	0.130	11 : 50 : 23.58	+00 : 08 : 39.2	0.31	18.59±0.037	18.49±0.014	18.17±0.024	17.76±0.025	17.69±0.026	0.03	1
LBQS 1148-0007	1.976	11 : 50 : 43.87	-00 : 23 : 54.2	0.17	17.19±0.029	17.12±0.011	17.08±0.018	16.86±0.022	16.68±0.024	0.03	1 2
LBQS 1148-0033	0.800	11 : 50 : 52.30	-00 : 50 : 16.4	1.62	18.27±0.027	17.91±0.013	17.86±0.018	17.86±0.017	17.67±0.043	0.02	1
LBQS 1148+0055	1.881	11 : 51 : 15.38	+00 : 38 : 27.0	0.02	17.98±0.036	17.99±0.015	17.89±0.010	17.60±0.011	17.53±0.025	0.02	1 2
LBQS 1148+0055B	1.409	11 : 51 : 15.62	+00 : 38 : 25.6	0.67	21.78±0.149	21.84±0.609	21.51±0.272	21.33±0.114	21.04±0.590	0.02	1
[VCV96] Q 1150+0010	0.130	11 : 52 : 35.00	-00 : 05 : 42.8	1.24	17.98±0.053	17.87±0.026	17.70±0.015	17.29±0.023	17.35±0.023	0.02	1
LBQS 1150+0127	1.636	11 : 52 : 39.27	+01 : 11 : 18.2	0.15	17.64±0.085	17.59±0.010	17.51±0.021	17.31±0.022	17.19±0.086	0.02	1 2
LBQS 1150+0041	0.783	11 : 52 : 46.56	+00 : 24 : 40.1	0.15	17.75±0.019	17.60±0.029	17.63±0.020	17.57±0.014	17.50±0.032	0.03	1 2
LBQS 1150-0054	1.332	11 : 53 : 06.91	-01 : 10 : 57.8	0.09	18.81±0.027	18.68±0.017	18.47±0.026	18.38±0.033	18.51±0.035	0.02	1 2
UM 464	1.550	11 : 53 : 47.79	-00 : 46 : 25.5	0.04	18.90±0.024	18.79±0.015	18.60±0.016	18.38±0.010	18.42±0.034	0.03	1 2
[HB89] 1157+014	1.989	11 : 59 : 44.81	+01 : 12 : 07.0	0.05	18.41±0.025	17.57±0.020	17.26±0.019	17.04±0.018	16.73±0.029	0.02	1 2
[HB89] 1158+007	1.365	12 : 01 : 23.25	+00 : 28 : 28.3	0.17	18.60±0.016	18.60±0.014	18.36±0.01	18.38±0.014	18.38±0.035	0.03	1 2
SDSSp J120210.09-005425.5	3.586	12 : 02 : 10.09	-00 : 54 : 25.5	0.07	23.54±0.576	20.10±0.018	19.05±0.011	18.94±0.014	18.93±0.039	0.02	2
SDSSp J120441.73-002149.6	5.020	12 : 04 : 41.72	-00 : 21 : 49.6	0.18	22.08±0.251	25.01±0.739	20.73±0.049	19.21±0.026	19.00±0.060	0.03	2
[HB89] 1203+011	0.104	12 : 05 : 48.49	+00 : 53 : 43.9	0.21	19.43±0.080	19.33±0.017	19.15±0.015	19.29±0.025	19.03±0.057	0.03	1
[HB89] 1205-008	1.002	12 : 07 : 41.68	-01 : 06 : 36.8	0.39	19.06±0.022	18.72±0.01	18.42±0.017	18.18±0.131	18.14±0.025	0.02	1
SDSSp J120823.82+001027.7	5.280	12 : 08 : 23.82	+00 : 10 : 27.8	0.13	24.66±0.709	25.04±0.645	22.70±0.283	20.73±0.070	20.73±0.261	0.03	2
UM 485	2.690	12 : 15 : 49.81	-00 : 34 : 32.2	1.82	19.08±0.032	17.52±0.024	17.36±0.020	17.15±0.018	16.89±0.051	0.03	1
PKS 1215-002	0.417	12 : 17 : 58.73	-00 : 29 : 46.3	0.81	18.64±0.031	18.18±0.014	17.72±0.010	17.44±0.010	17.15±0.045	0.03	1
SDSSp J122600.68+005923.6	4.270	12 : 26 : 00.68	+00 : 59 : 23.6	0.04	23.04±0.427	21.18±0.047	18.98±0.015	18.87±0.022	18.75±0.048	0.02	2
RX J1230.8+0115	0.117	12 : 30 : 50.02	+01 : 15 : 22.6	1.87	14.85±0.048	14.83±0.027	14.86±0.034	14.53±0.016	14.78±0.021	0.02	1
LBQS 1229+0106	0.477	12 : 32 : 09.68	+00 : 50 : 15.5	0.54	19.50±0.057	19.14±0.014	19.23±0.019	18.91±0.035	18.63±0.042	0.03	1
LBQS 1230-0015	0.470	12 : 33 : 04.05	-00 : 31 : 34.1	0.82	17.97±0.070	17.76±0.019	17.82±0.024	17.72±0.018	17.61±0.018	0.02	1
SDSSp J123503.04-000331.8	4.680	12 : 35 : 03.05	-00 : 03 : 31.7	0.16	23.54±0.467	23.37±0.220	21.41±0.055	20.07±0.027	20.04±0.107	0.02	2
[HB89] 1232-002	1.890	12 : 35 : 05.92	-00 : 30 : 22.4	0.70	18.78±0.103	18.78±0.016	18.77±0.018	18.57±0.021	18.55±0.042	0.03	1
LBQS 1232-0051	2.783	12 : 35 : 10.58	-01 : 07 : 45.7	0.42	19.49±0.034	18.80±0.013	18.73±0.01	18.62±0.012	18.60±0.033	0.02	1
[HB89] 1232-004	1.579	12 : 35 : 29.96	-00 : 41 : 41.0	0.86	19.24±0.048	18.98±0.020	18.82±0.020	18.51±0.039	18.52±0.039	0.02	1
[HB89] 1233-008	1.471	12 : 35 : 47.60	-01 : 09 : 05.4	0.61	19.95±0.034	19.75±0.022	19.44±0.015	19.20±0.020	19.24±0.051	0.03	1
[HB89] 1233-009	1.470	12 : 35 : 53.62	-01 : 11 : 48.6	0.53	18.95±0.020	18.74±0.018	18.65±0.011	18.51±0.016	18.52±0.031	0.03	1
[HB89] 1233-006NED01	1.097	12 : 36 : 02.43	-00 : 52 : 34.3	1.34	20.75±0.058	20.79±0.032	20.58±0.030	20.50±0.041	20.36±0.128	0.03	1
LBQS 1233+0040	1.573	12 : 36 : 02.83	+00 : 23 : 43.6	1.65	18.97±0.053	18.56±0.017	18.45±0.018	18.23±0.022	18.31±0.042	0.02	1
[HB89] 1233-007	0.417	12 : 36 : 08.83	-00 : 59 : 26.4	0.80	21.04±0.071	20.77±0.031	20.02±0.021	19.49±0.022	19.10±0.048	0.02	1
[HB89] 1233-005	0.308	12 : 36 : 08.93	-00 : 51 : 14.4	1.16	20.83±0.060	20.19±0.022	19.42±0.019	19.19±0.019	18.76±0.038	0.02	1
[HB89] 1233-006NED02	0.179	12 : 36 : 27.94	-00 : 53 : 57.6	1.02	21.76±0.157	21.06±0.042	20.68±0.031	20.24±0.035	19.95±0.092	0.02	1

Table 2—Continued

Name	z_{em}	RA(2000)	DEC(2000)	Δ''	u^*	g^*	r^*	i^*	z^*	$E(g^*-r^*)$	source
[HB89] 1233-006NED03	1.784	12 : 36 : 31.79	-00 : 53 : 00.0	0.14	21.02±0.076	20.80±0.036	20.80±0.033	20.42±0.038	20.41±0.134	0.02	1
[HB89] 1234-003	0.445	12 : 36 : 36.66	-00 : 37 : 23.8	1.14	21.05±0.083	20.86±0.033	20.53±0.035	20.15±0.035	20.14±0.104	0.02	1
[HB89] 1234-005	1.792	12 : 36 : 41.51	-00 : 49 : 54.8	0.84	19.50±0.038	19.49±0.018	19.39±0.020	19.10±0.022	19.03±0.040	0.03	1
[HB89] 1234-006NED01	0.135	12 : 36 : 45.97	-00 : 53 : 09.8	0.46	21.76±0.130	21.03±0.040	20.68±0.030	20.28±0.041	20.10±0.104	0.03	1
[HB89] 1234-006NED02	1.437	12 : 36 : 49.89	-00 : 57 : 08.7	0.37	21.14±0.079	21.12±0.043	20.98±0.039	20.81±0.058	20.35±0.131	0.03	1
[HB89] 1234-007	1.545	12 : 36 : 49.95	-00 : 59 : 25.3	0.82	18.89±0.037	18.39±0.021	18.23±0.01	18.06±0.014	18.03±0.031	0.02	1
[HB89] 1234-004NED01	1.686	12 : 36 : 56.97	-00 : 41 : 07.4	1.19	19.36±0.036	19.18±0.017	19.07±0.019	18.80±0.021	18.77±0.033	0.03	1
[HB89] 1234+001NED01	1.870	12 : 36 : 57.10	-00 : 06 : 18.1	1.50	19.98±0.086	19.85±0.041	19.76±0.019	19.46±0.033	19.44±0.059	0.02	1
QN Y1:33	0.753	12 : 37 : 02.03	-00 : 37 : 56.5	0.67	20.39±0.058	19.82±0.020	19.51±0.021	19.37±0.024	19.17±0.044	0.03	1
[HB89] 1234+005	1.581	12 : 37 : 02.56	+00 : 14 : 37.3	0.68	20.44±0.045	20.19±0.025	20.10±0.022	19.79±0.028	19.75±0.099	0.02	1
[HB89] 1234+002	2.038	12 : 37 : 04.40	-00 : 03 : 21.4	1.60	20.24±0.104	19.85±0.033	19.61±0.036	19.39±0.041	19.17±0.069	0.02	1
[HB89] 1234+003	2.003	12 : 37 : 08.64	+00 : 03 : 28.8	0.69	18.89±0.040	18.85±0.017	18.85±0.026	18.69±0.022	18.55±0.063	0.02	1
[HB89] 1234+004	2.003	12 : 37 : 12.87	+00 : 11 : 58.9	0.52	19.80±0.047	19.66±0.019	19.62±0.028	19.47±0.027	19.13±0.079	0.03	1
[HB89] 1234+001NED02	0.943	12 : 37 : 13.18	-00 : 09 : 38.4	1.42	20.66±0.109	20.04±0.034	19.54±0.036	19.44±0.041	19.23±0.055	0.02	1
LBQS 1234+0122	2.025	12 : 37 : 24.52	+01 : 06 : 15.5	1.56	18.53±0.063	18.07±0.012	17.89±0.019	17.79±0.030	17.68±0.045	0.02	1
[HB89] 1234-004NED02	2.193	12 : 37 : 27.99	-00 : 44 : 13.3	0.67	20.27±0.101	19.72±0.018	19.78±0.025	19.62±0.027	19.28±0.050	0.02	1
QN Y3:34	1.802	12 : 37 : 30.99	+00 : 44 : 28.5	0.56	19.57±0.049	19.60±0.025	19.68±0.018	19.35±0.028	19.25±0.051	0.02	1
[HB89] 1234-006NED03	0.788	12 : 37 : 33.43	-00 : 52 : 48.6	0.60	20.12±0.043	19.91±0.017	19.88±0.020	19.89±0.034	19.67±0.077	0.03	1
QN Y3:27	0.980	12 : 37 : 36.57	+00 : 38 : 34.3	0.55	19.21±0.047	19.04±0.024	18.76±0.013	18.79±0.026	18.64±0.035	0.02	1
[HB89] 1235+005NED01	0.820	12 : 37 : 38.16	+00 : 15 : 27.7	0.91	21.39±0.109	20.94±0.028	20.88±0.038	20.50±0.052	20.12±0.128	0.02	1
[HB89] 1235+005NED02	1.873	12 : 37 : 41.36	+00 : 17 : 28.1	1.22	21.03±0.080	21.17±0.042	21.16±0.051	20.65±0.046	20.48±0.157	0.02	1
[HB89] 1235+000NED01	0.169	12 : 37 : 43.62	-00 : 15 : 12.7	1.29	21.13±0.077	20.34±0.045	19.91±0.026	19.57±0.026	19.45±0.068	0.02	1
QN Y3:56	0.646	12 : 37 : 44.38	+01 : 04 : 32.6	1.38	18.96±0.048	18.55±0.026	18.65±0.012	18.62±0.023	18.67±0.041	0.02	1
QN Y3:53	0.922	12 : 37 : 45.72	+01 : 00 : 14.0	1.01	20.18±0.092	20.07±0.017	19.92±0.026	20.08±0.038	20.00±0.109	0.02	1
LBQS 1235-0019	0.944	12 : 37 : 49.64	-00 : 35 : 43.9	1.23	19.41±0.057	19.21±0.018	19.07±0.021	19.09±0.025	19.04±0.056	0.02	1
[HB89] 1235+005NED03	0.866	12 : 37 : 53.86	+00 : 16 : 38.3	0.65	20.30±0.053	20.04±0.030	20.06±0.026	20.01±0.029	19.62±0.077	0.02	1
[HB89] 1235+004	1.188	12 : 37 : 56.31	+00 : 09 : 15.7	0.27	22.05±0.187	21.60±0.051	21.58±0.069	21.15±0.071	20.88±0.258	0.02	1
[HB89] 1235+002	1.122	12 : 37 : 56.57	+00 : 00 : 59.8	1.27	21.12±0.110	20.73±0.027	20.20±0.030	20.20±0.031	20.13±0.145	0.03	1
QN Y3:22	1.890	12 : 37 : 57.22	+00 : 46 : 14.2	0.34	20.85±0.093	20.84±0.029	20.84±0.041	20.59±0.049	20.55±0.136	0.02	1
[HB89] 1235+006	1.948	12 : 37 : 58.20	+00 : 19 : 45.3	0.31	19.56±0.045	19.45±0.028	19.46±0.021	19.31±0.020	19.21±0.056	0.02	1
QN Y3:01	0.720	12 : 38 : 04.05	+00 : 51 : 13.5	0.93	20.05±0.064	19.65±0.014	19.57±0.018	19.60±0.027	19.35±0.063	0.02	1
QN Y3:20	0.794	12 : 38 : 06.83	+00 : 31 : 23.7	0.52	20.11±0.040	19.13±0.028	18.77±0.015	18.61±0.042	18.57±0.036	0.02	1
QN Y3:29	1.043	12 : 38 : 08.12	+00 : 32 : 17.2	0.12	19.02±0.028	19.07±0.028	18.94±0.015	18.98±0.043	18.83±0.042	0.02	1 2
QN Y3:07	0.808	12 : 38 : 08.38	+00 : 52 : 46.4	0.45	19.89±0.062	19.39±0.013	19.10±0.015	19.01±0.021	18.85±0.046	0.02	1
[HB89] 1235+005NED04	0.580	12 : 38 : 12.76	+00 : 15 : 16.4	0.73	19.33±0.043	18.93±0.028	19.00±0.019	18.79±0.017	18.77±0.042	0.02	1
APMUKS(BJ) B123542.93-004027.8	1.404	12 : 38 : 16.85	-00 : 56 : 56.6	0.80	19.08±0.027	19.04±0.011	18.84±0.011	18.76±0.016	18.84±0.039	0.02	1
QN Y3:49	1.220	12 : 38 : 23.08	+01 : 08 : 32.4	0.49	19.82±0.040	19.69±0.022	19.41±0.030	19.46±0.026	19.51±0.068	0.02	1
[HB89] 1235+005NED05	0.976	12 : 38 : 28.16	+00 : 19 : 06.0	0.63	20.74±0.121	20.61±0.029	20.34±0.035	20.16±0.040	20.07±0.113	0.02	1
[HB89] 1235+000NED02	1.571	12 : 38 : 28.81	-00 : 10 : 36.1	0.93	19.96±0.071	19.79±0.022	19.59±0.029	19.33±0.027	19.19±0.060	0.03	1
QN Y3:44	1.436	12 : 38 : 32.13	+01 : 08 : 13.6	0.76	19.12±0.032	19.08±0.020	18.91±0.028	18.88±0.021	18.88±0.043	0.02	1
QN Y4:30	1.073	12 : 38 : 37.11	-01 : 12 : 51.5	1.68	20.20±0.053	20.18±0.021	20.25±0.026	20.08±0.032	19.54±0.068	0.03	1
[HB89] 1236+001	1.610	12 : 38 : 40.52	-00 : 05 : 55.3	0.72	20.09±0.073	19.79±0.022	19.69±0.030	19.40±0.028	19.49±0.069	0.02	1
[HB89] 1236+000	0.868	12 : 38 : 44.42	-00 : 11 : 40.2	1.46	18.89±0.066	18.77±0.020	18.71±0.027	18.80±0.025	18.79±0.053	0.03	1
QN Y4:42	0.713	12 : 38 : 48.41	-01 : 07 : 00.5	1.71	21.92±0.165	21.51±0.056	21.47±0.069	21.47±0.099	20.94±0.205	0.03	1
LBQS 1236-0043	1.843	12 : 38 : 56.10	-00 : 59 : 30.9	1.09	18.35±0.048	18.48±0.010	18.31±0.01	17.97±0.010	18.01±0.019	0.02	1
QN Y4:45	0.208	12 : 38 : 56.17	-01 : 03 : 32.8	1.09	20.35±0.055	19.75±0.017	19.36±0.014	19.04±0.018	18.94±0.042	0.03	1
QN Y3:08	1.582	12 : 39 : 00.56	+00 : 51 : 38.0	0.13	19.44±0.081	19.03±0.011	18.93±0.014	18.74±0.017	18.70±0.078	0.02	1 2
QN Y4:33	0.727	12 : 39 : 02.71	-01 : 09 : 35.9	2.02	20.83±0.071	20.51±0.025	20.48±0.030	20.36±0.039	19.96±0.091	0.03	1
[HB89] 1236+004	0.526	12 : 39 : 05.36	+00 : 10 : 10.2	1.50	20.95±0.083	20.76±0.027	20.82±0.040	20.69±0.045	20.37±0.165	0.02	1
QN Y3:04	1.257	12 : 39 : 10.00	+00 : 49 : 28.9	0.89	20.77±0.056	20.93±0.029	20.76±0.037	20.76±0.056	20.90±0.190	0.02	1
LBQS 1236+0128	1.262	12 : 39 : 11.49	+01 : 12 : 13.9	0.90	17.96±0.076	17.81±0.026	17.53±0.011	17.60±0.011	17.66±0.040	0.02	1

Table 2—Continued

Name	z_{em}	RA(2000)	DEC(2000)	Δ''	u^*	g^*	r^*	i^*	z^*	$E(g^*-r^*)$	source
QN Y4:53	2.181	12 : 39 : 32.76	-00 : 38 : 38.2	0.94	19.18±0.115	18.69±0.021	18.32±0.017	18.11±0.016	17.96±0.060	0.02	1
QN Y4:50	1.281	12 : 39 : 44.95	-00 : 42 : 58.0	0.82	19.37±0.103	19.35±0.022	19.13±0.021	19.08±0.034	19.05±0.049	0.03	1
QN Y4:52	2.714	12 : 39 : 53.00	-00 : 41 : 11.8	0.18	21.49±0.158	20.67±0.032	20.49±0.033	20.41±0.050	20.29±0.116	0.02	1
QN Y4:15	1.055	12 : 39 : 57.81	-01 : 05 : 45.4	0.19	19.49±0.046	19.23±0.012	18.96±0.016	19.03±0.019	18.86±0.040	0.03	1 2
[HB89] 1237-009	0.819	12 : 39 : 59.80	-01 : 10 : 45.0	0.20	18.55±0.042	18.23±0.01	18.25±0.014	18.38±0.012	18.25±0.029	0.03	1 2
QN Y4:64	1.213	12 : 40 : 03.04	-00 : 40 : 54.4	1.12	20.93±0.125	20.91±0.036	20.76±0.037	20.81±0.064	20.72±0.164	0.02	1
LBQS 1237+0107	1.808	12 : 40 : 10.76	+00 : 51 : 29.4	1.48	18.44±0.111	18.32±0.018	18.35±0.023	18.13±0.023	18.20±0.047	0.02	1
LBQS 1238+0039	1.358	12 : 41 : 08.44	+00 : 22 : 56.9	0.18	18.12±0.034	17.91±0.017	17.61±0.022	17.55±0.011	17.58±0.025	0.02	1 2
F861:177	1.601	12 : 41 : 14.66	-00 : 22 : 10.6	1.01	21.58±0.111	21.06±0.039	20.93±0.051	20.63±0.049	20.92±0.193	0.03	1
F861:171	2.067	12 : 41 : 26.85	-00 : 27 : 14.2	0.79	20.26±0.083	19.82±0.029	19.60±0.026	19.44±0.023	19.22±0.047	0.03	1
F861:165	1.299	12 : 41 : 34.17	-00 : 42 : 57.0	0.52	19.71±0.085	19.77±0.021	19.51±0.016	19.54±0.020	19.60±0.064	0.02	1
F861:163	1.576	12 : 41 : 37.43	-00 : 20 : 31.2	0.93	20.39±0.049	19.90±0.040	19.75±0.018	19.50±0.025	19.54±0.062	0.03	1
F861:156	1.506	12 : 41 : 45.77	-00 : 38 : 54.2	1.37	21.02±0.113	20.72±0.031	20.45±0.030	20.17±0.032	20.10±0.100	0.02	1
F861:134	1.120	12 : 42 : 01.75	-00 : 42 : 15.3	0.81	21.02±0.111	21.18±0.040	20.66±0.038	20.69±0.048	20.67±0.160	0.02	1
LBQS 1239+0028	1.215	12 : 42 : 02.66	+00 : 12 : 29.1	0.28	17.87±0.040	17.43±0.026	16.98±0.017	16.91±0.018	16.87±0.033	0.03	1 2
F861:117	1.610	12 : 42 : 21.77	-00 : 39 : 02.3	0.49	21.98±0.194	21.67±0.059	21.67±0.076	21.27±0.076	20.75±0.282	0.02	1
F861:115	1.300	12 : 42 : 29.16	-00 : 32 : 58.5	0.96	21.86±0.160	21.60±0.054	21.44±0.064	21.11±0.066	20.82±0.163	0.03	1
F861:095	1.320	12 : 42 : 49.82	-00 : 25 : 41.8	0.34	22.67±0.292	21.44±0.048	21.14±0.049	20.89±0.055	20.53±0.127	0.03	1
F861:093	1.309	12 : 42 : 50.94	-00 : 36 : 41.7	2.13	20.80±0.099	20.78±0.033	20.52±0.032	20.67±0.044	20.47±0.121	0.02	1
F861:089	1.413	12 : 42 : 54.97	-00 : 33 : 59.9	1.09	21.17±0.112	21.15±0.040	20.80±0.039	20.61±0.042	20.63±0.141	0.03	1
F861:087	2.475	12 : 42 : 57.47	-00 : 30 : 17.8	1.07	23.25±0.419	22.27±0.088	22.53±0.163	22.01±0.141	22.18±0.378	0.03	1
F861:085	2.874	12 : 42 : 59.17	-00 : 19 : 43.2	1.33	22.40±0.222	21.50±0.048	21.26±0.052	21.36±0.077	21.83±0.357	0.02	1
F861:076	2.068	12 : 43 : 09.05	-00 : 24 : 03.6	0.90	21.11±0.081	20.95±0.032	20.58±0.033	20.17±0.030	19.86±0.092	0.03	1
F861:074	2.049	12 : 43 : 10.80	-00 : 36 : 40.8	0.13	19.76±0.164	19.53±0.027	19.25±0.025	19.08±0.020	18.94±0.052	0.02	1 2
F861:073	1.379	12 : 43 : 16.19	-00 : 38 : 10.1	0.10	21.23±0.115	20.88±0.038	20.46±0.028	20.32±0.036	20.59±0.165	0.02	1
F861:070	1.508	12 : 43 : 23.33	-00 : 18 : 44.2	0.48	21.14±0.079	21.03±0.036	20.84±0.036	20.61±0.043	20.39±0.132	0.02	1
F861:068	1.534	12 : 43 : 26.17	-00 : 26 : 51.3	1.11	21.83±0.212	21.62±0.053	21.25±0.057	21.22±0.070	21.24±0.238	0.03	1
F861:066	0.791	12 : 43 : 30.47	-00 : 20 : 43.2	1.10	20.63±0.055	19.83±0.022	20.02±0.021	20.08±0.031	19.78±0.074	0.03	1
LBQS 1241+0107	0.788	12 : 44 : 11.55	+00 : 50 : 38.5	0.12	18.27±0.073	17.93±0.015	17.88±0.01	17.93±0.014	17.87±0.041	0.01	1 2
LBQS 1241-0048	1.335	12 : 44 : 15.83	-01 : 04 : 29.6	0.13	18.28±0.030	18.05±0.01	18.08±0.016	18.21±0.012	18.25±0.022	0.04	1 2
LBQS 1242+0006	2.075	12 : 45 : 24.60	-00 : 09 : 38.1	0.23	18.10±0.033	18.12±0.011	17.96±0.012	17.80±0.012	17.59±0.033	0.01	1 2
LBQS 1243-0011	1.685	12 : 45 : 41.00	-00 : 27 : 44.9	0.23	18.93±0.022	18.77±0.017	18.57±0.015	18.20±0.017	18.13±0.025	0.02	1 2
LBQS 1243+0121	2.796	12 : 45 : 51.45	+01 : 05 : 05.1	1.29	20.30±0.048	18.21±0.017	18.13±0.014	17.91±0.017	17.63±0.150	0.03	1
LBQS 1243-0026	0.644	12 : 46 : 13.14	-00 : 42 : 33.0	1.17	17.18±0.023	16.90±0.021	16.99±0.024	16.84±0.019	16.86±0.014	0.03	1
UM 519	2.090	12 : 48 : 08.38	-00 : 43 : 24.0	1.15	18.26±0.027	18.03±0.016	17.91±0.014	17.82±0.021	17.57±0.030	0.04	1
LBQS 1246+0032	2.302	12 : 48 : 59.66	+00 : 15 : 45.5	0.01	18.91±0.137	18.25±0.018	18.30±0.014	18.08±0.013	17.69±0.028	0.02	1 2
LBQS 1249+0018	0.878	12 : 51 : 40.33	+00 : 02 : 10.9	1.02	18.39±0.026	17.89±0.018	17.60±0.014	17.53±0.011	17.37±0.031	0.02	1
UN J1252+0053	1.688	12 : 52 : 43.87	+00 : 53 : 20.1	0.17	18.55±0.033	18.33±0.020	18.16±0.028	17.86±0.027	17.93±0.034	0.02	1 2
LBQS 1250+0109	0.792	12 : 52 : 56.02	+00 : 53 : 39.5	0.13	18.30±0.023	17.99±0.011	17.95±0.010	18.09±0.015	18.00±0.045	0.02	1 2
UM 524	2.381	12 : 54 : 54.80	+01 : 00 : 07.9	0.32	18.97±0.031	18.31±0.012	18.37±0.016	18.28±0.017	17.96±0.025	0.02	1 2
EQS B1253-0002	0.717	12 : 55 : 50.31	-00 : 18 : 31.0	0.10	18.17±0.029	17.84±0.014	17.88±0.029	18.01±0.030	17.91±0.026	0.03	1 2
SDSSp J130348.94+002010.5	3.640	13 : 03 : 48.94	+00 : 20 : 10.5	0.06	24.56±0.533	20.87±0.033	18.95±0.014	18.71±0.015	18.32±0.043	0.02	2
EQS B1305+0100	0.763	13 : 07 : 54.27	+00 : 44 : 22.1	0.40	17.84±0.046	17.55±0.01	17.51±0.014	17.56±0.014	17.41±0.022	0.03	1
UM 545	2.110	13 : 08 : 01.36	-00 : 04 : 56.8	2.38	18.83±0.066	18.71±0.025	18.52±0.040	18.38±0.019	18.12±0.026	0.02	1
SDSSp J131052.52-005533.4	4.150	13 : 10 : 52.51	-00 : 55 : 33.3	0.22	23.25±0.710	20.86±0.033	18.88±0.013	18.84±0.013	18.82±0.037	0.03	2
LBQS 1308+0047	0.428	13 : 11 : 08.48	+00 : 31 : 51.8	1.47	18.09±0.077	17.90±0.016	17.92±0.011	17.91±0.015	17.73±0.022	0.04	1
LBQS 1308+0109	1.075	13 : 11 : 21.15	+00 : 53 : 19.5	0.88	18.15±0.045	17.90±0.015	17.62±0.010	17.64±0.017	17.76±0.028	0.04	1
LBQS 1308+0105	2.799	13 : 11 : 28.36	+00 : 49 : 29.8	0.21	19.96±0.051	18.92±0.016	18.76±0.015	18.74±0.013	18.51±0.054	0.03	1 2
LBQS 1311+0121	1.526	13 : 13 : 52.84	+01 : 05 : 11.1	0.03	19.35±0.056	19.19±0.015	18.98±0.013	18.71±0.016	18.69±0.043	0.03	1 2
LBQS 1313+0020	0.732	13 : 15 : 52.69	+00 : 04 : 54.4	0.16	18.44±0.025	18.06±0.034	18.23±0.022	18.19±0.030	18.13±0.034	0.02	1 2
LBQS 1313+0111	1.572	13 : 15 : 58.97	+00 : 55 : 11.2	0.06	19.25±0.040	19.07±0.017	18.92±0.012	18.69±0.021	18.68±0.036	0.04	1 2

Table 2—Continued

Name	z_{em}	RA(2000)	DEC(2000)	Δ''	u^*	g^*	r^*	i^*	z^*	$E(g^*-r^*)$	source
LBQS 1313+0107	2.403	13 : 16 : 30.46	+00 : 51 : 25.5	0.04	19.04±0.078	18.24±0.010	18.25±0.019	18.09±0.012	17.82±0.023	0.03	1 2
LBQS 1314-0008	1.742	13 : 16 : 48.00	−00 : 24 : 33.7	0.18	18.51±0.076	18.32±0.026	18.24±0.019	17.98±0.023	17.94±0.037	0.02	1 2
LBQS 1314+0116	2.692	13 : 17 : 14.22	+01 : 00 : 13.1	0.10	19.87±0.078	18.49±0.020	18.28±0.016	18.12±0.023	17.85±0.055	0.03	1 2
LBQS 1315+0002	0.918	13 : 17 : 44.92	−00 : 12 : 50.7	0.28	18.47±0.062	18.07±0.025	17.85±0.025	17.86±0.017	17.68±0.061	0.02	1 2
LBQS 1315+0127	1.650	13 : 18 : 10.73	+01 : 11 : 40.9	0.17	18.11±0.023	17.91±0.020	17.91±0.014	17.74±0.011	17.76±0.061	0.03	1 2
LBQS 1315+0014	0.889	13 : 18 : 17.78	−00 : 01 : 46.3	1.23	19.55±0.030	19.28±0.017	19.23±0.016	19.31±0.021	19.13±0.049	0.04	1
LBQS 1316+0023	0.492	13 : 18 : 40.21	+00 : 07 : 35.3	0.17	18.26±0.029	17.99±0.022	17.91±0.025	17.77±0.015	17.80±0.037	0.03	1 2
LBQS 1316+0103	0.392	13 : 18 : 43.86	+00 : 47 : 32.1	0.13	18.50±0.035	18.50±0.011	18.52±0.011	18.44±0.017	17.95±0.027	0.03	1 2
LBQS 1316+0044	1.131	13 : 19 : 08.14	+00 : 28 : 43.8	0.04	18.36±0.064	18.43±0.013	18.31±0.010	18.38±0.016	18.51±0.029	0.03	1 2
LBQS 1317-0033	0.890	13 : 19 : 38.76	−00 : 49 : 40.1	0.09	17.82±0.078	17.66±0.024	17.55±0.012	17.58±0.024	17.43±0.047	0.02	1 2
LBQS 1317-0018	0.354	13 : 20 : 20.28	−00 : 34 : 28.3	0.16	18.44±0.075	18.42±0.028	18.42±0.037	18.43±0.014	17.79±0.020	0.02	1 2
LBQS 1318+0100	1.102	13 : 20 : 37.54	+00 : 44 : 39.4	0.14	18.53±0.022	18.45±0.011	18.23±0.012	18.18±0.010	18.22±0.038	0.04	1 2
LBQS 1318-0006	1.588	13 : 21 : 08.63	−00 : 22 : 13.8	0.24	18.80±0.086	18.60±0.017	18.58±0.016	18.39±0.016	18.51±0.029	0.02	1 2
SDSSp J132110.82+003821.7	4.700	13 : 21 : 10.82	+00 : 38 : 21.7	0.05	23.28±0.445	23.27±0.195	21.45±0.067	20.04±0.034	20.05±0.100	0.03	2
LBQS 1319+0039	1.618	13 : 21 : 39.56	+00 : 23 : 57.6	0.08	18.12±0.065	17.84±0.023	17.65±0.015	17.39±0.016	17.36±0.032	0.03	1 2
LBQS 1319-0019	1.154	13 : 21 : 48.13	−00 : 35 : 16.9	0.17	18.75±0.079	18.64±0.016	18.47±0.015	18.52±0.030	18.66±0.064	0.03	1 2
LBQS 1319+0033	0.535	13 : 22 : 06.20	+00 : 17 : 59.7	0.06	18.25±0.070	17.89±0.012	18.04±0.021	17.95±0.023	17.90±0.070	0.03	1 2
LBQS 1319+0110	2.151	13 : 22 : 14.82	+00 : 54 : 19.9	0.07	18.75±0.027	18.44±0.022	18.27±0.015	18.22±0.018	18.02±0.030	0.02	1 2
LBQS 1320-0033	1.144	13 : 22 : 36.00	−00 : 49 : 12.3	0.32	18.66±0.065	18.36±0.042	18.03±0.018	17.92±0.020	17.80±0.031	0.03	1
LBQS 1320+0048	1.968	13 : 23 : 14.50	+00 : 32 : 50.9	0.16	19.11±0.067	19.24±0.030	19.21±0.025	18.97±0.024	18.85±0.041	0.03	1 2
LBQS 1320-0006	1.392	13 : 23 : 23.79	−00 : 21 : 55.2	0.08	19.01±0.113	18.48±0.020	17.89±0.024	17.68±0.015	17.59±0.048	0.03	1 2
LBQS 1320+0103	1.784	13 : 23 : 33.04	+00 : 47 : 50.3	0.03	17.94±0.035	17.90±0.023	17.71±0.015	17.37±0.020	17.27±0.018	0.03	1 2
LBQS 1324+0125	0.970	13 : 27 : 11.13	+01 : 10 : 09.7	0.91	18.92±0.068	18.84±0.022	18.67±0.013	18.76±0.031	18.58±0.082	0.02	1
LBQS 1324+0126	0.868	13 : 27 : 24.04	+01 : 11 : 23.9	0.14	18.33±0.062	18.19±0.013	18.06±0.016	18.10±0.017	17.89±0.058	0.03	1 2
LBQS 1325+0027	2.524	13 : 27 : 50.45	+00 : 11 : 56.9	0.17	19.35±0.037	18.66±0.021	18.37±0.017	18.18±0.021	17.92±0.050	0.03	1 2
LBQS 1325-0038	0.959	13 : 28 : 11.36	−00 : 53 : 43.1	0.07	19.07±0.061	18.92±0.011	18.73±0.013	18.77±0.011	18.65±0.033	0.03	1 2
LBQS 1327+0055	2.298	13 : 29 : 44.36	+00 : 40 : 04.6	1.01	18.54±0.022	17.93±0.01	17.88±0.01	17.86±0.021	17.70±0.020	0.03	1
LBQS 1328+0047	1.475	13 : 30 : 52.37	+00 : 32 : 18.3	0.15	18.39±0.050	18.28±0.022	18.17±0.014	18.02±0.018	18.03±0.028	0.03	1 2
LBQS 1329+0018	2.351	13 : 32 : 15.04	+00 : 02 : 52.6	0.87	19.21±0.025	18.51±0.037	18.31±0.015	18.24±0.013	18.00±0.050	0.02	1
LBQS 1329-0007	0.960	13 : 32 : 31.09	−00 : 23 : 18.2	0.22	18.47±0.063	18.29±0.013	18.14±0.013	18.26±0.020	18.12±0.059	0.04	1 2
[MMB90] 133021.15+010814.0	3.510	13 : 32 : 54.51	+00 : 52 : 50.6	1.71	23.82±0.405	19.15±0.028	18.33±0.016	18.12±0.018	18.07±0.056	0.03	1
LBQS 1330+0113	1.509	13 : 33 : 21.90	+00 : 58 : 24.3	0.04	18.35±0.030	18.22±0.027	18.01±0.016	17.79±0.018	17.85±0.056	0.03	1 2
LBQS 1332-0045	0.672	13 : 35 : 26.00	−01 : 00 : 28.1	0.09	17.51±0.021	17.31±0.01	17.31±0.01	17.18±0.01	17.20±0.022	0.03	1 2
LBQS 1334-0033	2.801	13 : 36 : 47.15	−00 : 48 : 57.1	1.15	18.26±0.058	17.48±0.016	17.50±0.055	17.46±0.035	17.26±0.037	0.03	1
LBQS 1334-0005	0.295	13 : 36 : 49.11	−00 : 20 : 57.4	0.17	18.15±0.094	18.19±0.031	18.11±0.019	18.13±0.033	17.64±0.027	0.03	1 2
LBQS 1334+0053	0.647	13 : 37 : 22.59	+00 : 38 : 11.5	0.21	19.26±0.034	18.88±0.012	19.03±0.017	18.99±0.021	19.08±0.056	0.03	1 2
LBQS 1334+0113	0.330	13 : 37 : 26.48	+00 : 58 : 28.7	0.11	18.18±0.041	18.28±0.021	18.14±0.019	18.09±0.025	17.57±0.081	0.03	1 2
[HB89] 1335+005NED01	0.336	13 : 37 : 49.84	+00 : 16 : 52.6	1.09	21.06±0.080	20.30±0.022	19.59±0.020	19.66±0.024	19.23±0.114	0.02	1
[HB89] 1335+005NED02	2.163	13 : 38 : 23.04	+00 : 16 : 12.0	0.16	18.79±0.032	18.60±0.022	18.50±0.014	18.37±0.020	18.20±0.059	0.03	1 2
[HB89] 1335+005NED03	1.014	13 : 38 : 28.31	+00 : 17 : 32.4	0.44	19.59±0.037	19.43±0.024	19.22±0.017	19.34±0.024	19.30±0.080	0.03	1
[HB89] 1336+006NED01	2.103	13 : 38 : 39.80	+00 : 23 : 32.4	0.37	20.87±0.067	20.69±0.031	20.71±0.037	20.51±0.046	20.51±0.177	0.03	1
[HB89] 1336+007	1.953	13 : 38 : 56.85	+00 : 27 : 18.4	0.04	19.05±0.021	18.94±0.018	18.86±0.012	18.69±0.015	18.54±0.030	0.03	1 2
[HB89] 1336+004NED01	1.648	13 : 38 : 59.10	+00 : 11 : 30.0	1.03	20.35±0.130	20.11±0.018	20.01±0.025	19.63±0.029	19.69±0.081	0.03	1
[HB89] 1336+004NED02	2.242	13 : 39 : 04.03	+00 : 09 : 45.0	0.43	21.14±0.142	20.65±0.023	20.85±0.036	20.63±0.043	20.43±0.138	0.03	1
[HB89] 1336+004NED03	1.050	13 : 39 : 04.86	+00 : 10 : 11.3	0.98	20.33±0.130	20.33±0.020	20.06±0.025	20.15±0.034	20.56±0.152	0.03	1
[HB89] 1336+001	1.062	13 : 39 : 06.78	−00 : 04 : 23.7	1.29	19.60±0.066	19.37±0.024	19.24±0.014	19.24±0.029	19.14±0.103	0.02	1
[HB89] 1336-000	1.808	13 : 39 : 34.24	−00 : 16 : 35.5	1.05	20.78±0.057	18.70±0.036	17.58±0.019	17.17±0.024	16.81±0.066	0.03	1
[HB89] 1337+004NED01	2.122	13 : 39 : 39.02	+00 : 10 : 21.9	0.27	19.37±0.106	19.23±0.023	19.11±0.025	18.76±0.019	18.44±0.066	0.04	1
[HB89] 1337+004NED02	1.880	13 : 39 : 45.37	+00 : 09 : 46.3	0.22	19.27±0.106	19.22±0.023	19.21±0.025	18.94±0.019	18.82±0.070	0.04	1 2
[HB89] 1337+005	1.906	13 : 40 : 31.37	+00 : 15 : 07.8	0.33	18.61±0.018	18.68±0.017	18.74±0.013	18.50±0.017	18.48±0.080	0.03	1 2
LBQS 1338-0030	0.388	13 : 40 : 44.52	−00 : 45 : 16.6	0.09	17.26±0.144	17.20±0.026	17.32±0.016	17.36±0.024	16.95±0.042	0.03	1 2

Table 2—Continued

Name	z_{em}	RA(2000)	DEC(2000)	Δ''	u^*	g^*	r^*	i^*	z^*	$E(g^*-r^*)$	source
LBQS 1338-0038	0.237	13 : 41 : 13.93	-00 : 53 : 15.0	0.11	17.66±0.016	17.74±0.014	17.54±0.01	17.10±0.01	17.28±0.017	0.02	1 2
F864:137	0.169	13 : 42 : 30.42	-00 : 07 : 09.8	1.19	21.97±0.147	21.01±0.034	20.68±0.036	20.53±0.041	20.33±0.134	0.03	1
F864:093	0.378	13 : 42 : 32.95	-00 : 15 : 50.6	0.84	20.48±0.045	20.05±0.026	19.75±0.022	19.70±0.024	19.68±0.061	0.03	1
F864:094	2.439	13 : 42 : 33.09	-00 : 07 : 52.5	0.55	20.77±0.069	20.01±0.023	19.90±0.025	19.80±0.024	19.49±0.086	0.03	1
F864:076	0.515	13 : 42 : 33.71	-00 : 11 : 48.0	0.10	19.41±0.048	19.01±0.020	19.13±0.021	18.93±0.018	18.81±0.071	0.03	1 2
F864:169	1.717	13 : 42 : 37.81	-00 : 15 : 22.6	1.46	21.78±0.111	20.90±0.033	20.39±0.027	19.93±0.027	19.74±0.064	0.03	1
F864:115	1.754	13 : 42 : 38.01	-00 : 09 : 27.6	1.41	21.43±0.100	21.10±0.036	21.26±0.053	20.85±0.053	20.94±0.206	0.03	1
LBQS 1340-0020	0.788	13 : 42 : 46.26	-00 : 35 : 43.7	0.04	18.27±0.035	18.12±0.014	18.19±0.037	18.38±0.021	18.24±0.047	0.03	1 2
LBQS 1340-0038	0.326	13 : 42 : 51.61	-00 : 53 : 45.3	0.15	16.90±0.024	16.90±0.013	16.88±0.012	17.06±0.020	16.51±0.016	0.04	1 2
F864:072	0.803	13 : 42 : 56.52	+00 : 00 : 57.3	0.01	19.37±0.174	18.92±0.021	18.85±0.029	19.05±0.035	18.88±0.043	0.03	1 2
F864:162	1.507	13 : 42 : 58.94	-00 : 23 : 36.9	0.94	23.30±0.340	22.33±0.078	21.92±0.077	21.54±0.079	20.84±0.152	0.03	1
LBQS 1340+0107	1.067	13 : 42 : 59.05	+00 : 51 : 57.7	0.10	17.95±0.102	17.72±0.025	17.55±0.013	17.58±0.022	17.61±0.087	0.03	1 2
F864:124	2.386	13 : 43 : 01.27	-00 : 14 : 09.6	1.71	21.28±0.077	20.34±0.027	20.26±0.026	20.15±0.031	19.86±0.070	0.03	1
F864:082	2.053	13 : 43 : 01.58	-00 : 29 : 50.6	0.50	20.18±0.047	20.07±0.021	20.02±0.029	19.95±0.033	19.71±0.075	0.03	1
F864:119	0.667	13 : 43 : 13.37	-00 : 05 : 01.2	2.02	21.52±0.101	20.98±0.037	20.78±0.035	20.23±0.033	19.83±0.082	0.03	1
F864:114	1.976	13 : 43 : 22.03	+00 : 00 : 10.1	0.43	20.47±0.116	20.34±0.021	20.33±0.030	20.06±0.033	19.96±0.109	0.02	1
F864:102	1.886	13 : 43 : 24.28	-00 : 20 : 29.7	0.45	19.92±0.039	19.90±0.029	19.86±0.021	19.56±0.022	19.48±0.077	0.03	1
F864:080	1.513	13 : 43 : 25.84	-00 : 16 : 12.2	0.07	19.51±0.035	19.24±0.027	19.03±0.018	18.80±0.018	18.77±0.066	0.03	1 2
RX J1343.4+0001	2.347	13 : 43 : 29.22	+00 : 01 : 32.8	0.35	22.40±0.217	21.54±0.040	21.12±0.044	20.72±0.045	20.22±0.126	0.02	1
F864:081	1.055	13 : 43 : 47.58	-00 : 23 : 36.3	0.78	20.27±0.042	20.07±0.026	19.70±0.026	19.74±0.021	19.82±0.079	0.03	1
F864:097	1.140	13 : 43 : 53.48	-00 : 05 : 20.0	1.18	20.64±0.060	20.66±0.025	20.39±0.028	20.33±0.036	20.57±0.149	0.02	1
F864:113	1.410	13 : 43 : 59.90	+00 : 00 : 46.1	0.07	20.20±0.091	20.14±0.019	19.97±0.019	19.89±0.026	19.86±0.087	0.03	1
F864:108	1.188	13 : 44 : 12.29	-00 : 24 : 47.2	0.84	19.88±0.036	19.81±0.025	19.64±0.026	19.66±0.020	19.66±0.073	0.03	1
F864:112	1.884	13 : 44 : 20.89	+00 : 02 : 27.0	1.06	20.43±0.098	20.27±0.021	20.26±0.027	20.00±0.024	19.69±0.072	0.03	1
F864:158	2.235	13 : 44 : 23.95	-00 : 28 : 46.4	1.00	22.15±0.189	21.47±0.049	21.61±0.073	21.20±0.073	21.12±0.247	0.02	1
F864:148	1.767	13 : 44 : 24.54	-00 : 24 : 12.7	0.90	21.38±0.086	21.25±0.033	21.32±0.049	20.96±0.050	21.18±0.194	0.02	1
F864:069	1.373	13 : 44 : 27.91	-00 : 30 : 28.6	1.76	19.26±0.031	19.09±0.025	18.58±0.020	18.54±0.011	18.54±0.056	0.02	1
F864:111	0.852	13 : 44 : 54.64	-00 : 19 : 07.6	0.74	20.94±0.059	20.59±0.031	20.44±0.031	20.45±0.043	20.28±0.098	0.03	1
LBQS 1342-0000	0.245	13 : 44 : 59.44	-00 : 15 : 59.5	0.10	17.71±0.015	17.69±0.025	17.58±0.021	17.44±0.030	17.44±0.041	0.03	1 2
LBQS 1343-0008	1.097	13 : 45 : 47.87	-00 : 23 : 23.4	0.11	18.00±0.041	17.74±0.039	17.42±0.027	17.44±0.018	17.41±0.022	0.03	1 2
[HB89] 1343+012	0.487	13 : 46 : 14.99	+00 : 57 : 06.1	1.38	19.57±0.111	19.43±0.021	19.65±0.019	19.43±0.021	19.18±0.048	0.03	1
LBQS 1345-0000	0.553	13 : 47 : 51.71	-00 : 15 : 18.4	0.09	18.14±0.041	17.89±0.025	18.05±0.020	17.98±0.014	18.02±0.032	0.03	1 2
SDSSp J134755.68+003935.1	3.800	13 : 47 : 55.67	+00 : 39 : 35.1	0.08	23.97±0.454	20.52±0.022	19.47±0.013	19.36±0.025	19.35±0.053	0.03	2
LBQS 1346+0121A	1.949	13 : 48 : 34.97	+01 : 06 : 26.2	0.06	18.31±0.020	18.25±0.019	18.14±0.020	17.98±0.026	17.89±0.048	0.03	1 2
[HB89] 1346+001	3.268	13 : 49 : 17.79	-00 : 07 : 02.2	0.80	19.66±0.102	18.73±0.025	18.42±0.025	18.28±0.022	18.29±0.031	0.04	1
LBQS 1346+0007	1.128	13 : 49 : 22.12	-00 : 06 : 57.7	0.39	18.91±0.100	18.54±0.025	18.30±0.025	18.25±0.022	18.21±0.030	0.04	1
LBQS 1347-0026	0.516	13 : 49 : 34.31	-00 : 41 : 02.9	0.21	18.13±0.128	17.81±0.018	17.91±0.018	17.72±0.021	17.65±0.030	0.03	1 2
1RXS J134948.2-010619	0.599	13 : 49 : 48.40	-01 : 06 : 21.8	0.09	16.98±0.053	16.41±0.023	16.32±0.01	16.10±0.01	16.17±0.01	0.04	1 2
LBQS 1348-0054	1.479	13 : 50 : 44.67	-01 : 08 : 59.2	0.06	18.43±0.047	18.20±0.01	17.95±0.035	17.72±0.012	17.69±0.030	0.05	1 2
PKS 1348+007	2.084	13 : 51 : 04.43	+00 : 31 : 19.5	0.62	22.74±0.228	22.36±0.085	22.43±0.118	22.17±0.156	21.60±0.349	0.03	1
LBQS 1348+0118	1.085	13 : 51 : 28.32	+01 : 03 : 38.6	0.18	17.49±0.023	17.26±0.016	17.02±0.020	17.03±0.014	17.09±0.047	0.03	1 2
UM 617	1.444	13 : 51 : 50.49	-00 : 07 : 38.8	0.28	16.97±0.151	16.88±0.044	16.72±0.033	16.60±0.027	16.65±0.077	0.04	1 2
LBQS 1349+0057	1.158	13 : 52 : 32.58	+00 : 42 : 52.5	0.02	18.44±0.023	18.21±0.01	17.90±0.010	17.86±0.013	17.90±0.027	0.04	1 2
LBQS 1350+0052	0.485	13 : 52 : 52.15	+00 : 37 : 58.6	0.10	18.37±0.023	18.05±0.01	18.09±0.011	17.93±0.014	17.92±0.026	0.04	1 2
PG 1352+011	1.117	13 : 54 : 58.68	+00 : 52 : 10.9	0.94	16.27±0.075	16.08±0.014	15.89±0.036	15.93±0.015	15.98±0.042	0.04	1
[HB89] 1352-007	0.895	13 : 55 : 25.66	-00 : 57 : 40.6	0.11	19.02±0.020	18.76±0.016	18.66±0.01	18.82±0.013	18.65±0.031	0.05	1 2
DMS 0726 14n	1.340	14 : 00 : 44.04	-00 : 54 : 10.4	0.68	21.78±0.116	21.85±0.066	21.36±0.053	21.17±0.071	21.02±0.219	0.05	1
DMS 1358-0047	2.040	14 : 00 : 51.73	-01 : 02 : 11.1	0.95	20.59±0.041	20.56±0.025	20.57±0.029	20.25±0.034	20.08±0.105	0.05	1
DMS 1358-0052	0.850	14 : 00 : 57.02	-01 : 06 : 47.0	1.00	20.38±0.044	20.22±0.021	20.05±0.020	19.75±0.028	19.67±0.064	0.05	1
DMS 1358-0054	2.810	14 : 01 : 02.18	-01 : 08 : 44.3	0.72	21.88±0.137	20.67±0.027	20.53±0.027	20.43±0.040	20.16±0.095	0.04	1
DMS 1175 14n	0.928	14 : 01 : 03.31	-00 : 50 : 30.8	0.28	18.60±0.023	18.42±0.01	18.32±0.01	18.44±0.010	18.45±0.028	0.04	1 2

Table 2—Continued

Name	z_{em}	RA(2000)	DEC(2000)	Δ''	u^*	g^*	r^*	i^*	z^*	$E(g^*-r^*)$	source
EQS B1358+0058	0.667	14 : 01 : 04.87	+00 : 43 : 32.6	0.08	17.63±0.075	17.29±0.01	17.27±0.017	17.09±0.022	17.04±0.023	0.04	1 2
UM 627	1.865	14 : 01 : 10.81	−00 : 13 : 03.7	0.37	16.81±0.025	16.64±0.025	16.75±0.016	16.53±0.030	16.48±0.054	0.05	1
DMS 1358-0100	0.820	14 : 01 : 11.07	−01 : 15 : 19.7	0.59	21.32±0.086	20.98±0.034	20.76±0.041	20.73±0.047	20.46±0.127	0.05	1
DMS 1358-0031	2.522	14 : 01 : 14.29	−00 : 45 : 37.0	0.17	19.32±0.038	18.84±0.022	18.73±0.016	18.72±0.015	18.45±0.026	0.05	1 2
DMS 1358-0050	1.340	14 : 01 : 21.63	−01 : 04 : 50.8	0.47	21.50±0.101	21.52±0.052	21.21±0.046	21.13±0.063	20.93±0.177	0.05	1
DMS 1359-0030	0.860	14 : 01 : 35.26	−00 : 45 : 17.3	0.97	20.96±0.078	20.83±0.033	20.70±0.033	20.53±0.039	20.24±0.097	0.05	1
DMS 1359-0056	1.850	14 : 01 : 40.23	−01 : 11 : 18.3	0.88	22.18±0.177	22.24±0.095	22.58±0.144	21.85±0.121	21.58±0.300	0.05	1
DMS 1076 14n	1.140	14 : 01 : 45.20	−00 : 51 : 11.5	0.53	20.32±0.041	20.22±0.020	19.98±0.018	20.01±0.027	20.09±0.099	0.04	1
UM 629	2.465	14 : 03 : 23.39	−00 : 06 : 06.9	0.03	18.66±0.071	17.98±0.014	17.95±0.012	17.90±0.011	17.67±0.037	0.05	1 2
SDSSp J140554.07-000037.0	3.650	14 : 05 : 54.07	−00 : 00 : 37.0	0.07	23.59±0.453	20.15±0.025	18.79±0.023	18.54±0.029	18.31±0.045	0.05	2
UM 638	1.960	14 : 08 : 17.56	−01 : 14 : 32.1	0.68	18.13±0.027	18.00±0.012	17.94±0.010	17.68±0.01	17.62±0.030	0.06	1
UM 645	2.262	14 : 11 : 23.52	+00 : 42 : 53.0	0.13	18.77±0.037	18.18±0.010	18.16±0.012	17.98±0.026	17.77±0.027	0.04	1 2
SDSSp J141205.78-010152.6	3.730	14 : 12 : 05.80	−01 : 01 : 52.7	0.39	23.52±0.513	20.61±0.028	19.44±0.014	19.25±0.016	18.95±0.047	0.06	2
SDSSp J141315.36+000032.1	4.090	14 : 13 : 15.36	+00 : 00 : 32.4	0.26	23.80±0.564	21.43±0.044	19.79±0.026	19.75±0.024	19.73±0.104	0.04	2
SDSSp J141332.35-004909.7	4.140	14 : 13 : 32.35	−00 : 49 : 09.6	0.10	25.46±0.872	21.14±0.038	19.59±0.023	19.30±0.018	19.05±0.052	0.05	2
EQS B1413+0107	1.041	14 : 15 : 49.71	+00 : 53 : 56.5	0.15	17.54±0.106	17.21±0.015	16.87±0.011	16.93±0.025	16.86±0.077	0.04	1 2
EQS B1420-0053	0.717	14 : 22 : 40.36	−01 : 06 : 46.1	0.16	17.82±0.022	17.44±0.01	17.63±0.023	17.45±0.013	17.29±0.016	0.04	1 2
SDSSp J142329.98+004138.4	3.760	14 : 23 : 29.99	+00 : 41 : 38.4	0.08	23.87±0.376	20.80±0.028	19.51±0.016	19.49±0.020	19.41±0.054	0.03	2
[VCV96] Q 1421-0013	0.151	14 : 24 : 03.81	−00 : 26 : 58.1	0.13	16.44±0.022	16.34±0.018	16.22±0.024	15.85±0.012	15.98±0.033	0.04	1
EQS B1421+0108	1.059	14 : 24 : 30.42	+00 : 54 : 59.2	0.02	18.01±0.131	17.94±0.024	17.78±0.027	17.87±0.020	17.90±0.053	0.03	1 2
EQS B1423-0013	1.075	14 : 26 : 00.22	−00 : 27 : 00.4	0.16	17.99±0.145	17.77±0.018	17.59±0.021	17.49±0.027	17.47±0.073	0.05	1 2
SDSSp J142647.82+002740.4	3.690	14 : 26 : 47.80	+00 : 27 : 40.0	0.45	22.38±0.206	20.55±0.022	19.40±0.015	19.36±0.029	19.25±0.048	0.04	2
EQS B1424-0007	0.629	14 : 26 : 58.58	−00 : 20 : 56.4	0.15	17.15±0.068	16.72±0.014	16.84±0.029	16.78±0.016	16.88±0.036	0.04	1 2
LBQS 1429-0100	0.657	14 : 31 : 41.90	−01 : 13 : 30.6	0.07	17.76±0.018	17.42±0.012	17.55±0.010	17.52±0.015	17.56±0.025	0.05	1 2
LBQS 1429-0036	1.190	14 : 31 : 43.80	−00 : 50 : 11.5	0.06	18.54±0.028	18.25±0.020	18.05±0.033	17.90±0.013	17.94±0.034	0.04	1 2
LBQS 1429+0127	1.094	14 : 31 : 49.41	+01 : 14 : 29.9	0.12	18.31±0.055	18.23±0.016	18.08±0.018	18.11±0.018	18.19±0.040	0.04	1 2
LBQS 1429-0053	2.089	14 : 32 : 29.25	−01 : 06 : 16.1	0.11	18.06±0.013	17.91±0.01	17.82±0.016	17.57±0.010	17.25±0.035	0.05	1 2
LBQS 1429-0039B	0.362	14 : 32 : 30.99	−00 : 52 : 29.0	0.06	19.69±0.028	19.44±0.014	19.02±0.013	18.83±0.018	18.33±0.026	0.04	1 2
LBQS 1430-0046	1.023	14 : 32 : 44.44	−00 : 59 : 15.1	0.03	17.80±0.023	17.57±0.01	17.26±0.01	17.26±0.01	17.31±0.025	0.05	1 2
LBQS 1430-0041	1.116	14 : 33 : 21.42	−00 : 54 : 45.8	1.84	16.84±0.022	16.62±0.01	16.48±0.01	16.52±0.013	16.49±0.012	0.05	1
LBQS 1431-0029	1.263	14 : 33 : 57.00	−00 : 42 : 41.0	1.48	18.39±0.070	17.70±0.029	17.41±0.019	17.39±0.021	17.43±0.023	0.04	1
LBQS 1433+0007	0.967	14 : 35 : 42.69	−00 : 05 : 41.8	0.12	18.89±0.114	18.75±0.019	18.57±0.016	18.71±0.032	18.68±0.052	0.05	1 2
LBQS 1433+0011	0.582	14 : 36 : 20.04	−00 : 01 : 12.9	0.06	19.51±0.116	19.17±0.032	19.39±0.019	19.19±0.018	19.13±0.057	0.04	1 2
LBQS 1433-0016	0.325	14 : 36 : 24.82	−00 : 29 : 05.4	0.12	18.43±0.050	18.20±0.015	17.91±0.022	17.85±0.016	17.31±0.064	0.04	1 2
LBQS 1433-0025	2.060	14 : 36 : 28.46	−00 : 38 : 40.3	0.05	18.69±0.069	18.57±0.016	18.48±0.032	18.28±0.033	18.02±0.045	0.04	1 2
LBQS 1434-0038	1.273	14 : 36 : 45.06	−00 : 51 : 50.6	0.07	18.66±0.040	18.78±0.015	18.28±0.012	18.26±0.010	18.30±0.034	0.04	1 2
LBQS 1434-0059	1.684	14 : 36 : 50.18	−01 : 12 : 28.1	0.04	18.70±0.020	18.56±0.014	18.53±0.037	18.22±0.014	18.18±0.026	0.04	1 2
[VCV96] Q 1434+0020	0.140	14 : 37 : 04.12	+00 : 07 : 05.1	0.14	17.92±0.055	18.03±0.024	18.02±0.028	17.50±0.021	17.67±0.055	0.04	1 2
LBQS 1436+0017	1.407	14 : 39 : 31.89	+00 : 04 : 52.2	0.02	18.13±0.037	17.96±0.022	17.85±0.019	17.77±0.011	17.73±0.038	0.05	1 2
SDSSp J143951.60-003429.2	4.258	14 : 39 : 51.60	−00 : 34 : 29.1	0.06	23.08±0.388	23.53±0.223	21.87±0.103	21.47±0.103	20.98±0.209	0.04	2
SDSSp J143952.58-003359.2	4.255	14 : 39 : 52.58	−00 : 33 : 59.1	0.15	24.20±0.591	23.23±0.177	20.90±0.053	20.55±0.048	20.27±0.117	0.04	2
LBQS 1437+0002	1.410	14 : 40 : 24.17	−00 : 10 : 38.5	0.15	19.37±0.073	19.32±0.026	18.94±0.031	18.79±0.021	18.77±0.052	0.04	1 2
LBQS 1438+0002	1.446	14 : 40 : 57.21	−00 : 09 : 51.4	0.60	18.35±0.071	17.76±0.025	17.46±0.029	17.27±0.018	17.31±0.042	0.04	1
LBQS 1439+0047	1.857	14 : 42 : 01.80	+00 : 34 : 48.9	0.16	18.57±0.041	18.28±0.012	18.21±0.021	17.93±0.024	17.94±0.038	0.05	1
LBQS 1440-0024	1.821	14 : 42 : 59.91	−00 : 37 : 25.0	0.06	17.77±0.076	17.74±0.017	17.74±0.01	17.48±0.031	17.48±0.068	0.04	1 2
LBQS 1442-0011	2.226	14 : 45 : 14.87	−00 : 23 : 58.2	1.30	19.02±0.021	18.31±0.013	17.84±0.027	17.77±0.016	17.58±0.065	0.03	1
LBQS 1443-0004	1.795	14 : 45 : 44.62	−00 : 17 : 14.9	0.06	18.26±0.030	18.16±0.016	18.14±0.018	17.95±0.026	17.93±0.025	0.04	1 2
LBQS 1443-0100	1.801	14 : 45 : 59.55	−01 : 13 : 17.5	0.16	18.55±0.069	18.40±0.015	18.22±0.014	17.83±0.012	17.75±0.026	0.05	1 2
LBQS 1443+0013	1.015	14 : 46 : 25.13	+00 : 00 : 41.5	0.19	18.77±0.130	18.46±0.021	18.17±0.026	18.17±0.019	18.03±0.041	0.04	1 2
LBQS 1444-0019	0.696	14 : 46 : 46.38	−00 : 31 : 43.8	0.17	18.21±0.059	17.83±0.026	17.88±0.017	17.94±0.021	17.87±0.020	0.04	1 2
LBQS 1444+0126	2.206	14 : 46 : 53.04	+01 : 13 : 56.0	0.53	19.39±0.050	18.77±0.030	18.61±0.017	18.46±0.036	18.11±0.050	0.05	1

Table 2—Continued

Name	z_{em}	RA(2000)	DEC(2000)	Δ''	u^*	g^*	r^*	i^*	z^*	$E(g^*-r^*)$	source
SDSSp J144758.44-005055.4	3.800	14 : 47 : 58.43	-00 : 50 : 55.4	0.14	23.93±0.917	21.06±0.036	19.61±0.017	19.38±0.021	19.14±0.048	0.05	2
LBQS 1446+0027	0.832	14 : 48 : 56.71	+00 : 15 : 10.3	0.19	19.21±0.043	18.88±0.036	18.79±0.016	18.88±0.021	18.70±0.084	0.05	1 2
LBQS 1446+0020	1.650	14 : 49 : 08.24	+00 : 08 : 24.3	0.19	18.49±0.029	18.23±0.029	18.23±0.020	18.07±0.020	18.02±0.045	0.05	1 2
LBQS 1446-0035	0.253	14 : 49 : 30.48	-00 : 47 : 46.4	0.12	18.12±0.099	18.00±0.036	17.64±0.019	17.48±0.017	17.24±0.024	0.05	1 2
LBQS 1448+0049	1.079	14 : 50 : 36.64	+00 : 37 : 24.3	0.63	18.12±0.054	18.06±0.026	17.77±0.014	17.80±0.017	17.90±0.037	0.04	1
SDSSp J145118.78-010446.2	4.660	14 : 51 : 18.78	-01 : 04 : 46.2	0.04	24.65±0.442	24.39±0.439	22.70±0.151	20.73±0.042	20.55±0.124	0.05	2
[HGP92] 151245.6+000000	1.568	15 : 15 : 19.40	-00 : 11 : 03.5	0.25	19.99±0.083	19.62±0.018	19.47±0.016	19.13±0.018	19.11±0.052	0.06	1 2
[HGP92] 151333.3-000443	1.490	15 : 16 : 07.15	-00 : 15 : 43.9	0.10	19.48±0.071	19.02±0.034	18.74±0.017	18.45±0.034	18.50±0.050	0.05	1 2
SDSSp J151618.44-000544.3	3.700	15 : 16 : 18.44	-00 : 05 : 44.1	0.17	24.61±0.448	21.76±0.051	20.26±0.025	20.03±0.030	19.78±0.079	0.06	2
[HGP92] 151422.7-000340	1.812	15 : 16 : 56.60	-00 : 14 : 38.8	0.08	20.01±0.068	19.53±0.026	19.32±0.017	19.33±0.027	18.93±0.049	0.06	1 2
QN Z3:33	1.382	15 : 18 : 34.28	+01 : 07 : 03.3	0.09	18.52±0.031	18.13±0.028	17.82±0.015	17.76±0.017	17.73±0.024	0.05	1 2
QN Z3:22	0.210	15 : 18 : 46.44	+01 : 13 : 51.2	0.67	19.12±0.040	18.99±0.025	18.74±0.014	18.44±0.019	18.43±0.048	0.05	1
SDSSp J152740.52-010602.6	4.410	15 : 27 : 40.52	-01 : 06 : 02.7	0.15	24.41±0.525	22.81±0.149	20.53±0.026	20.00±0.026	19.67±0.067	0.16	2
SDSSp J154014.57+001854.7	3.829	15 : 40 : 14.53	+00 : 18 : 54.2	0.85	24.64±0.519	21.75±0.054	20.42±0.038	20.26±0.036	20.34±0.168	0.09	2
[HB89] 1602-001	1.639	16 : 04 : 56.15	-00 : 19 : 07.1	0.15	17.90±0.038	17.59±0.011	17.35±0.015	17.11±0.017	17.02±0.018	0.14	1 2
SDSSp J162116.91-004251.1	3.740	16 : 21 : 16.92	-00 : 42 : 50.9	0.30	22.07±0.172	18.63±0.011	17.32±0.012	17.29±0.01	17.23±0.022	0.10	2
SDSSp J162448.30-003839.4	2.950	16 : 24 : 48.32	-00 : 38 : 39.1	0.41	22.13±0.187	20.37±0.022	20.13±0.021	20.20±0.028	20.03±0.085	0.10	2
LBQS 2231-0048	1.209	22 : 33 : 59.93	-00 : 33 : 15.8	0.94	17.79±0.010	17.79±0.01	17.36±0.01	17.30±0.01	17.37±0.015	0.06	1
LBQS 2231-0015	3.015	22 : 34 : 08.99	+00 : 00 : 01.7	0.36	19.16±0.021	17.57±0.01	17.26±0.01	17.13±0.01	17.01±0.013	0.06	1
LBQS 2235-0112	0.361	22 : 38 : 23.26	-00 : 57 : 08.2	0.65	18.27±0.012	18.22±0.01	18.23±0.01	18.21±0.01	17.54±0.019	0.05	1
LBQS 2236-0023	1.500	22 : 39 : 19.36	-00 : 08 : 18.1	0.90	18.62±0.016	18.48±0.01	18.35±0.01	18.16±0.01	18.18±0.031	0.06	1
[HB89] 2237+003	2.200	22 : 40 : 26.22	+00 : 39 : 40.1	0.27	19.13±0.021	18.56±0.01	18.29±0.01	18.23±0.01	18.06±0.027	0.08	1
[HB89] 2238+004	2.200	22 : 40 : 40.07	+00 : 40 : 25.1	2.14	21.43±0.130	20.42±0.024	20.03±0.023	19.83±0.035	19.42±0.088	0.07	1
[HB89] 2238+001	2.200	22 : 41 : 28.25	+00 : 23 : 07.1	2.25	20.38±0.055	19.93±0.016	19.75±0.019	19.65±0.028	19.25±0.093	0.07	1
LBQS 2239+0007	1.440	22 : 41 : 47.35	+00 : 22 : 54.7	1.01	18.54±0.015	18.33±0.01	18.14±0.01	17.99±0.01	17.97±0.030	0.07	1
LBQS 2244-0105	2.030	22 : 46 : 49.30	-00 : 49 : 54.3	1.53	17.73±0.01	17.58±0.01	17.38±0.01	17.21±0.01	17.00±0.012	0.08	1
LBQS 2244-0020	1.051	22 : 47 : 10.36	-00 : 05 : 07.3	0.88	18.62±0.015	18.42±0.01	18.10±0.01	18.11±0.01	18.02±0.026	0.09	1
LBQS 2250-0002	1.572	22 : 52 : 51.62	+00 : 13 : 39.0	1.75	19.70±0.032	19.41±0.012	19.26±0.012	18.98±0.016	18.90±0.075	0.08	1
SDSSp J225452.88+004822.7	3.696	22 : 54 : 52.88	+00 : 48 : 22.7	0.05	23.15±0.559	21.54±0.066	20.24±0.030	20.12±0.046	19.91±0.154	0.09	2
SDSSp J225624.35+004720.2	4.081	22 : 56 : 24.35	+00 : 47 : 20.3	0.16	24.11±0.884	21.98±0.098	20.30±0.050	20.27±0.093	19.94±0.161	0.07	2
SDSSp J230323.77+001615.2	3.696	23 : 03 : 23.77	+00 : 16 : 15.1	0.11	25.58±0.380	21.25±0.045	20.09±0.026	20.02±0.041	20.00±0.197	0.06	2
SDSSp J230639.65+010855.2	3.639	23 : 06 : 39.65	+01 : 08 : 55.1	0.11	23.42±0.552	20.61±0.028	19.24±0.014	18.95±0.019	18.83±0.059	0.05	2
SDSSp J232201.37+000035.5	3.843	23 : 22 : 01.37	+00 : 00 : 35.4	0.08	24.78±0.614	21.39±0.051	20.16±0.026	20.04±0.038	20.04±0.154	0.04	2
SDSSp J232717.99+000546.1	3.660	23 : 27 : 17.96	+00 : 05 : 45.9	0.50	24.57±0.947	20.93±0.045	19.82±0.025	19.81±0.037	20.03±0.167	0.04	2
PMN J2336+0002	1.096	23 : 36 : 24.05	+00 : 02 : 46.0	0.24	17.85±0.011	17.84±0.01	17.61±0.01	17.64±0.01	17.88±0.026	0.04	1 2
FIRST J233818.2-005610	0.898	23 : 38 : 18.27	-00 : 56 : 10.4	0.10	19.47±0.028	19.17±0.011	19.11±0.013	19.05±0.017	18.88±0.061	0.04	2
FIRST J233838.2-003514	2.676	23 : 38 : 38.23	-00 : 35 : 13.7	0.14	19.93±0.041	19.04±0.01	18.78±0.010	18.75±0.014	18.62±0.046	0.04	2
FIRST J233930.0+003017	3.033	23 : 39 : 30.01	+00 : 30 : 17.2	0.13	19.62±0.038	18.67±0.01	18.59±0.01	18.47±0.011	18.35±0.035	0.04	2
FIRST J234023.6-005327	2.092	23 : 40 : 23.67	-00 : 53 : 27.1	0.21	18.27±0.012	17.85±0.01	17.53±0.01	17.22±0.01	16.90±0.011	0.03	2
[HB89] 2340+009	2.370	23 : 42 : 53.59	+01 : 15 : 21.1	0.10	20.23±0.051	19.57±0.012	19.35±0.014	19.18±0.021	18.98±0.063	0.03	1
[HB89] 2340+008NED01	1.370	23 : 42 : 54.97	+01 : 08 : 04.5	1.22	20.23±0.050	20.17±0.019	19.82±0.020	19.73±0.032	19.74±0.121	0.03	1
[HB89] 2340+008NED02	2.140	23 : 43 : 22.96	+01 : 07 : 29.5	0.80	20.11±0.046	19.85±0.015	19.85±0.019	19.70±0.032	19.31±0.083	0.03	1
UM 173	1.371	23 : 43 : 26.60	-00 : 03 : 17.4	0.07	18.05±0.011	17.98±0.01	17.79±0.01	17.80±0.01	17.84±0.022	0.03	1 2
[HB89] 2341+009	1.400	23 : 43 : 40.34	+01 : 12 : 54.5	1.01	19.30±0.025	19.13±0.01	19.10±0.012	18.92±0.017	18.73±0.051	0.03	1
FIRST J234440.0-003231	0.503	23 : 44 : 40.04	-00 : 32 : 31.7	0.15	17.88±0.010	17.56±0.01	17.65±0.01	17.52±0.01	17.40±0.015	0.04	1 2
[HB89] 2342+008	1.570	23 : 44 : 42.48	+01 : 05 : 50.1	1.13	20.44±0.062	20.27±0.021	20.04±0.024	20.03±0.040	20.04±0.157	0.03	1
[HB89] 2342+007	2.700	23 : 45 : 06.34	+01 : 01 : 35.7	0.85	19.43±0.035	19.21±0.011	19.01±0.015	18.68±0.015	18.61±0.043	0.03	1
[HB89] 2343+008NED02	2.900	23 : 45 : 45.30	+01 : 08 : 54.3	0.67	21.84±0.201	20.73±0.033	20.47±0.034	20.12±0.045	20.11±0.181	0.04	1
[HB89] 2344+002	2.060	23 : 47 : 09.99	+00 : 28 : 56.3	2.69	21.57±0.185	21.16±0.054	21.34±0.091	20.95±0.092	20.84±0.292	0.04	1
[HB89] 2345+005	2.100	23 : 48 : 08.14	+00 : 48 : 29.7	1.80	20.55±0.058	20.31±0.022	20.64±0.038	20.30±0.051	20.31±0.196	0.02	1
[HB89] 2345+002NED01	3.060	23 : 48 : 12.38	+00 : 29 : 39.6	0.67	20.55±0.063	20.21±0.025	19.37±0.016	18.97±0.017	18.87±0.049	0.03	1

Table 2—Continued

Name	z_{em}	RA(2000)	DEC(2000)	Δ''	u^*	g^*	r^*	i^*	z^*	$E(g^*-r^*)$	source
[VCV96] 2345+007C	2.653	23 : 48 : 13.76	+00 : 56 : 39.9	1.28	20.87 \pm 0.119	20.87 \pm 0.044	20.42 \pm 0.041	20.47 \pm 0.065	20.06 \pm 0.153	0.02	1
[HB89] 2345+006	2.152	23 : 48 : 19.19	+00 : 57 : 17.5	1.50	20.88 \pm 0.116	20.69 \pm 0.039	20.60 \pm 0.047	20.57 \pm 0.070	20.03 \pm 0.152	0.02	1
[HB89] 2345+000	2.650	23 : 48 : 25.38	+00 : 20 : 40.1	2.12	20.74 \pm 0.069	19.89 \pm 0.016	19.78 \pm 0.019	19.77 \pm 0.031	19.66 \pm 0.147	0.03	1
UM 180	1.960	23 : 48 : 30.41	+00 : 39 : 18.6	0.17	17.84 \pm 0.010	17.68 \pm 0.01	17.68 \pm 0.01	17.41 \pm 0.01	17.23 \pm 0.014	0.03	1
[HB89] 2346+000	1.480	23 : 48 : 45.01	+00 : 22 : 37.8	1.82	20.43 \pm 0.054	20.08 \pm 0.019	19.95 \pm 0.022	19.78 \pm 0.031	19.69 \pm 0.151	0.03	1
[HB89] 2346+001NED01	2.520	23 : 48 : 47.18	+00 : 27 : 39.1	1.19	21.59 \pm 0.194	20.34 \pm 0.028	19.69 \pm 0.021	19.52 \pm 0.027	19.20 \pm 0.067	0.03	1
[HB89] 2346+001NED02	1.530	23 : 48 : 54.05	+00 : 28 : 40.6	1.76	20.73 \pm 0.090	20.62 \pm 0.035	20.83 \pm 0.055	20.35 \pm 0.056	20.03 \pm 0.141	0.03	1
[HB89] 2346+005	1.800	23 : 48 : 59.41	+00 : 51 : 26.8	0.80	19.45 \pm 0.034	19.43 \pm 0.014	19.39 \pm 0.017	19.09 \pm 0.019	19.08 \pm 0.065	0.03	1
[HB89] 2346+002	2.270	23 : 49 : 05.01	+00 : 28 : 54.9	2.12	21.45 \pm 0.168	20.36 \pm 0.029	20.01 \pm 0.027	19.83 \pm 0.036	19.62 \pm 0.098	0.03	1
[HB89] 2346+007	2.480	23 : 49 : 12.62	+00 : 59 : 46.1	2.76	21.58 \pm 0.212	21.03 \pm 0.052	20.99 \pm 0.067	20.72 \pm 0.084	21.92 \pm 0.605	0.03	1
[HB89] 2346+009	2.350	23 : 49 : 16.15	+01 : 12 : 53.5	0.92	20.30 \pm 0.053	19.86 \pm 0.015	19.81 \pm 0.021	19.82 \pm 0.036	19.83 \pm 0.135	0.02	1
[HB89] 2347+002	2.120	23 : 49 : 34.28	+00 : 30 : 23.7	2.69	21.09 \pm 0.101	21.10 \pm 0.055	20.45 \pm 0.040	20.32 \pm 0.055	20.27 \pm 0.185	0.04	1
UM 183	1.136	23 : 50 : 08.89	-00 : 29 : 12.5	2.54	19.02 \pm 0.021	18.87 \pm 0.01	18.63 \pm 0.01	18.61 \pm 0.011	18.70 \pm 0.043	0.04	1
SDSSp J235053.55-004810.3	3.840	23 : 50 : 53.54	-00 : 48 : 10.4	0.19	23.70 \pm 0.943	21.13 \pm 0.054	19.78 \pm 0.023	19.60 \pm 0.028	19.54 \pm 0.102	0.03	2
UM 184	3.020	23 : 50 : 57.87	-00 : 52 : 10.0	0.18	20.70 \pm 0.066	18.72 \pm 0.01	18.31 \pm 0.01	18.25 \pm 0.01	18.17 \pm 0.029	0.03	1 2
[HB89] 2349+002	2.495	23 : 51 : 51.25	+00 : 34 : 33.8	0.70	20.74 \pm 0.098	19.89 \pm 0.020	19.75 \pm 0.023	19.65 \pm 0.033	19.29 \pm 0.074	0.03	1
LBQS 2349+0059	2.040	23 : 51 : 53.34	+01 : 15 : 56.8	0.61	19.01 \pm 0.021	18.85 \pm 0.01	18.77 \pm 0.010	18.72 \pm 0.014	18.56 \pm 0.048	0.02	1
[HB89] 2349-014	0.172	23 : 51 : 56.13	-01 : 09 : 13.4	0.19	16.06 \pm 0.01	16.13 \pm 0.01	16.15 \pm 0.01	15.56 \pm 0.01	15.77 \pm 0.01	0.03	1 2
LBQS 2349+0019	1.356	23 : 51 : 57.60	+00 : 36 : 10.5	1.58	18.87 \pm 0.021	18.73 \pm 0.01	18.52 \pm 0.01	18.46 \pm 0.012	18.50 \pm 0.037	0.03	1
LBQS 2349+0022	1.237	23 : 52 : 17.25	+00 : 39 : 03.9	0.22	18.25 \pm 0.012	18.11 \pm 0.01	17.83 \pm 0.01	17.82 \pm 0.01	17.95 \pm 0.026	0.03	1 2
LBQS 2350-0045A	1.614	23 : 52 : 53.52	-00 : 28 : 50.5	0.05	18.94 \pm 0.020	18.17 \pm 0.01	18.15 \pm 0.01	17.93 \pm 0.01	17.86 \pm 0.023	0.03	1 2
LBQS 2350-0045B	0.764	23 : 53 : 21.63	-00 : 28 : 40.7	0.26	18.38 \pm 0.014	17.92 \pm 0.01	17.86 \pm 0.01	17.95 \pm 0.01	17.79 \pm 0.023	0.03	1 2
LBQS 2350-0012	0.561	23 : 53 : 24.08	+00 : 03 : 58.2	0.07	17.52 \pm 0.01	17.23 \pm 0.01	17.42 \pm 0.01	17.29 \pm 0.01	17.52 \pm 0.020	0.04	1 2
LBQS 2351-0036	0.462	23 : 54 : 09.18	-00 : 19 : 47.8	0.31	18.51 \pm 0.017	18.14 \pm 0.01	17.98 \pm 0.01	17.69 \pm 0.01	17.57 \pm 0.020	0.04	1 2
LBQS 2352+0025	0.271	23 : 54 : 57.09	+00 : 42 : 20.0	0.99	18.13 \pm 0.012	18.08 \pm 0.01	17.89 \pm 0.01	17.87 \pm 0.01	17.31 \pm 0.015	0.03	1
FIRST J235520.5+000747	1.060	23 : 55 : 20.59	+00 : 07 : 47.6	0.07	18.38 \pm 0.017	18.06 \pm 0.01	17.85 \pm 0.01	17.89 \pm 0.01	17.92 \pm 0.029	0.04	2
LBQS 2353+0032	0.558	23 : 55 : 45.51	+00 : 49 : 23.2	1.17	18.24 \pm 0.012	17.95 \pm 0.01	18.09 \pm 0.01	17.98 \pm 0.01	17.91 \pm 0.025	0.03	1
LBQS 2354+0048	1.004	23 : 56 : 49.92	+01 : 05 : 31.5	0.14	18.29 \pm 0.014	18.08 \pm 0.01	17.99 \pm 0.01	18.01 \pm 0.01	17.86 \pm 0.025	0.02	1 2
SDSSp J235718.35+004350.4	4.340	23 : 57 : 18.36	+00 : 43 : 50.4	0.19	24.00 \pm 0.782	22.44 \pm 0.144	20.07 \pm 0.026	19.83 \pm 0.036	19.61 \pm 0.105	0.04	2
LBQS 2356-0127	1.119	23 : 59 : 17.03	-01 : 10 : 29.1	0.39	18.60 \pm 0.018	18.40 \pm 0.01	18.14 \pm 0.01	18.08 \pm 0.01	18.01 \pm 0.028	0.05	1
PKS 2357-007	1.107	23 : 59 : 36.82	-00 : 31 : 12.9	0.96	21.09 \pm 0.105	21.12 \pm 0.043	20.73 \pm 0.042	20.61 \pm 0.061	20.20 \pm 0.171	0.05	1

Note. — Object sources listed in the last column are NED (1) and SDSS (2).

Table 3. Color-Redshift Relation

z	$u^* - g^*$				$g^* - r^*$				$r^* - i^*$				$i^* - z^*$			
	Median	Low ^a	High ^b	N	Median	Low ^a	High ^b	N	Median	Low ^a	High ^b	N	Median	Low ^a	High ^b	N
0.05	0.326	0.183	0.380	4	0.282	0.278	0.369	4	0.379	0.340	0.392	4	0.088	0.024	0.126	4
0.10	0.253	-0.002	0.450	11	0.356	0.156	0.564	14	0.453	0.323	0.705	14	0.135	-0.271	0.242	14
0.15	0.159	-0.170	0.756	25	0.358	-0.101	0.681	31	0.410	0.219	0.569	31	0.056	-0.229	0.258	29
0.20	0.225	-0.180	0.814	29	0.397	0.091	0.826	33	0.362	0.158	0.530	33	0.092	-0.151	0.295	33
0.25	0.153	-0.245	0.458	39	0.348	0.038	0.846	42	0.236	-0.023	0.447	42	0.243	-0.017	0.571	42
0.30	0.208	-0.129	0.615	36	0.385	-0.056	0.784	41	0.154	-0.094	0.339	39	0.486	0.241	0.627	39
0.35	0.131	-0.132	0.677	59	0.254	-0.168	0.956	66	0.092	-0.165	0.364	66	0.513	0.295	0.788	63
0.40	0.183	-0.105	0.492	46	0.095	-0.236	0.725	49	0.122	-0.133	0.411	49	0.370	0.011	0.723	48
0.45	0.239	0.021	0.466	42	0.103	-0.231	0.596	52	0.189	-0.007	0.563	51	0.197	-0.133	0.487	47
0.50	0.278	0.036	0.576	45	-0.059	-0.306	0.458	58	0.214	0.029	0.512	58	0.097	-0.087	0.330	57
0.55	0.322	0.127	0.537	40	-0.084	-0.259	0.267	42	0.179	0.031	0.456	42	0.032	-0.195	0.292	40
0.60	0.339	0.138	0.519	35	-0.068	-0.302	0.458	39	0.161	-0.087	0.548	39	-0.039	-0.197	0.151	38
0.65	0.318	0.109	0.555	48	-0.019	-0.270	0.316	56	0.125	-0.073	0.539	55	-0.017	-0.282	0.221	52
0.70	0.329	0.108	0.567	39	0.015	-0.132	0.227	43	0.019	-0.202	0.216	43	0.129	-0.053	0.345	41
0.75	0.285	0.074	0.517	56	0.040	-0.197	0.377	62	-0.002	-0.247	0.403	62	0.136	-0.100	0.387	61
0.80	0.295	0.113	0.722	53	0.041	-0.213	0.342	57	-0.069	-0.220	0.147	57	0.139	0.008	0.311	55
0.85	0.231	0.009	0.527	46	0.058	-0.105	0.196	48	-0.041	-0.289	0.144	48	0.125	-0.027	0.331	45
0.90	0.250	-0.047	0.548	47	0.119	-0.107	0.297	54	-0.069	-0.192	0.091	54	0.127	-0.027	0.314	50
0.95	0.138	-0.093	0.362	51	0.159	-0.014	0.342	57	-0.056	-0.180	0.083	57	0.092	-0.038	0.213	54
1.00	0.157	-0.026	0.377	41	0.239	0.066	0.418	45	-0.039	-0.211	0.089	44	0.032	-0.137	0.194	39
1.05	0.152	-0.074	0.399	57	0.230	0.025	0.463	65	-0.045	-0.166	0.149	64	0.030	-0.147	0.203	57
1.10	0.114	-0.072	0.362	51	0.214	0.064	0.457	56	-0.042	-0.162	0.079	56	-0.065	-0.268	0.124	49
1.15	0.082	-0.151	0.397	57	0.249	0.010	0.539	62	0.010	-0.146	0.158	62	-0.074	-0.310	0.147	57
1.20	0.056	-0.181	0.369	62	0.268	0.053	0.500	67	0.032	-0.107	0.165	67	-0.070	-0.242	0.141	62
1.25	0.063	-0.178	0.309	64	0.253	0.039	0.473	70	0.004	-0.173	0.169	70	-0.076	-0.194	0.056	65
1.30	0.065	-0.186	0.410	56	0.259	0.035	0.582	60	0.025	-0.159	0.309	61	-0.059	-0.246	0.185	58
1.35	0.046	-0.297	0.396	53	0.252	0.036	0.456	58	0.036	-0.100	0.164	58	-0.042	-0.170	0.080	50
1.40	0.069	-0.114	0.328	48	0.247	0.042	0.437	56	0.086	-0.031	0.232	56	-0.032	-0.167	0.137	50
1.45	0.172	-0.036	0.368	50	0.148	-0.004	0.326	55	0.123	-0.026	0.269	54	-0.022	-0.173	0.130	51
1.50	0.169	-0.056	0.744	68	0.150	-0.003	0.578	73	0.182	0.071	0.365	72	-0.028	-0.223	0.198	66
1.55	0.203	0.036	0.437	70	0.092	-0.101	0.370	75	0.206	0.016	0.382	75	-0.022	-0.170	0.163	68
1.60	0.210	0.037	0.419	73	0.070	-0.092	0.240	81	0.217	0.102	0.341	81	-0.002	-0.163	0.182	75
1.65	0.162	-0.001	0.483	52	0.074	-0.124	0.455	58	0.213	0.059	0.370	57	0.012	-0.155	0.175	57
1.70	0.106	-0.071	0.319	51	0.035	-0.101	0.484	59	0.251	0.033	0.504	59	0.024	-0.132	0.183	54
1.75	0.077	-0.113	0.278	63	0.023	-0.192	0.247	67	0.259	0.100	0.447	67	0.014	-0.163	0.179	63

Table 3—Continued

z	$u^* - g^*$				$g^* - r^*$				$r^* - i^*$				$i^* - z^*$			
	Median	Low ^a	High ^b	N	Median	Low ^a	High ^b	N	Median	Low ^a	High ^b	N	Median	Low ^a	High ^b	N
1.80	0.079	−0.252	0.474	59	0.044	−0.198	0.344	67	0.270	0.133	0.492	67	0.030	−0.138	0.214	63
1.85	0.048	−0.174	0.373	48	0.015	−0.173	0.214	51	0.262	0.128	0.472	51	0.049	−0.131	0.157	45
1.90	−0.009	−0.416	0.300	51	0.046	−0.171	0.305	58	0.251	0.108	0.423	58	0.057	−0.071	0.243	53
1.95	0.039	−0.162	0.232	50	0.032	−0.174	0.221	50	0.209	0.044	0.380	50	0.134	0.021	0.261	47
2.00	0.036	−0.299	0.366	44	0.064	−0.073	0.276	50	0.174	0.031	0.365	49	0.177	0.017	0.381	45
2.05	0.133	−0.109	0.457	43	0.121	−0.212	0.459	49	0.148	−0.043	0.389	48	0.205	0.063	0.352	43
2.10	0.184	−0.076	0.422	42	0.100	−0.351	0.345	48	0.112	−0.065	0.321	48	0.217	0.061	0.409	41
2.20	0.289	−0.048	0.647	117	0.072	−0.228	0.421	135	0.119	−0.085	0.355	135	0.224	0.067	0.396	124
2.40	0.570	0.148	1.082	42	0.062	−0.218	0.568	55	0.077	−0.085	0.354	54	0.250	0.061	0.570	50
2.60	0.795	0.419	1.343	29	0.172	−0.084	0.649	39	0.083	−0.072	0.406	38	0.252	0.038	0.517	35
2.80	1.046	0.185	1.648	18	0.145	−0.050	0.545	32	0.107	−0.114	0.437	32	0.174	−0.027	0.502	29
3.00	1.475	0.905	2.049	8	0.245	0.004	0.804	20	0.088	−0.126	0.486	20	0.112	−0.136	0.280	19
3.20	0	0.217	0.123	0.496	13	0.104	−0.050	0.337	13	0.051	−0.040	0.171	11
3.40	0	0.414	0.276	0.829	7	0.115	0.004	0.145	7	0.087	−0.029	0.098	7
3.60	0	1.084	0.570	1.544	24	0.093	−0.017	0.252	25	0.094	−0.106	0.318	15
3.80	0	1.257	1.021	1.815	29	0.076	−0.043	0.203	31	0.180	−0.103	0.258	19
4.00	0	1.406	1.069	1.638	17	0.145	−0.013	0.270	19	0.121	0.029	0.168	7
4.20	0	1.813	1.492	2.183	7	0.295	0.018	0.443	10	0.096	0.003	0.140	8
4.40	0	0	0.334	0.213	0.428	6	0.239	0.235	0.286	4
4.60	0	0	1.074	0.887	1.452	8	0.084	−0.047	0.127	4
4.80	0	0	0	0

^aColor at the 95% confidence limit to the blue of the median^bColor at the 95% confidence limit to the red of the median

Table 4. Power-law Colors of Quasars

α_ν	α_λ	$u' - g'$	$g' - r'$	$r' - i'$	$i' - z'$
−2.5	0.5	0.756	0.739	0.523	0.459
−2.0	0.0	0.602	0.594	0.419	0.367
−1.5	−0.5	0.450	0.447	0.315	0.275
−1.0	−1.0	0.299	0.299	0.210	0.184
−0.5	−1.5	0.149	0.150	0.105	0.092
0.0	−2.0	0.000	0.000	0.000	0.000

Table 5. Scatter in Corrected Colors (95% Confidence)

Color	Δ Blue Color	Δ Red Color	$\Delta\alpha$ Blue	$\Delta\alpha$ Red
u^*-g^*	−0.209	0.402	0.69	1.34
g^*-r^*	−0.190	0.319	0.64	1.07
r^*-i^*	−0.161	0.198	0.77	0.94
i^*-z^*	−0.173	0.211	0.95	1.15